

# ROBUST AND ADAPTIVE CONTROL VIA BACKSTEPPING TECHNIQUE

ANTOINE G. IBRAHIM

A THESIS SUBMITTED IN PARTIAL FULFILLMENT OF THE  
REQUIREMENTS OF MScEng DEGREE IN CONTROL ENGINEERING

FACULTY OF ENGINEERING

LAKEHEAD UNIVERSITY

THUNDER BAY, ONTARIO

P7B 5E1

OCTOBER 24<sup>st</sup>, 2005



Library and  
Archives Canada

Bibliothèque et  
Archives Canada

Published Heritage  
Branch

Direction du  
Patrimoine de l'édition

395 Wellington Street  
Ottawa ON K1A 0N4  
Canada

395, rue Wellington  
Ottawa ON K1A 0N4  
Canada

*Your file* *Votre référence*  
*ISBN: 978-0-494-15620-9*  
*Our file* *Notre référence*  
*ISBN: 978-0-494-15620-9*

**NOTICE:**

The author has granted a non-exclusive license allowing Library and Archives Canada to reproduce, publish, archive, preserve, conserve, communicate to the public by telecommunication or on the Internet, loan, distribute and sell theses worldwide, for commercial or non-commercial purposes, in microform, paper, electronic and/or any other formats.

The author retains copyright ownership and moral rights in this thesis. Neither the thesis nor substantial extracts from it may be printed or otherwise reproduced without the author's permission.

**AVIS:**

L'auteur a accordé une licence non exclusive permettant à la Bibliothèque et Archives Canada de reproduire, publier, archiver, sauvegarder, conserver, transmettre au public par télécommunication ou par l'Internet, prêter, distribuer et vendre des thèses partout dans le monde, à des fins commerciales ou autres, sur support microforme, papier, électronique et/ou autres formats.

L'auteur conserve la propriété du droit d'auteur et des droits moraux qui protègent cette thèse. Ni la thèse ni des extraits substantiels de celle-ci ne doivent être imprimés ou autrement reproduits sans son autorisation.

---

In compliance with the Canadian Privacy Act some supporting forms may have been removed from this thesis.

Conformément à la loi canadienne sur la protection de la vie privée, quelques formulaires secondaires ont été enlevés de cette thèse.

While these forms may be included in the document page count, their removal does not represent any loss of content from the thesis.

Bien que ces formulaires aient inclus dans la pagination, il n'y aura aucun contenu manquant.

  
**Canada**

# ABSTRACT

Most of the control systems are designed using linear techniques, which have been well developed. Practical physical systems are typically nonlinear. Nonlinear control is one of the biggest challenges in modern control theory. Nonlinear processes are difficult to control because there can be so many variations of the nonlinear behavior.

One of the main recursive procedures to design a nonlinear controller is the backstepping. Adaptive backstepping achieved global stabilization in the presence of unknown parameters and robust backstepping achieved it in the presence of disturbances. The ease with which backstepping incorporated uncertainties and unknown parameters, contributed to its instant popularity and rapid acceptance. The backstepping provides a powerful design tool for nonlinear systems in the lower triangular form.

The first part of the thesis is to explain backstepping technique for third order nonlinear systems. Robust backstepping technique for a system with bounded uncertainties and adaptive backstepping technique for a system with linear unknown parameters are illustrated and simulated.

The second part of the thesis is to apply the adaptive backstepping and robust backstepping technique to a 2-DOF (degree of freedom) planar manipulator. Experimental and simulation results are obtained and compared with linear (PD) controller and nonlinear controller (Lyapunov based algorithm).

## ACKNOWLEDGEMENTS

I would like to express my deepest gratitude to my supervisor Dr. X. Liu for his guidance and mentorship, which were more than effective. I would like to thank my co-supervisor Dr. A. Tayebi for his suggestions and help. I am grateful to Mr. Manfred Klein, Greg Jollimore and Mr. Kailash Bhatia who helped me in the experimental part of the thesis.

I extend my thanks to my fellow graduate students for their suggestions and discussions, which were valuable and positive.

Finally, I would like to thank my family for many reasons, which allow me to accomplish this work.

# Contents

<b>I</b>	<b>INTRODUCTION</b>	<b>1</b>
<b>1</b>	<b>Introduction</b>	<b>2</b>
1.1	Nonlinear Control . . . . .	2
1.2	Basic Concepts and Definitions . . . . .	5
1.3	Literature Review . . . . .	8
1.4	Thesis Overview . . . . .	10
<b>II</b>	<b>NONLINEAR ADAPTIVE AND ROBUST BACKSTEPPING CONTROL DESIGN</b>	<b>12</b>
<b>2</b>	<b>Nonlinear Backstepping Control Design</b>	<b>13</b>
2.1	Theory . . . . .	13
2.2	Example . . . . .	17
<b>3</b>	<b>Robust Backstepping Control Design</b>	<b>22</b>

3.1	Theory . . . . .	22
3.2	Example . . . . .	27
<b>4</b>	<b>Adaptive Backstepping Control Design</b>	<b>41</b>
4.1	Theory . . . . .	41
4.2	Example . . . . .	48
 <b>III APPLICATION OF DIFFERENT CONTROLLERS ON 2-DOF PLANAR MANIPULATOR</b>		 <b>55</b>
<b>5</b>	<b>System and Experimental Setup</b>	<b>56</b>
5.1	Robotics Background . . . . .	56
5.2	Experimental Setup . . . . .	59
5.2.1	Mechanical Assembly . . . . .	60
5.2.2	Circuitry . . . . .	62
5.2.3	Data Acquisition Module . . . . .	64
<b>6</b>	<b>PD Controller</b>	<b>66</b>
6.1	Theory . . . . .	66
6.2	Control Design . . . . .	69
6.3	Experimental Results . . . . .	72

<b>7 Nonlinear Controller</b>	<b>77</b>
7.1 Control Design . . . . .	77
7.2 Experimental Results . . . . .	80
<b>8 Robust Controller</b>	<b>85</b>
8.1 Control Design . . . . .	85
8.2 Experimental Results . . . . .	90
<b>9 Adaptive Controller</b>	<b>96</b>
9.1 Control Design . . . . .	96
9.2 Experimental Results . . . . .	101
<b>IV CONCLUSION</b>	<b>107</b>
<b>10 Conclusion and future work</b>	<b>108</b>
10.1 Conclusion . . . . .	108
10.2 Future work . . . . .	110
<b>A Block Diagrams</b>	<b>115</b>
<b>B Cut Sheets - LMD18200, 55V H-bridge</b>	<b>120</b>
<b>C Cut Sheets - TL494, PWM Control Circuit</b>	<b>131</b>

<b>D Cut Sheets - Servo Systems Encoder</b>	<b>140</b>
<b>E Cut Sheets - DC Motor</b>	<b>142</b>



# List of Figures

2.1	$x_1$ -Nonlinear backstepping control . . . . .	20
2.2	$x_2$ -Nonlinear backstepping control . . . . .	20
2.3	$x_3$ -Nonlinear backstepping control . . . . .	21
2.4	$u$ -Nonlinear backstepping control . . . . .	21
3.1	$x_1$ -Nonlinear robust backstepping control - $\theta_1 = 1.5, \theta_2 = 2, \theta_3 = 3$ . . . . .	36
3.2	$x_2$ -Nonlinear robust backstepping control - $\theta_1 = 1.5, \theta_2 = 2, \theta_3 = 3$ . . . . .	36
3.3	$x_3$ -Nonlinear robust backstepping control - $\theta_1 = 1.5, \theta_2 = 2, \theta_3 = 3$ . . . . .	37
3.4	$u$ -Nonlinear robust backstepping control - $\theta_1 = 1.5, \theta_2 = 2, \theta_3 = 3$ . . . . .	37
3.5	$x_1$ -Nonlinear robust backstepping control - $\theta_1 = 0, \theta_2 = 0, \theta_3 = 0$ . . . . .	37
3.6	$x_2$ -Nonlinear robust backstepping control - $\theta_1 = 0, \theta_2 = 0, \theta_3 = 0$ . . . . .	37
3.7	$x_3$ -Nonlinear robust backstepping control - $\theta_1 = 0, \theta_2 = 0, \theta_3 = 0$ . . . . .	38
3.8	$u$ -Nonlinear robust backstepping control - $\theta_1 = 0, \theta_2 = 0, \theta_3 = 0$ . . . . .	38
3.9	$x_1$ -Nonlinear robust backstepping control - $\theta_1 = -1, \theta_2 = -1, \theta_3 = -1$ . . . . .	38
3.10	$x_2$ -Nonlinear robust backstepping control - $\theta_1 = -1, \theta_2 = -1, \theta_3 = -1$ . . . . .	38

3.11	$x_3$ -Nonlinear robust backstepping control - $\theta_1 = -1, \theta_2 = -1, \theta_3 = -1$ . . . . .	39
3.12	$u$ -Nonlinear robust backstepping control - $\theta_1 = -1, \theta_2 = -1, \theta_3 = -1$ . . . . .	39
3.13	$x_1$ -Nonlinear robust backstepping control - $\theta_1 = 1, \theta_2 = 1, \theta_3 = 1$ . . . . .	39
3.14	$x_2$ -Nonlinear robust backstepping control - $\theta_1 = 1, \theta_2 = 1, \theta_3 = 1$ . . . . .	39
3.15	$x_3$ -Nonlinear robust backstepping control - $\theta_1 = 1, \theta_2 = 1, \theta_3 = 1$ . . . . .	40
3.16	$u$ -Nonlinear robust backstepping control - $\theta_1 = 1, \theta_2 = 1, \theta_3 = 1$ . . . . .	40
4.1	$x_1$ -Nonlinear adaptive backstepping control - $\theta = 1$ . . . . .	52
4.2	$x_2$ -Nonlinear adaptive backstepping control - $\theta = 1$ . . . . .	52
4.3	$x_3$ -Nonlinear adaptive backstepping control - $\theta = 1$ . . . . .	53
4.4	$\hat{\theta}$ -Nonlinear adaptive backstepping control - $\theta = 1$ . . . . .	53
4.5	$u$ -Nonlinear adaptive backstepping control - $\theta = 1$ . . . . .	53
4.6	$x_1$ -Nonlinear adaptive backstepping control - $\theta = 2$ . . . . .	53
4.7	$x_2$ -Nonlinear adaptive backstepping control - $\theta = 2$ . . . . .	54
4.8	$x_3$ -Nonlinear adaptive backstepping control - $\theta = 2$ . . . . .	54
4.9	$\hat{\theta}$ -Nonlinear adaptive backstepping control - $\theta = 2$ . . . . .	54
4.10	$u$ -Nonlinear adaptive backstepping control - $\theta = 2$ . . . . .	54
5.1	2 DOF robot manipulator . . . . .	57
6.1	$q_1$ - Simulation result with PD control . . . . .	72
6.2	$q_2$ - Simulation result with PD control . . . . .	72

6.3	$\dot{q}_1$ - Simulation result with PD control . . . . .	73
6.4	$\dot{q}_2$ - Simulation result with PD control . . . . .	73
6.5	$e_1$ - Simulation result with PD control . . . . .	74
6.6	$e_2$ - Simulation result with PD control . . . . .	74
6.7	$v_1$ - Simulation result with PD control . . . . .	74
6.8	$v_2$ - Simulation result with PD control . . . . .	74
6.9	$q_1$ - Experimental result with PD control . . . . .	75
6.10	$q_2$ - Experimental result with PD control . . . . .	75
6.11	$\dot{q}_1$ - Experimental result with PD control . . . . .	75
6.12	$\dot{q}_2$ - Experimental result with PD control . . . . .	75
6.13	$e_1$ - Experimental result with PD control . . . . .	76
6.14	$e_2$ - Experimental result with PD control . . . . .	76
6.15	$v_1$ - Experimental result with PD control . . . . .	76
6.16	$v_2$ - Experimental result with PD control . . . . .	76
7.1	$q_1$ - Simulation result with nonlinear stabilizing control based on Lyapunov method	80
7.2	$q_2$ - Simulation result with nonlinear stabilizing control based on Lyapunov method	80
7.3	$\dot{q}_1$ - Simulation result with nonlinear stabilizing control based on Lyapunov method	81
7.4	$\dot{q}_2$ - Simulation result with nonlinear stabilizing control based on Lyapunov method	81
7.5	$e_1$ - Simulation result with nonlinear stabilizing control based on Lyapunov method	82
7.6	$e_2$ - Simulation result with nonlinear stabilizing control based on Lyapunov method	82

7.7	$v_1$ - Simulation result with nonlinear stabilizing control based on Lyapunov method	82
7.8	$v_2$ - Simulation result with nonlinear stabilizing control based on Lyapunov method	82
7.9	$q_1$ - Experimental result with nonlinear stabilizing control based on Lyapunov method	83
7.10	$q_2$ - Experimental result with nonlinear stabilizing control based on Lyapunov method	83
7.11	$\dot{q}_1$ - Experimental result with nonlinear stabilizing control based on Lyapunov method	83
7.12	$\dot{q}_2$ - Experimental result with nonlinear stabilizing control based on Lyapunov method	83
7.13	$e_1$ - Experimental result with nonlinear stabilizing control based on Lyapunov method	84
7.14	$e_2$ - Experimental result with nonlinear stabilizing control based on Lyapunov method	84
7.15	$v_1$ - Experimental result with nonlinear stabilizing control based on Lyapunov method	84
7.16	$v_2$ - Experimental result with nonlinear stabilizing control based on Lyapunov method	84
8.1	$q_1$ - Simulation result with robust control . . . . .	91
8.2	$q_2$ - Simulation result with robust control . . . . .	91
8.3	$\dot{q}_1$ - Simulation result with robust control . . . . .	92
8.4	$\dot{q}_2$ - Simulation result with robust control . . . . .	92
8.5	$e_1$ - Simulation result with robust control . . . . .	92
8.6	$e_2$ - Simulation result with robust control . . . . .	92
8.7	$v_1$ - Simulation result with robust control . . . . .	93
8.8	$v_2$ - Simulation result with robust control . . . . .	93
8.9	$q_1$ - Experimental result with robust control . . . . .	93
8.10	$q_2$ - Experimental result with robust control . . . . .	93

8.11	$\dot{q}_1$ - Experimental result with robust control . . . . .	94
8.12	$\dot{q}_2$ - Experimental result with robust control . . . . .	94
8.13	$e_1$ - Experimental result with robust control . . . . .	94
8.14	$e_2$ - Experimental result with robust control . . . . .	94
8.15	$v_1$ - Experimental result with robust control . . . . .	95
8.16	$v_2$ - Experimental result with robust control . . . . .	95
9.1	$q_1$ - Simulation result with adaptive control . . . . .	101
9.2	$q_2$ - Simulation result with adaptive control . . . . .	101
9.3	$\dot{q}_1$ - Simulation result with adaptive control . . . . .	102
9.4	$\dot{q}_2$ - Simulation result with adaptive control . . . . .	102
9.5	$e_1$ - Simulation result with adaptive control . . . . .	103
9.6	$e_2$ - Simulation result with adaptive control . . . . .	103
9.7	$v_1$ - Simulation result with adaptive control . . . . .	103
9.8	$v_2$ - Simulation result with adaptive control . . . . .	103
9.9	$\hat{\theta}_1$ - Simulation result with adaptive control . . . . .	104
9.10	$\hat{\theta}_2$ - Simulation result with adaptive control . . . . .	104
9.11	$q_1$ - Experimental result with adaptive control . . . . .	104
9.12	$q_2$ - Experimental result with adaptive control . . . . .	104
9.13	$\dot{q}_1$ - Experimental result with adaptive control . . . . .	105
9.14	$\dot{q}_2$ - Experimental result with adaptive control . . . . .	105

9.15	$e_1$ - Experimental result with adaptive control . . . . .	105
9.16	$e_2$ - Experimental result with adaptive control . . . . .	105
9.17	$v_1$ - Experimental result with adaptive control . . . . .	106
9.18	$v_2$ - Experimental result with adaptive control . . . . .	106
9.19	$\hat{\theta}_1$ - Experimental result with adaptive control . . . . .	106
9.20	$\hat{\theta}_2$ - Experimental result with adaptive control . . . . .	106
A.1	Experimental Block Diagram . . . . .	115
A.2	PD Controller - Simulink Block . . . . .	116
A.3	Nonlinear Controller - Simulink Block . . . . .	117
A.4	Robust Controller - Simulink Block . . . . .	118
A.5	Adaptive Controller - Simulink Block . . . . .	119
B.1	LMD18200, 55V H-bridge - Page1 . . . . .	121
B.2	LMD18200, 55V H-bridge - Page2 . . . . .	122
B.3	LMD18200, 55V H-bridge - Page3 . . . . .	123
B.4	LMD18200, 55V H-bridge - Page4 . . . . .	124
B.5	LMD18200, 55V H-bridge - Page5 . . . . .	125
B.6	LMD18200, 55V H-bridge - Page6 . . . . .	126
B.7	LMD18200, 55V H-bridge - Page7 . . . . .	127
B.8	LMD18200, 55V H-bridge - Page8 . . . . .	128

B.9	LMD18200, 55V H-bridge - Page9 . . . . .	129
B.10	LMD18200, 55V H-bridge - Page 10 . . . . .	130
C.1	TL494, PWM Control Circuit - Page1 . . . . .	132
C.2	TL494, PWM Control Circuit - Page2 . . . . .	133
C.3	TL494, PWM Control Circuit - Page3 . . . . .	134
C.4	TL494, PWM Control Circuit - Page4 . . . . .	135
C.5	TL494, PWM Control Circuit - Page5 . . . . .	136
C.6	TL494, PWM Control Circuit - Page6 . . . . .	137
C.7	TL494, PWM Control Circuit - Page7 . . . . .	138
C.8	TL494, PWM Control Circuit - Page8 . . . . .	139
D.1	Servo Systems Encoder . . . . .	141
E.1	DC Motor - Page1 . . . . .	143
E.2	DC Motor - Page2 . . . . .	144

## List of Acronyms and Notations

P	Proportional
PD	Proportional plus Derivative
PID	Proportional plus Integral plus Derivative
DOF	Degree of Freedom
SISO	Single Input Single Output
DAQ	Data Acquisition
DAC	Digital to Analog Converter
ADC	Analog to Digital Converter
DC	Direct Current
PWM	Pulse Width Modulation
RFI	Radio Frequency Interference
clf	Control Lyapunov Function
$A^{-1}$	Inverse of Matrix A
$A^T$	Transpose of Matrix A



# Part I

## INTRODUCTION

# Chapter 1

## Introduction

### 1.1 Nonlinear Control

Control theory can be described as the process of influencing the behavior of a physical system to achieve a desired goal, primarily through the use of feedback. It is important in a diverse range of scientific and engineering disciplines, including such things as the design of robotic systems.

Linear control is widely used in industrial applications. Most physical systems are nonlinear to various extents. However, if the range of variations of the system variables is not wide, then the system may be linearized within relatively small range of variation of variables [1]. While linearizing the behavior of the system and applying traditional linear control methods is an effective method of controlling the system,

there are many reasons, which justify the effort in the development of nonlinear control methodologies, as follows:

- **Improvement of Existing Control Systems** [2] Linear control methods are only effective around the chosen operating point. Large deviations from this point lead to instabilities and the eventual failure of the system to remain in the desired position. It is therefore important to develop techniques of analysis and control design for nonlinear systems.
- **Analysis of Hard Nonlinearities** [2] In some cases a linear approximation of the system is a good enough model for analysis and design, while in others the system has dominating nonlinear effects that make a linear approximation a non-satisfactory model for the system. Saturation and hysteresis are good examples for the so-called 'hard nonlinearities'. Their effects cannot be derived from linear methods, and nonlinear controllers must be developed to deal with the system in the presence of these inherent nonlinearities.
- **Dealing with Model Uncertainties** [2] It is not practical to assume that all the parameters are exactly known for a system to be controlled. There are systems whose parameters and models can be accurately obtained. On the other hand, there are systems to be controlled with unknown or uncertain parameters. Uncertainties may result from disturbances or inaccurate knowledge

of the system parameters. In such cases linear controllers may act poorly in controlling these systems. Two classes of nonlinear controllers can stabilize the system in the presence of such uncertainties. These controllers are called robust controllers and adaptive controllers. The adaptive controller estimates parameters and calculates the control accordingly. The robust controller allows for uncertainty in the design of the fixed controller so it becomes insensitive to parameter variations or disturbances [3].

The application of nonlinear control methods was limited due to the mathematical complexity associated with the nonlinear control laws. Over the last few years, the evolution in computer technology has solved a lot of problems related to the implementation of nonlinear controllers. Moreover, most of modern applications require more stringent control systems.

The most important approach for studying the stability of nonlinear control systems is the theory introduced in the late 19th century by the Russian mathematician Alexandr Mikhailovich Lyapunov. There are two methods introduced by Lyapunov for stability analysis of a nonlinear system.

The indirect method, or linearization method, states that the stability properties of a nonlinear system in the close vicinity of an equilibrium point are essentially the same as those of its linearized approximation. The method serves as the theoretical justification for using linear control for physical systems, which are always inherently

nonlinear. The direct method is a powerful tool for nonlinear system analysis, and therefore, the so-called Lyapunov analysis often actually refers to the direct method. The direct method is a generalization of the energy concepts associated with a mechanical system: the motion of a mechanical system is stable if its total mechanical energy decreases all the time. In using the direct method to analyze the stability of a nonlinear system, the idea is to construct a scalar energy-like function (a Lyapunov function) for the system, and to see whether it decreases. The limitation of this method lies in the fact that it is often difficult to find a Lyapunov function for a given system [2].

Lyapunov functions are of fundamental importance in the study of nonlinear systems. Not only Lyapunov functions are useful in proving stability of nonlinear systems, they are also an important part of certain nonlinear control design methods.

## 1.2 Basic Concepts and Definitions

Some basic concepts and definitions are introduced below.

**Equilibrium Point:** A state vector  $x^*$  is an equilibrium point of the system if once  $x(t)$  is equal to  $x^*$ , it remains equal to  $x^*$  for all future time.

**Definition of Stability:** Let  $B_R$  denote the spherical region (or ball) defined by  $\|x\| < R$  in state space, and  $S_R$  the sphere itself defined by  $\|x\| = R$ .

The equilibrium point  $x = 0$  is said to be stable if, for any  $R > 0$ , there exists

$r > 0$ , such that if  $\|x(0)\| < r$ , then  $\|x(t)\| < R$  for all  $t \geq 0$ . Otherwise the equilibrium point is unstable.

**Asymptotic Stability:** An equilibrium point is called locally asymptotically stable if it is stable, and if in addition there exists some  $r > 0$  such that  $\|x(0)\| < r$  implies that  $x(t) \rightarrow 0$  as  $t \rightarrow \infty$ . The ball  $B_r$  of radius  $r$  is called the domain of attraction of the equilibrium point. If the convergence to zero occurs for any initial condition  $x(0)$ , the equilibrium point is globally asymptotically stable (GAS).

**Smooth Function:** A smooth function is a function that has continuous derivatives up to some desired order over some domain. A function can therefore be said to be smooth over a restricted interval such as  $(a, b)$  or  $[a, b]$ . The number of continuous derivatives necessary for a function to be considered smooth depends on the problem at hand, and may vary from two to infinity. A function for which all orders of derivatives are continuous is called a C-infinity function.

**Symmetric Matrix:** A square matrix  $P$  is symmetric if  $P = P^T$ .

**Skew-Symmetric Matrix:** If a matrix  $P$  is equal to the negative of its transpose  $P^T = -P$  then it is called a skew-symmetric matrix.

**Positive Definite:** A square matrix  $P$  is positive definite if  $x^T P x > 0$  for non-zero  $x$ .

**Positive Semidefinite:** A square matrix  $P$  is positive semidefinite if  $x^T P x \geq 0$  for non-zero  $x$ .

**Negative Definite:** A square matrix  $P$  is negative definite if  $x^T P x < 0$  for non-zero  $x$ .

**Negative Semidefinite:** A square matrix  $P$  is negative semidefinite if  $x^T P x \leq 0$  for non-zero  $x$ .

**Lyapunov Function Candidate:** Let  $V(x): R^n \rightarrow R$  be a continuous function with continuous first partial derivatives in the neighborhood of the origin in  $R^n$ . If  $V$  is positive definite then it is called a Lyapunov function candidate.

**Lyapunov Function:** Consider the system

$$\dot{x} = f(x), \tag{1.1}$$

where  $x \in R^n$ . Suppose that the origin is an equilibrium point i.e.,  $f(0) = 0$ . The equilibrium point  $x = 0$  is asymptotically stable if there exists a Lyapunov function candidate  $V$  such that  $\dot{V}$  is negative definite along the solution trajectories of the system, that is, if

$$\dot{V} = \frac{dV}{dx} f(x) < 0, \quad \forall x \neq 0,$$

Then  $V$  is called a Lyapunov function.

**LaSalle's Theorem:** Given the system (1.1), suppose that a Lyapunov function candidate  $V$  is found such that  $\dot{V} \leq 0$  along solution trajectories. Then the equilibrium point  $x = 0$  of (1.1) is asymptotically stable if  $\dot{V}$  does not vanish identically along any solution of (1.1) other than the null solution, i.e., if and only if the only

solution of (1.1) satisfying  $\dot{V} = 0$  is the null solution.

### 1.3 Literature Review

Nonlinear feedback control has been the topic of hundreds of publications, numerous monographs and several comprehensive textbooks such as Khalil (1996b), Vidyasagar (1993), and Sastry (1999) [4].

For nonlinear control the 1990s started with a breakthrough: *backstepping*, a recursive design for systems with nonlinearities not constrained by linear bounds. The true potential of backstepping was discovered only when this approach was developed for nonlinear systems with structured uncertainty [4] [5].

The ease with which backstepping incorporated uncertainties and unknown parameters contributed to its instant popularity and rapid acceptance. At the same time, its limitation to a class of pure feedback (lower triangular) systems stimulated the development of other recursive procedures such as *forwarding* [4].

Models of physical non-linear systems are prone to different kinds of uncertainties [6].

With *adaptive backstepping*, Kanellakopoulos, Kokotovic, and Morse (1991a,b) achieved global stabilization in the presence of unknown parameters and with *robust backstepping*, Freeman and Kokotovic (1992,1993), and Marino and Tomei (1993b) achieved it in the presence of disturbances [4].



There are many papers, which develop the design methodology and technique for adaptive and robust backstepping control on many physical systems [7] [8] [9] [10] [11].

Sliding mode control [12] and Lyapunov redesign are used to robustly stabilize an uncertain system when the uncertainty satisfies the matching condition. Backstepping can be used to relax the matching condition.[13].

Motivated by the backstepping design technique, a robust and adaptive control technique has been introduced using neural networks [14] [15].

The considerable number of publications on the robust and adaptive control of robot manipulators has brought many interesting results [16]. Recursive design of robust and robust adaptive control with  $L_2$ -gain performance for two-link robot manipulator has been developed and applied experimentally [17]. A general approach for the design of an adaptive position control for robotic systems by the backstepping passivity strict-feedback technique has been illustrated by simulation results [18].

To deal with the uncertainties in the dynamics of robotic systems, various control methods have been developed, including robust control schemes (e.g. Dawson et al. 1992) and adaptive control schemes (e.g. Yuan 1995) [5] [16] [17].

In this thesis, we will develop the adaptive and the robust recursive design methods (*backstepping*) for the two-link robot manipulator and compare them with other well-developed controllers.

The advantage of this control technique is that it imposes desired properties of stability by fixing the candidate Lyapunov functions initially, then by calculating the other functions in a recursive way [5].

## 1.4 Thesis Overview

The thesis is mainly divided into two parts besides the introduction and the conclusion. Nonlinear backstepping design procedures are explained in the first part. The application of different controllers on a 2-DOF planar manipulator, including adaptive backstepping and robust backstepping, discussed in the first part, are shown in the second part. Simulation and experimental results are analyzed and compared.

A general background on nonlinear system and Lyapunov stability theorem is discussed in the introduction.

Chapter 2 gives the theoretical background needed in order to understand the backstepping design followed by an example and simulations to show the design method.

Chapter 3 presents the robust backstepping design procedure theoretically. An example and simulations are provided to demonstrate the procedure.

Chapter 4 explains the adaptive backstepping design theoretically with an example and simulations to illustrate the design method.

Chapter 5 provides some basic knowledge about robots and describes the experi-

mental setup used.

Chapter 6 shows the application of PD controller on the 2-link robot manipulator. Simulation and experimental results are shown and discussed.

Chapter 7 discusses the performance of nonlinear controllers based on Lyapunov direct method on the 2-link robot manipulator by simulation and experimental results.

Chapter 8 demonstrates the robust backstepping controller design on the 2-link robot manipulator. Simulation and experimental results are studied.

Chapter 9 illustrates the adaptive backstepping controller design on the 2-link robot manipulator. Simulations and experimental results are analyzed.

Chapter 10 concludes the thesis by comparing the main results that have been reached. Moreover, it includes some proposals for future work.

## Part II

# NONLINEAR ADAPTIVE AND ROBUST BACKSTEPPING CONTROL DESIGN

# Chapter 2

## Nonlinear Backstepping Control Design

### 2.1 Theory

Lyapunov functions are of fundamental importance in the study of nonlinear systems and the design procedure of nonlinear controllers including backstepping. Backstepping is a recursive design procedure for systematically selecting the control Lyapunov functions (clf) that allow the design of nonlinear controllers for a nonlinear system. Backstepping is applicable to the systems in the lower triangular form [19].

In this chapter, we will explain the procedure to design backstepping-based controllers for a nonlinear system assuming that all parameters are known. This chapter

is considered an introduction for the next two chapters, which explain the robust backstepping techniques for nonlinear systems with bounded uncertainties and the adaptive backstepping techniques for nonlinear systems with unknown linear parameters.

In what follows, we will illustrate the application of backstepping procedure on a nonlinear system in the lower triangular structure.

Consider a SISO nonlinear system of the form

$$\begin{aligned}
 \dot{\xi}_1 &= f_1(\xi_1) + g_1(\xi_1)\xi_2 \\
 \dot{\xi}_2 &= f_2(\xi_1, \xi_2) + g_2(\xi_1, \xi_2)\xi_3 \\
 \dot{\xi}_3 &= f_3(\xi_1, \xi_2, \xi_3) + g_3(\xi_1, \xi_2, \xi_3)\xi_4 \\
 &\vdots \\
 \dot{\xi}_r &= f_r(\xi_1, \dots, \xi_r) + g_r(\xi_1, \dots, \xi_r)u
 \end{aligned} \tag{2.1}$$

with  $g_i(\xi_1, \dots, \xi_i) \neq 0$  for all  $1 \leq i \leq r$ ,  $f_i(0, \dots, 0) = 0$  for all  $1 \leq i \leq r$ , and all functions are smooth.  $u$  is the control input.

For simplicity, let  $r = 3$  to show the backstepping design procedure. Equation (2.1) can be written as follows

$$\begin{aligned}
\dot{\xi}_1 &= f_1(\xi_1) + g_1(\xi_1)\xi_2 \\
\dot{\xi}_2 &= f_2(\xi_1, \xi_2) + g_2(\xi_1, \xi_2)\xi_3 \\
\dot{\xi}_3 &= f_3(\xi_1, \xi_2, \xi_3) + g_3(\xi_1, \xi_2, \xi_3)u
\end{aligned} \tag{2.2}$$

We start by choosing the Lyapunov function  $V_1$  as follows

$$V_1(\xi_1) = \frac{1}{2}\xi_1^2 \tag{2.3}$$

The derivative of the Lyapunov function is

$$\dot{V}_1 = \xi_1 \dot{\xi}_1 \tag{2.4}$$

If  $\xi_2$  were the control, a controller for the first equation of (2.2) would be given by

$$\xi_2 = \alpha_1(\xi_1) = \frac{1}{g_1(\xi_1)}(-c_1\xi_1 - f_1(\xi_1)) \tag{2.5}$$

where  $\alpha_1(\xi_1)$  is an intermediate control law called virtual control. We need to make the derivative of  $V_1$  negative definite when  $\xi_2 = \alpha_1(\xi_1)$ . This is possible when the constant  $c_1 > 0$ . The derivative of  $V_1$  would be

$$\dot{V}_1 = -c_1\xi_1^2 \tag{2.6}$$

To find a function  $\alpha_2(\xi_1, \xi_2)$  for  $\xi_3$ , the virtual control in the second equation of (2.2), we introduce the new error variable  $\xi_2 - \alpha_1$ . Choose the Lyapunov function

$$V_2(\xi_1, \xi_2) = V_1 + \frac{1}{2}(\xi_2 - \alpha_1)^2 \tag{2.7}$$

Then, the derivative of the Lyapunov function is

$$\dot{V}_2 = \dot{V}_1 + (\xi_2 - \alpha_1)(f_2(\xi_1, \xi_2) + g_2(\xi_1, \xi_2)\xi_3) - \frac{\partial \alpha_1}{\partial \xi_1}(f_1(\xi_1) + g_1(\xi_1)\xi_2) \quad (2.8)$$

If  $\xi_3$  were the control, a controller for the second equation of (2.2) would be given by

$$\xi_3 = \alpha_2(\xi_1, \xi_2) = \frac{1}{g_2(\xi_1, \xi_2)}(-c_2(\xi_2 - \alpha_1) - f_2(\xi_1, \xi_2) + \frac{\partial \alpha_1}{\partial \xi_1}(f_1(\xi_1) + g_1(\xi_1)\xi_2)) \quad (2.9)$$

which results that

$$\dot{V}_2 = -c_1\xi_1^2 - c_2(\xi_2 - \alpha_1)^2 \quad (2.10)$$

is negative definite where  $c_2 > 0$ .

Introducing the new error variable  $\xi_3 - \alpha_2$ , we are finally in the position to design our actual feedback control  $u$  to stabilize the system by using the Lyapunov function

$$V_3(\xi_1, \xi_2, \xi_3) = V_2 + \frac{1}{2}(\xi_3 - \alpha_2)^2 \quad (2.11)$$

The derivative of the Lyapunov function is

$$\begin{aligned} \dot{V}_3 &= \dot{V}_2 + (\xi_3 - \alpha_2)(f_3(\xi_1, \xi_2, \xi_3) + g_3(\xi_1, \xi_2, \xi_3)u) \\ &\quad - \frac{\partial \alpha_2}{\partial \xi_1}(f_1(\xi_1) + g_1(\xi_1)\xi_2) - \frac{\partial \alpha_2}{\partial \xi_2}(f_2(\xi_1, \xi_2) + g_2(\xi_1, \xi_2)\xi_3) \end{aligned} \quad (2.12)$$

Knowing that  $g_1 \neq 0$ ,  $g_2 \neq 0$ , and  $g_3 \neq 0$ , we can choose the control  $u$  as follows

$$u = \frac{1}{g_3(\xi_1, \xi_2, \xi_3)}(-c_3(\xi_3 - \alpha_2) - f_3(\xi_1, \xi_2, \xi_3) + \frac{\partial \alpha_2}{\partial \xi_1}(f_1(\xi_1) + g_1(\xi_1)\xi_2) + \frac{\partial \alpha_2}{\partial \xi_2}(f_2(\xi_1, \xi_2) + g_2(\xi_1, \xi_2)\xi_3)) \quad (2.13)$$



to make  $\dot{V}_3$  negative definite, that is

$$\dot{V}_3 = -c_1\xi_1^2 - c_2(\xi_2 - \alpha_1)^2 - c_3(\xi_3 - \alpha_2)^2 \quad (2.14)$$

where  $c_3 > 0$ . By Lyapunov stability theorem, the controller (2.13) can stabilize the system.

## 2.2 Example

We will illustrate the design procedure explained in the previous section by the following example

$$\begin{aligned} \dot{x}_1 &= x_2 + x_1^2 \\ \dot{x}_2 &= x_1^3 + x_2^2 + x_3 \\ \dot{x}_3 &= x_1x_2 + x_2x_3 + u \end{aligned} \quad (2.15)$$

Comparing (2.15) to (2.2):

$$\begin{aligned} x_1 &= \xi_1, \quad x_2 = \xi_2, \quad x_3 = \xi_3 \\ f_1(\xi_1) &= x_1^2 \\ g_1(\xi_1) &= 1 \\ f_2(\xi_1, \xi_2) &= x_1^3 + x_2^2 \end{aligned}$$

$$\begin{aligned}
g_2(\xi_1, \xi_2) &= 1 \\
f_3(\xi_1, \xi_2, \xi_3) &= x_1 x_2 + x_2 x_3 \\
g_3(\xi_1, \xi_2, \xi_3) &= 1
\end{aligned} \tag{2.16}$$

First step is by choosing the Lyapunov function  $V_1$

$$V_1 = \frac{1}{2}x_1^2 \tag{2.17}$$

The derivative of the Lyapunov function is given by

$$\dot{V}_1 = x_1 \dot{x}_1 \tag{2.18}$$

If  $x_2$  were the control, a controller for the first equation of (2.15) would be given by

$$x_2 = \alpha_1 = -x_1^2 - c_1 x_1 \tag{2.19}$$

Applying (2.19) in  $\dot{V}_1$ , then

$$\dot{V}_1 = -c_1 x_1^2 \tag{2.20}$$

becomes negative definite where  $c_1 > 0$ .

Introducing the error variable  $\hat{x}_2 = x_2 - \alpha_1$ , the derivative of the Lyapunov function

$$V_2 = V_1 + \frac{1}{2}\hat{x}_2^2 \tag{2.21}$$

is as follows

$$\begin{aligned}\dot{V}_2 &= \dot{V}_1 + \hat{x}_2 \dot{\hat{x}}_2 \\ &= x_1(\hat{x}_2 - c_1 x_1) + \hat{x}_2(x_1^3 + (\hat{x}_2 + \alpha_1)^2 + x_3 - \dot{\alpha}_1)\end{aligned}\quad (2.22)$$

If  $x_3$  were the control, a controller for the second equation of (2.15) would be given by

$$x_3 = \alpha_2 = \dot{\alpha}_1 - (\hat{x}_2 + \alpha_1)^2 - x_1^3 - x_1 - c_2 \hat{x}_2 \quad (2.23)$$

which makes  $\dot{V}_2$  negative definite by choosing  $c_2 > 0$ .  $\dot{V}_2$  can be written as follows

$$\dot{V}_2 = -c_1 x_1^2 - c_2 \hat{x}_2^2 \quad (2.24)$$

The new error variable is  $\hat{x}_3 = x_3 - \alpha_2$ . The derivative of the Lyapunov function

$$V_3 = V_2 + \frac{1}{2} \hat{x}_3^2 \quad (2.25)$$

is given by

$$\begin{aligned}\dot{V}_3 &= \dot{V}_2 + \hat{x}_3 \dot{\hat{x}}_3 \\ &= x_1(\hat{x}_2 - c_1 x_1) + \hat{x}_2(x_1^3 + (\hat{x}_2 + \alpha_1)^2 + (\hat{x}_3 + \alpha_2) - \dot{\alpha}_1) \\ &\quad + \hat{x}_3(-\dot{\alpha}_2 + x_1(\hat{x}_2 + \alpha_1) + (\hat{x}_2 + \alpha_1)(\hat{x}_3 + \alpha_2) + u)\end{aligned}\quad (2.26)$$

We are finally in the position to design our feedback control  $u$  to stabilize the system.

$$u = \dot{\alpha}_2 - x_1(\hat{x}_2 + \alpha_1) - (\hat{x}_2 + \alpha_1)(\hat{x}_3 + \alpha_2) - \hat{x}_2 - c_3 \hat{x}_3 \quad (2.27)$$

where  $c_3 > 0$ .

The feedback control  $u$  is able to stabilize the system by making

$$\dot{V}_3 = -c_1 x_1^2 - c_2 \hat{x}_2^2 - c_3 \hat{x}_3^2 \quad (2.28)$$

negative definite.

The simulation results shown in figures 2.1, 2.2, 2.3, and 2.4 were realized using Matlab. These figures show the system response for nonlinear backstepping control.  $u$  is the control effort. The control parameters are chosen as follows  $c_1 = 10$ ,  $c_2 = 1$ , and  $c_3 = 2$ .  $T = 10s$  with initial values  $x_{1_0} = 0.1$ ,  $x_{2_0} = 0.1$ , and  $x_{3_0} = 0.1$ .

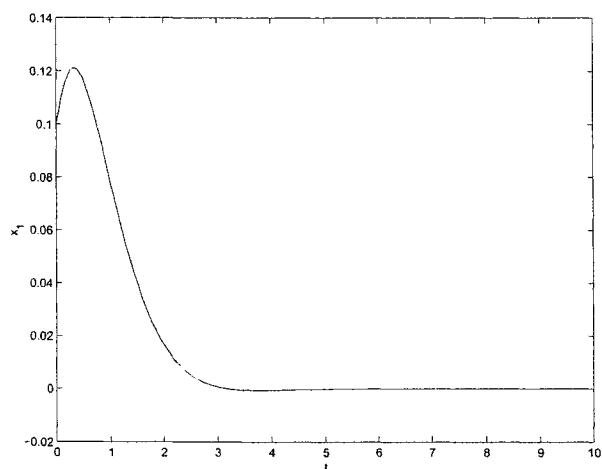


Figure 2.1:  $x_1$ -Nonlinear backstepping control

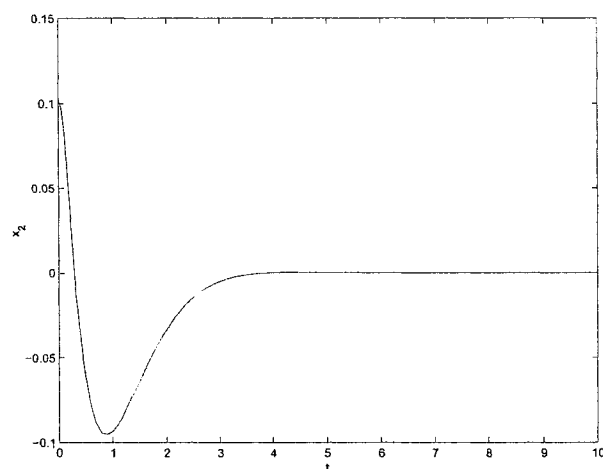


Figure 2.2:  $x_2$ -Nonlinear backstepping control

Assuming that all parameters of the system are accurately known, nonlinear backstepping controller causes the closed loop states to converge to zero.

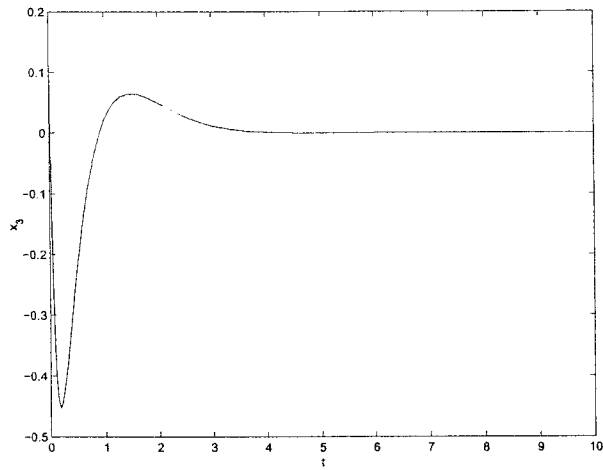


Figure 2.3:  $x_3$ -Nonlinear backstepping control

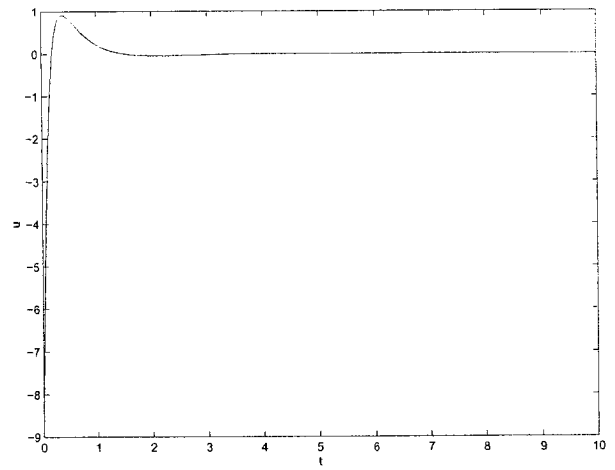


Figure 2.4:  $u$ -Nonlinear backstepping control

In the previous example, overshoots and/or undershoots can't be totally eliminated. However, they can be controlled by changing the control parameters.

# Chapter 3

## Robust Backstepping Control

### Design

#### 3.1 Theory

Every mathematical model for a real system is more or less uncertain. The uncertainties may result from disturbances or inaccurate knowledge of the system parameters (such as mass, inertia, friction, etc). The need of controllers with high performance and guaranteed robustness properties has increased during the last decade.

Model uncertainties should always be bounded; otherwise with absolutely no knowledge of the system, the problem becomes ill posed. Given any controller connected to a completely uncertain system, there is always the possibility of making the

closed loop unstable [20].

Robust controllers are introduced to stabilize the system in spite of parameter uncertainties. In this chapter, we will explain the robust control design using backstepping. It is a procedure by which both a Control Lyapunov Function (clf) and a control law can be determined simultaneously. The robust backstepping technique for a third order system in the lower triangular form is developed in this chapter.

The lower triangular structure for a system with uncertainties is:

$$\begin{aligned}
\dot{x}_1 &= \phi_1(x_1)x_2 + \psi_1(x_1) + \delta_1(x) \\
\dot{x}_2 &= \phi_2(x_1, x_2)x_3 + \psi_2(x_1, x_2) + \delta_2(x) \\
\dot{x}_3 &= \phi_3(x_1, x_2, x_3)x_4 + \psi_3(x_1, x_2, x_3) + \delta_3(x) \\
&\vdots \\
\dot{x}_r &= \phi_r(x_1, \dots, x_r)u + \psi_r(x_1, \dots, x_r) + \delta_r(x)
\end{aligned} \tag{3.1}$$

where  $x_1 \in R$ ,  $x_2 \in R$ ,  $x_3 \in R \dots x_r \in R$  are state variables and  $u \in R$  is the control input.  $\delta_1(x)$ ,  $\delta_2(x)$ ,  $\delta_3(x) \dots \delta_r(x)$  are uncertain nonlinearities which are uniformly bounded for all values of  $x$ .  $\phi_i(x_1, \dots, x_i) \neq 0$  where  $1 \leq i \leq r$

**(Structural Condition)**

The uncertainty terms  $\delta_i(x)$  for  $1 \leq i \leq r$  satisfy the following structural conditions

$$|\delta_i(x)| \leq \sum_{j=1}^i k_j^i(x_1, \dots, x_i) |x_j|, \quad i = 1, \dots, r$$

where the nonnegative functions  $k_j^i$  for  $1 \leq j \leq i$  and  $1 \leq i \leq r$  are known.

For simplicity, we will explain the robust backstepping design procedure by assuming that  $r = 3$ . The lower triangular form for the third order system is as follows:

$$\begin{aligned}\dot{x}_1 &= \phi_1(x_1)x_2 + \psi_1(x_1) + \delta_1(x) \\ \dot{x}_2 &= \phi_2(x_1, x_2)x_3 + \psi_2(x_1, x_2) + \delta_2(x) \\ \dot{x}_3 &= \phi_3(x_1, x_2, x_3)u + \psi_3(x_1, x_2, x_3) + \delta_3(x)\end{aligned}\tag{3.2}$$

**Step 1:** First  $x_2$  is regarded as a control input for the first equation of (3.2). A control Lyapunov Function,  $V_1(x_1)$ , can be chosen as follows:

$$V_1(x_1) = \frac{1}{2}x_1^2\tag{3.3}$$

We start by designing the smooth function  $\alpha_1(x_1)$ , as will be shown in the example, with  $\alpha_1(0) = 0$ , so that the derivative of the Lyapunov function  $V_1(x_1)$  satisfies the following inequality

$$\dot{V}_1 \leq -b_1x_1^2\tag{3.4}$$

along the trajectories of the first equation of the system (3.2) with  $x_2 = \alpha_1(x_1)$ .

**Step 2:** Let us introduce the change of coordinate  $\hat{x}_2 = x_2 - \alpha_1(x_1)$ . Then, by taking the derivative of  $\hat{x}_2$ , we have

$$\begin{aligned}\dot{\hat{x}}_2 &= \dot{x}_2 - \frac{\partial \alpha_1}{\partial x_1} \dot{x}_1 \\ &= \phi_2(x_1, x_2)x_3 + \psi_2(x_1, x_2) + \delta_2(x)\end{aligned}$$



$$\begin{aligned}
& - \frac{\partial \alpha_1}{\partial x_1} [\phi_1(x_1)x_2 + \psi_1(x_1) + \delta_1(x)] \\
& = \hat{\phi}_2(x_1, \hat{x}_2)x_3 + \hat{\psi}_2(x_1, \hat{x}_2) + \hat{\delta}_2(x)
\end{aligned}$$

where

$$\begin{aligned}
\hat{\phi}_2(x_1, \hat{x}_2) & = \phi_2(x_1, x_2) \\
\hat{\psi}_2(x_1, \hat{x}_2) & = \psi_2(x_1, x_2) - \frac{\partial \alpha_1}{\partial x_1} [\phi_1(x_1)x_2 + \psi_1(x_1)] \\
\hat{\delta}_2(x) & = \delta_2(x) - \frac{\partial \alpha_1}{\partial x_1} \delta_1(x)
\end{aligned}$$

We can rewrite the equation of  $\dot{x}_1$  as follows

$$\dot{x}_1 = \phi_1(x_1)\alpha_1(x_1) + \psi_1(x_1) + \delta_1(x) + \hat{x}_2\phi_1(x_1) \quad (3.5)$$

From the structural condition,  $\hat{\delta}_2(x)$  satisfies

$$\begin{aligned}
|\hat{\delta}_2(x)| & \leq |\delta_2(x)| + \left| \frac{\partial \alpha_1}{\partial x_1} \right| |\delta_1(x)| \\
& \leq k_1^2 |x_1| + k_2^2 |x_2| + \left| \frac{\partial \alpha_1}{\partial x_1} \right| k_1^1 |x_1| \\
& \leq k_1^2 |x_1| + k_2^2 |\hat{x}_2| + k_2^2 |\alpha_1(x_1)| + \left| \frac{\partial \alpha_1}{\partial x_1} \right| k_1^1 |x_1|
\end{aligned}$$

Now we can design the smooth function  $\alpha_2(x_1, \hat{x}_2)$ , as will be shown in the example,

with  $\alpha_2(0, 0) = 0$ , so that the derivative of

$$V_2(x_1, \hat{x}_2) = \frac{1}{2}x_1^2 + \frac{1}{2}\hat{x}_2^2$$

satisfies the following inequality

$$\dot{V}_2 \leq -b_1x_1^2 - b_2\hat{x}_2^2$$

along the trajectories of the second equation of the system (3.2) with  $x_3 = \alpha_2(x_1, \hat{x}_2)$ .

**Step 3:** Let us introduce the change of coordinate  $\hat{x}_3 = x_3 - \alpha_2(x_1, \hat{x}_2)$ . Then, by taking the derivative of  $\hat{x}_3$ , we have

$$\begin{aligned}
\dot{\hat{x}}_3 &= \dot{x}_3 - \frac{\partial \alpha_2}{\partial x_1} \dot{x}_1 - \frac{\partial \alpha_2}{\partial \hat{x}_2} \dot{\hat{x}}_2 \\
&= \phi_3(x_1, x_2, x_3)u + \psi_3(x_1, x_2, x_3) + \delta_3(x) \\
&\quad - \frac{\partial \alpha_2}{\partial x_1} [\phi_1(x_1)x_2 + \psi_1(x_1) + \delta_1(x)] \\
&\quad - \frac{\partial \alpha_2}{\partial \hat{x}_2} [\hat{\phi}_2(x_1, \hat{x}_2)x_3 + \hat{\psi}_2(x_1, \hat{x}_2) + \hat{\delta}_2(x)] \\
&= \hat{\phi}_3(x_1, \hat{x}_2, \hat{x}_3)u + \hat{\psi}_3(x_1, \hat{x}_2, \hat{x}_3) + \hat{\delta}_3(x)
\end{aligned}$$

where

$$\begin{aligned}
\hat{\phi}_3(x_1, \hat{x}_2, \hat{x}_3) &= \phi_3(x_1, x_2, x_3) \\
\hat{\psi}_3(x_1, \hat{x}_2, \hat{x}_3) &= \psi_3(x_1, x_2, x_3) - \frac{\partial \alpha_2}{\partial x_1} [\phi_1(x_1)x_2 + \psi_1(x_1)] \\
&\quad - \frac{\partial \alpha_2}{\partial \hat{x}_2} [\hat{\phi}_2(x_1, \hat{x}_2)x_3 + \hat{\psi}_2(x_1, \hat{x}_2)] \\
\hat{\delta}_3(x) &= \delta_3(x) - \frac{\partial \alpha_2}{\partial x_1} \delta_1(x) - \frac{\partial \alpha_2}{\partial \hat{x}_2} \delta_2(x)
\end{aligned}$$

We can rewrite the equation of  $\hat{x}_2$  as follows

$$\dot{\hat{x}}_2 = \hat{\phi}_2(x_1, \hat{x}_2)\alpha_2(x_1, \hat{x}_2) + \hat{\psi}_2(x_1, \hat{x}_2) + \hat{\delta}_2(x) + \hat{\phi}_2(x_1, \hat{x}_2)\hat{x}_3 \quad (3.6)$$

The upper bound for  $\delta_3(x)$  can be estimated

$$|\hat{\delta}_3(x)| \leq |\delta_3(x)| + \left| \frac{\partial \alpha_2}{\partial x_1} \right| |\delta_1(x)| + \left| \frac{\partial \alpha_2}{\partial x_2} \right| |\delta_2(x)|$$

$$\begin{aligned}
&\leq k_1^3 |x_1| + k_2^3 |x_2| + k_3^3 |x_3| + \left| \frac{\partial \alpha_2}{\partial x_1} \right| k_1^1 |x_1| \\
&+ \left| \frac{\partial \alpha_2}{\partial x_2} \right| (k_1^2 |x_1| + k_2^2 |x_2|) \\
&\leq k_1^3 |x_1| + k_2^3 |\hat{x}_2| + k_3^3 |\alpha_1(x_1)| + k_3^3 |\hat{x}_3| + k_3^3 |\alpha_2(x_1, \hat{x}_2)| \\
&+ \left| \frac{\partial \alpha_2}{\partial x_1} \right| k_1^1 |x_1| + \left| \frac{\partial \alpha_2}{\partial x_2} \right| (k_1^2 |x_1| + k_2^2 |\hat{x}_2| + k_2^2 |\alpha_2(x_1, \hat{x}_2)|)
\end{aligned}$$

We are finally in the position to design our actual feedback control  $u$  to stabilize the system with respect to

$$V_3(x_1, \hat{x}_2, \hat{x}_3) = \frac{1}{2}x_1^2 + \frac{1}{2}\hat{x}_2^2 + \frac{1}{2}\hat{x}_3^2$$

so that it satisfies the following inequality

$$\dot{V}_3 \leq -b_1x_1^2 - b_2\hat{x}_2^2 - b_3\hat{x}_3^2$$

where  $b_1 > 0$ ,  $b_2 > 0$ , and  $b_3 > 0$ .

The steps above have demonstrated the design procedure of the robust backstepping control. In the following example, the same procedure will be applied on a given system.

## 3.2 Example

We will illustrate the design procedure explained in the previous section by the following example

$$\dot{x}_1 = x_2 + x_1\theta_1$$

$$\begin{aligned}
\dot{x}_2 &= x_3 + x_2^2 x_1 \theta_2 \\
\dot{x}_3 &= u + x_1 x_2 \theta_3
\end{aligned} \tag{3.7}$$

Comparing (3.7) to (3.2):

$$\begin{aligned}
\phi_1(x_1) &= 1 \\
\phi_2(x_1, x_2) &= 1 \\
\phi_3(x_1, x_2, x_3) &= 1 \\
\psi_1(x_1) &= 0 \\
\psi_2(x_1, x_2) &= 0 \\
\psi_3(x_1, x_2, x_3) &= 0 \\
\delta_1(x) &= x_1 \theta_1 \\
\delta_2(x) &= x_2^2 x_1 \theta_2 \\
\delta_3(x) &= x_1 x_2 \theta_3
\end{aligned} \tag{3.8}$$

where  $\theta_1$ ,  $\theta_2$ , and  $\theta_3$  are unknown parameters that satisfy

$$|\theta_1| \leq a, \quad |\theta_2| \leq b, \quad |\theta_3| \leq c$$

for some known bounds  $a$ ,  $b$ , and  $c$ .

The function  $\delta_1$  satisfies the inequality  $|\delta_1| \leq a |x_1|$  globally. The function  $\delta_2$  satisfies the inequality  $|\delta_2| \leq b x_2^2 |x_1|$  globally. The function  $\delta_3$  satisfies the inequality  $|\delta_3| \leq c |x_1| |x_2|$  globally.

Starting with the equation

$$\dot{x}_1 = x_2 + \theta_1 x_1$$

we take  $V_1(x_1) = \frac{1}{2}x_1^2$  to obtain

$$\dot{V}_1 = x_1 x_2 + \theta_1 x_1^2$$

If  $x_2$  were the control, a controller for the first equation of (3.7) would be given by

$$x_2 = \alpha_1 = -(b_1 + a)x_1 \quad (3.9)$$

We can rewrite  $\dot{V}_1$  as follows

$$\begin{aligned} \dot{V}_1 &= -(b_1 + a)x_1^2 + \theta_1 x_1^2 \\ &\leq -(b_1 + a)x_1^2 + ax_1^2 \\ &\leq -b_1 x_1^2 \end{aligned} \quad (3.10)$$

Set the new error variable  $\hat{x}_2 = x_2 - \alpha_1 = x_2 + (b_1 + a)x_1$ . Then, we have

$$\begin{aligned} \dot{\hat{x}}_2 &= \dot{x}_2 - \frac{\partial \alpha_1}{\partial x_1} \dot{x}_1 \\ &= \dot{x}_2 + (b_1 + a)\dot{x}_1 \\ &= x_3 + x_2^2 x_1 \theta_2 + (b_1 + a)(x_2 + x_1 \theta_1) \\ &= x_3 + (\hat{x}_2 + \alpha_1)^2 x_1 \theta_2 + (b_1 + a)(\hat{x}_2 + \alpha_1 + x_1 \theta_1) \\ &= x_3 + (b_1 + a)(\hat{x}_2 + \alpha_1) + \hat{\delta}_2(x_1, \hat{x}_2) \end{aligned}$$

where  $\hat{\delta}_2(x_1, \hat{x}_2) = (\hat{x}_2 + \alpha_1)^2 x_1 \theta_2 + (b_1 + a)x_1 \theta_1$

$$|\hat{\delta}_2(x_1, \hat{x}_2)| \leq b(\hat{x}_2 + \alpha_1)^2 |x_1| + (b_1 + a)a |x_1|$$

We can choose the Lyapunov function  $V_2$

$$V_2 = V_1 + \frac{1}{2}\hat{x}_2^2 \quad (3.11)$$

The derivative of the Lyapunov function is given by

$$\begin{aligned} \dot{V}_2 &= \dot{V}_1 + \dot{\hat{x}}_2 \hat{x}_2 \\ &= x_1(\hat{x}_2 + \alpha_1 + \theta_1 x_1) + \hat{x}_2(x_3 + (b_1 + a)(\hat{x}_2 + \alpha_1) + \hat{\delta}_2) \\ &= x_1(\alpha_1 + \theta_1 x_1) + \hat{x}_2(x_1 + x_3 + (b_1 + a)(\hat{x}_2 + \alpha_1)) + \hat{x}_2 \hat{\delta}_2 \\ &\leq -b_1 x_1^2 + \hat{x}_2(x_1 + x_3 + (b_1 + a)(\hat{x}_2 + \alpha_1)) \\ &\quad + |\hat{x}_2| (b(\hat{x}_2 + \alpha_1)^2 |x_1| + (b_1 + a)a |x_1|) \\ &\leq -b_1 x_1^2 + \hat{x}_2(x_1 + x_3 + (b_1 + a)(\hat{x}_2 + \alpha_1)) \\ &\quad + |\hat{x}_2| (b(\hat{x}_2 + \alpha_1)^2 + (b_1 + a)a) |x_1| \\ &\leq -b_1 x_1^2 + \hat{x}_2(x_1 + x_3 + (b_1 + a)(\hat{x}_2 + \alpha_1)) \\ &\quad + \frac{1}{2}\hat{x}_2^2 (b(\hat{x}_2 + \alpha_1)^2 + (b_1 + a)a)^2 + \frac{1}{2}x_1^2 \end{aligned} \quad (3.12)$$

We now consider  $x_3$  as the control variable for the second equation of (3.7). We can design the smooth function  $\alpha_2$  as follows

$$x_3 = \alpha_2 = -b_2 \hat{x}_2 - x_1 - (b_1 + a)(\hat{x}_2 + \alpha_1)$$

$$- \frac{1}{2} \hat{x}_2 (b(\hat{x}_2 + \alpha_1)^2 + (b_1 + a)a)^2 \quad (3.13)$$

Applying (3.13) in (3.12), we can rewrite  $\dot{V}_2$  as follows

$$\dot{V}_2 \leq (-b_1 + \frac{1}{2})x_1^2 - b_2 \hat{x}_2^2 \quad (3.14)$$

Set the new error variable  $\hat{x}_3 = x_3 - \alpha_2$ . Then, we have

$$\dot{\hat{x}}_3 = \dot{x}_3 - \dot{\alpha}_2$$

$\dot{\alpha}_1$  can be written as follows

$$\dot{\alpha}_1 = -(b_1 + a)\dot{x}_1$$

Replacing  $\alpha_1$  by its equivalence from equation (3.9),  $\dot{\hat{x}}_2$  can be written as follows

$$\dot{\hat{x}}_2 = -(b_1 + a)^2 x_1 + (b_1 + a)\dot{x}_2 + \dot{x}_3 + (\hat{x}_2 - (b_1 + a)x_1)^2 x_1 \theta_2 + (b_1 + a)x_1 \theta_1 \quad (3.15)$$

$\dot{\alpha}_2$  can be written as follows

$$\begin{aligned} \dot{\alpha}_2 &= \frac{\partial \alpha_2}{\partial x_1} \dot{x}_1 + \frac{\partial \alpha_2}{\partial x_2} \dot{x}_2 \\ &= -b_2 \dot{\hat{x}}_2 - \dot{x}_1 - (b_1 + a)\dot{\hat{x}}_2 - (b_1 + a)\dot{\alpha}_1 \\ &\quad - \hat{x}_2 (b(\hat{x}_2 + \alpha_1)^2 + (b_1 + a)a)(2b(\hat{x}_2 + \alpha_1)(\dot{\hat{x}}_2 + \dot{\alpha}_1)) \\ &\quad - \frac{1}{2} \dot{\hat{x}}_2 (b(\hat{x}_2 + \alpha_1)^2 + (b_1 + a)a)^2 \\ &= -b_2 \dot{\hat{x}}_2 - \dot{x}_1 - (b_1 + a)\dot{\hat{x}}_2 + (b_1 + a)^2 \dot{x}_1 \\ &\quad - \hat{x}_2 (b(\hat{x}_2 - (b_1 + a)x_1)^2 + (b_1 + a)a)(2b(\hat{x}_2 - (b_1 + a)x_1)(\dot{\hat{x}}_2 - (b_1 + a)\dot{x}_1)) \end{aligned}$$

$$\begin{aligned}
& - \frac{1}{2} \dot{\hat{x}}_2 (b(\hat{x}_2 - (b_1 + a)x_1)^2 + (b_1 + a)a)^2 \\
& = \dot{\hat{x}}_2 (-b_1 - a - b_2) - \dot{x}_1 ((b_1 + a)^2 - 1) \\
& - \hat{x}_2 (b(\hat{x}_2 - (b_1 + a)x_1)^2 + (b_1 + a)a) (2b(\hat{x}_2 - (b_1 + a)x_1)(\dot{\hat{x}}_2 - (b_1 + a)\dot{x}_1)) \\
& - \frac{1}{2} \dot{\hat{x}}_2 (b(\hat{x}_2 - (b_1 + a)x_1)^2 + (b_1 + a)a)^2 \tag{3.16}
\end{aligned}$$

From equation (3.16), we can rewrite  $\dot{\hat{x}}_3$  as follows

$$\begin{aligned}
\dot{\hat{x}}_3 & = \dot{x}_3 + b_2 \dot{\hat{x}}_2 + \dot{x}_1 + (b_1 + a) \dot{\hat{x}}_2 - (b_1 + a)^2 \dot{x}_1 \\
& + \hat{x}_2 (b(\hat{x}_2 - (b_1 + a)x_1)^2 + (b_1 + a)a) (2b(\hat{x}_2 - (b_1 + a)x_1)(\dot{\hat{x}}_2 - (b_1 + a)\dot{x}_1)) \\
& + \frac{1}{2} \dot{\hat{x}}_2 (b(\hat{x}_2 - (b_1 + a)x_1)^2 + (b_1 + a)a)^2
\end{aligned}$$

and from equation (3.15),  $\dot{\hat{x}}_2$  can be written as follows

$$\dot{\hat{x}}_2 = \dot{x}_3 + (\hat{x}_2 + \alpha_1)^2 x_1 \theta_2 + (b_1 + a)(\hat{x}_2 + \alpha_1 + x_1 \theta_1) \tag{3.17}$$

To simplify the equation, the following variables are introduced

$$\begin{aligned}
m & = (\hat{x}_2 - (b_1 + a)x_1) \\
k & = bm^2 + (b_1 + a)a \\
l & = b_1 + a
\end{aligned}$$

We can rewrite  $\dot{\hat{x}}_2$  as follows

$$\dot{\hat{x}}_2 = \dot{\hat{x}}_3 + \alpha_2 + m^2 x_1 \theta_2 + l(\hat{x}_2 + \alpha_1 + x_1 \theta_1) \tag{3.18}$$



We can rewrite  $\dot{\hat{x}}_3$  as follows

$$\begin{aligned}
\dot{\hat{x}}_3 &= u + x_1 m \theta_3 - (\hat{x}_3 - b_2 \hat{x}_2 - x_1 - \frac{1}{2} \hat{x}_2 k^2 + m^2 x_1 \theta_2 + l x_1 \theta_1) \\
&\quad (-b_1 - a - b_2) + (m + x_1 \theta_1)(l^2 - 1) + 2 \hat{x}_2 k b m (\hat{x}_3 - b_2 \hat{x}_2) \\
&\quad - x_1 - \frac{1}{2} \hat{x}_2 k^2 + m^2 x_1 \theta_2 + l x_1 \theta_1 - l(m + x_1 \theta_1) \\
&\quad + \frac{1}{2} k^2 (\hat{x}_3 - b_2 \hat{x}_2 - x_1 - \frac{1}{2} \hat{x}_2 k^2 + m^2 x_1 \theta_2 + l x_1 \theta_1) \\
&= u - (\hat{x}_3 - b_2 \hat{x}_2 - x_1 - \frac{1}{2} \hat{x}_2 k^2) (-b_1 - a - b_2) \\
&\quad + m(l^2 - 1) + 2 \hat{x}_2 k b m (\hat{x}_3 - b_2 \hat{x}_2 - x_1 - \frac{1}{2} \hat{x}_2 k^2 - l m) \\
&\quad + \frac{1}{2} k^2 (\hat{x}_3 - b_2 \hat{x}_2 - x_1 - \frac{1}{2} \hat{x}_2 k^2) + \hat{\delta}_3 \tag{3.19}
\end{aligned}$$

where

$$\hat{\delta}_3 = (m \theta_3 - (-b_1 - a - b_2)(m^2 \theta_2 + l \theta_1) + (l^2 - 1) \theta_1 + 2 \hat{x}_2 k b m^3 \theta_2 + \frac{1}{2} k^2 (m^2 \theta_2 + l \theta_1)) x_1 \tag{3.20}$$

We can choose the Lyapunov function  $V_3$

$$V_3 = V_2 + \frac{1}{2} \hat{x}_3^2 \tag{3.21}$$

The derivative of the Lyapunov function is given by

$$\begin{aligned}
\dot{V}_3 &= \dot{V}_2 + \dot{\hat{x}}_3 \hat{x}_3 \\
&\leq -(b_1 - \frac{1}{2}) x_1^2 - b_2 \hat{x}_2^2 + \hat{x}_3 (\hat{x}_2 + \dot{\hat{x}}_3) \tag{3.22}
\end{aligned}$$

The uncertain term in  $\dot{V}_3$  can be written as follows

$$\begin{aligned}
\hat{x}_3 \hat{\delta}_3 &= \hat{x}_3(m\theta_3 - (-b_1 - a - b_2)(m^2\theta_2 + l\theta_1) + (l^2 - 1)\theta_1 + 2\hat{x}_2 k b m^3 \theta_2 \\
&+ \frac{1}{2}k^2(m^2\theta_2 + l\theta_1))x_1 \\
&\leq c |x_1| |m| |\hat{x}_3| + b(b_1 + a + b_2)m^2 |\hat{x}_3| |x_1| \\
&+ (b_1 + a + b_2)la |\hat{x}_3| |x_1| + (l^2 - 1)a |\hat{x}_3| |x_1| \\
&+ 2kb^2m^2 |\hat{x}_2| |m| |\hat{x}_3| |x_1| + \frac{1}{2}k^2m^2b |\hat{x}_3| |x_1| \\
&+ \frac{1}{2}k^2la |\hat{x}_3| |x_1| \\
&\leq \frac{1}{8}x_1^2 + 2c^2m^2\hat{x}_3^2 + \frac{1}{8}x_1^2 + 2b^2(b_1 + a + b_2)^2m^4\hat{x}_3^2 \\
&+ \frac{1}{8}x_1^2 + 2((b_1 + a + b_2)la + (l^2 - 1)a)^2\hat{x}_3^2 \\
&+ \frac{1}{2}\hat{x}_2^2 + 2k^2b^4m^4m^2\hat{x}_3^2x_1^2 + \frac{1}{8}x_1^2 + \frac{1}{2}k^4m^4b^2\hat{x}_3^2 \\
&+ \frac{1}{8}x_1^2 + \frac{1}{2}k^4l^2a^2\hat{x}_3^2 \tag{3.23}
\end{aligned}$$

From equations (3.22), (3.23), and (3.19), we are in the position to design our actual feedback control  $u$  to stabilize the system.

$$\begin{aligned}
u &= -b_3\hat{x}_3 - \hat{x}_2 + (\hat{x}_3 - b_2\hat{x}_2 - x_1 - \frac{1}{2}\hat{x}_2k^2)(-b_1 - a - b_2) - m(l^2 - 1) \\
&- 2\hat{x}_2 k b m(\hat{x}_3 - b_2\hat{x}_2 - x_1 - \frac{1}{2}\hat{x}_2k^2 - lm) - \frac{1}{2}k^2(\hat{x}_3 - b_2\hat{x}_2 - x_1 - \frac{1}{2}\hat{x}_2k^2) \\
&- 2c^2m^2\hat{x}_3 - 2b^2(b_1 + a + b_2)^2m^4\hat{x}_3 - 2((b_1 + a + b_2)la + (l^2 - 1)a)^2\hat{x}_3 \\
&- 2k^2b^4m^4m^2\hat{x}_3x_1^2 - \frac{1}{2}k^4m^4b^2\hat{x}_3 - \frac{1}{2}k^4l^2a^2\hat{x}_3 \tag{3.24}
\end{aligned}$$

The derivative of the Lyapunov function  $V_3$  is given by

$$\dot{V}_3 \leq -(b_1 - \frac{9}{8})x_1^2 - (b_2 - \frac{1}{2})\hat{x}_2^2 - b_3\hat{x}_3^2 \quad (3.25)$$

which implies that the controller given by (3.24) will stabilize the system and as will be shown in the following figures.

Figures 3.1 - 3.16 show the simulation results, which were carried out on Matlab. The control parameters are as follows  $b_1 = 1.9$ ,  $b_2 = 0.6$ , and  $b_3 = 1$ .  $T = 10s$  with initial values  $x_{10} = 0.1$ ,  $x_{20} = 0.1$ , and  $x_{30} = 0$ . The upper bounds are chosen as follows  $a = 2$ ,  $b = 3$ , and  $c = 4$ .

Simulations were performed using different values of  $\theta_1$ ,  $\theta_2$  and  $\theta_3$  as follows:

First set:  $\theta_1 = 1.5$ ,  $\theta_2 = 2$ ,  $\theta_3 = 3$ . Results are shown in figures 3.1, 3.2, 3.3, and 3.4.

Second set:  $\theta_1 = 0$ ,  $\theta_2 = 0$ ,  $\theta_3 = 0$ . Results are shown in figures 3.5, 3.6, 3.7, and 3.8.

Third set:  $\theta_1 = -1$ ,  $\theta_2 = -1$ ,  $\theta_3 = -1$ . Results are shown in figures 3.9, 3.10, 3.11, and 3.12.

Fourth set:  $\theta_1 = 1$ ,  $\theta_2 = 1$ ,  $\theta_3 = 1$ . Results are shown in figures 3.13, 3.14, 3.15, and 3.16.

The fourth set will be compared with the results of the adaptive backstepping control, as will be shown in the next chapter, where the value of  $\theta$  is chosen equal to 1.

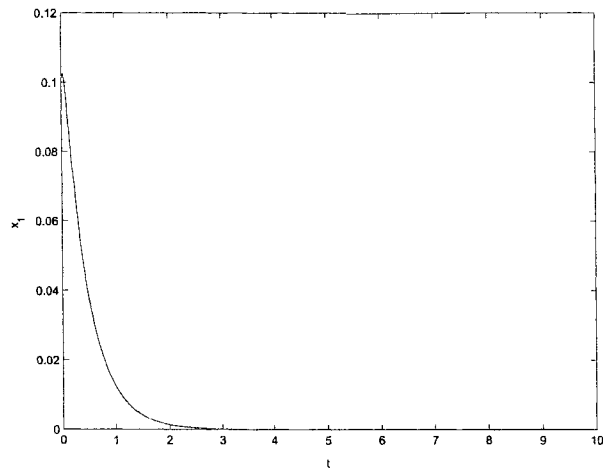


Figure 3.1:  $x_1$ -Nonlinear robust backstepping control -  $\theta_1 = 1.5, \theta_2 = 2, \theta_3 = 3$

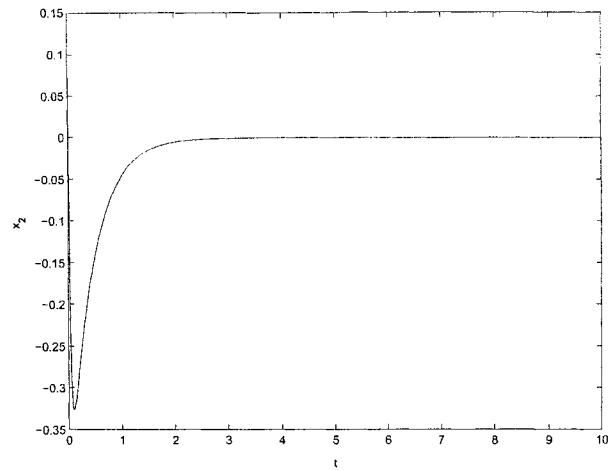


Figure 3.2:  $x_2$ -Nonlinear robust backstepping control -  $\theta_1 = 1.5, \theta_2 = 2, \theta_3 = 3$

Robust backstepping control makes the closed loop states to converge to zero in the presence of bounded uncertainties. However, the control effort is very high. The simulation results are quite similar for the four cases, which prove that the robust controller is able to stabilize the system even if we change the values of  $\theta_1$ ,  $\theta_2$  and  $\theta_3$  as long as their absolute values are less than the upper bounds.

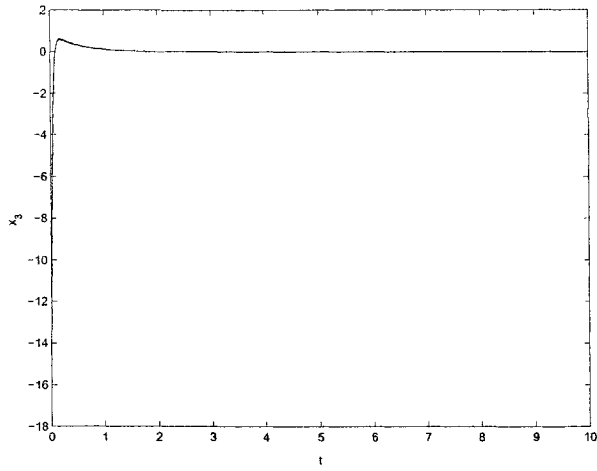


Figure 3.3:  $x_3$ -Nonlinear robust back-stepping control -  $\theta_1 = 1.5, \theta_2 = 2, \theta_3 = 3$

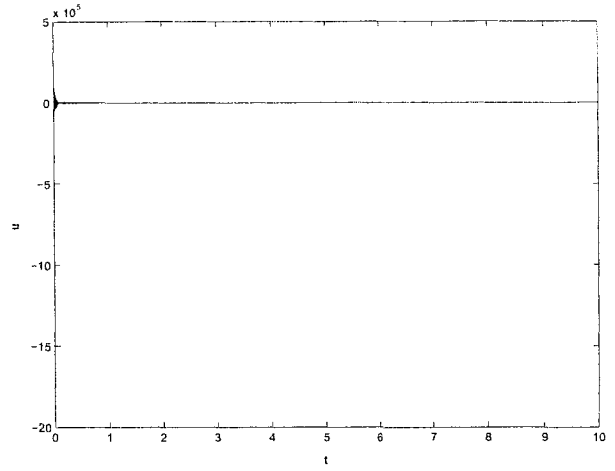


Figure 3.4:  $u$ -Nonlinear robust back-stepping control -  $\theta_1 = 1.5, \theta_2 = 2, \theta_3 = 3$

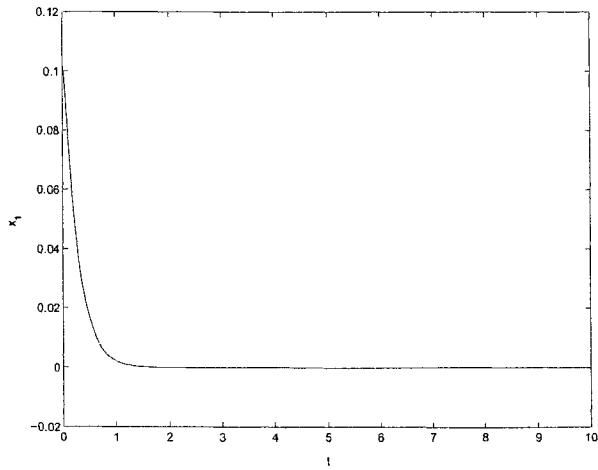


Figure 3.5:  $x_1$ -Nonlinear robust back-stepping control -  $\theta_1 = 0, \theta_2 = 0, \theta_3 = 0$

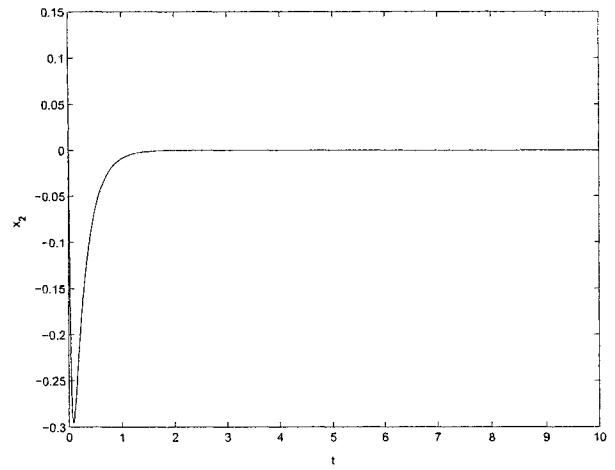


Figure 3.6:  $x_2$ -Nonlinear robust back-stepping control -  $\theta_1 = 0, \theta_2 = 0, \theta_3 = 0$

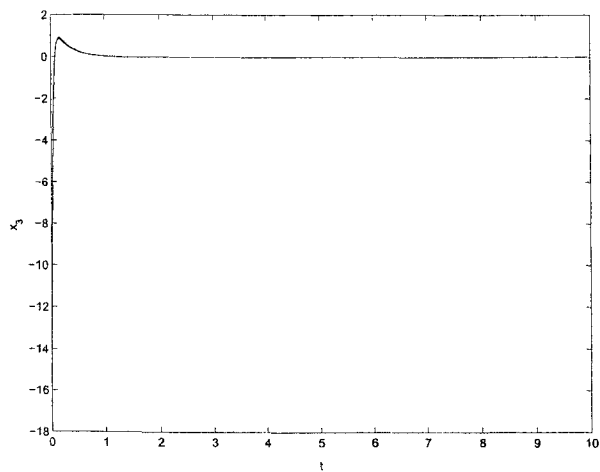


Figure 3.7:  $x_3$ -Nonlinear robust backstepping control -  $\theta_1 = 0, \theta_2 = 0, \theta_3 = 0$

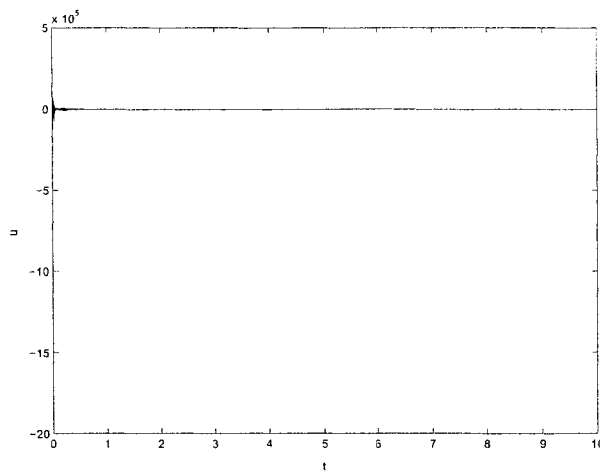


Figure 3.8:  $u$ -Nonlinear robust backstepping control -  $\theta_1 = 0, \theta_2 = 0, \theta_3 = 0$

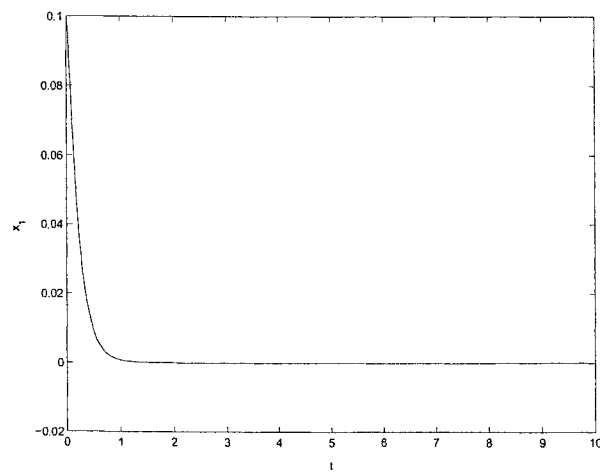


Figure 3.9:  $x_1$ -Nonlinear robust backstepping control -  $\theta_1 = -1, \theta_2 = -1, \theta_3 = -1$

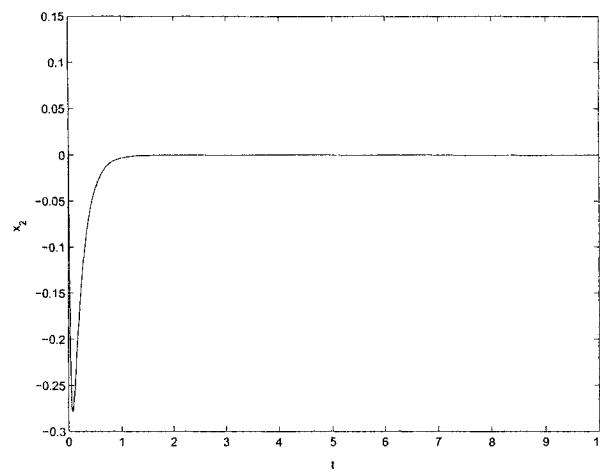


Figure 3.10:  $x_2$ -Nonlinear robust backstepping control -  $\theta_1 = -1, \theta_2 = -1, \theta_3 = -1$

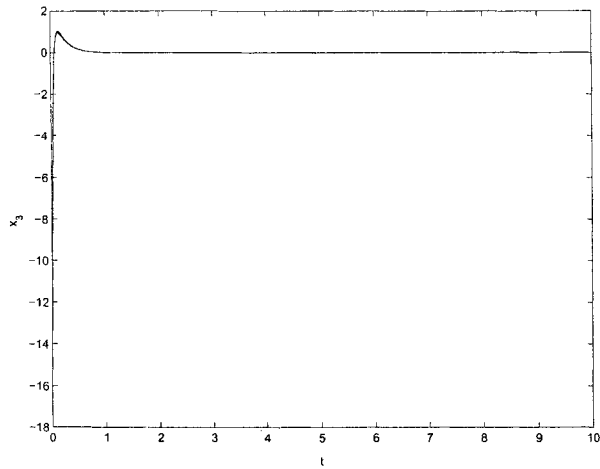


Figure 3.11:  $x_3$ -Nonlinear robust backstepping control -  $\theta_1 = -1, \theta_2 = -1, \theta_3 = -1$

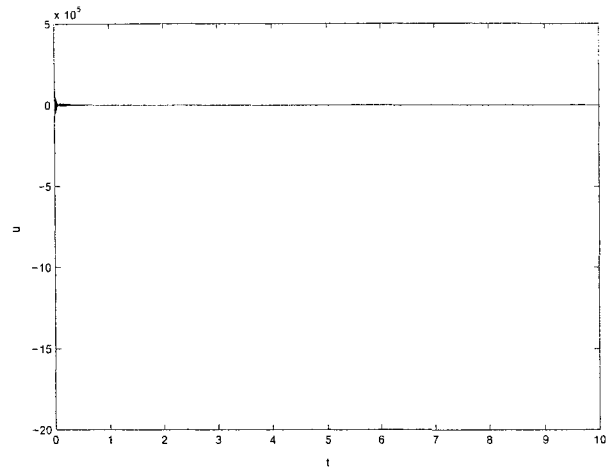


Figure 3.12:  $u$ -Nonlinear robust backstepping control -  $\theta_1 = -1, \theta_2 = -1, \theta_3 = -1$

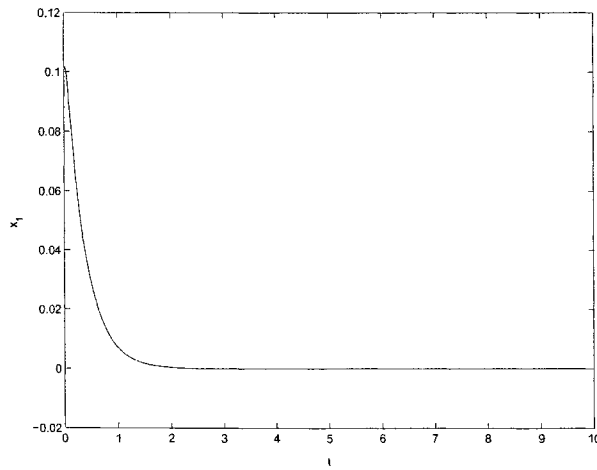


Figure 3.13:  $x_1$ -Nonlinear robust backstepping control -  $\theta_1 = 1, \theta_2 = 1, \theta_3 = 1$

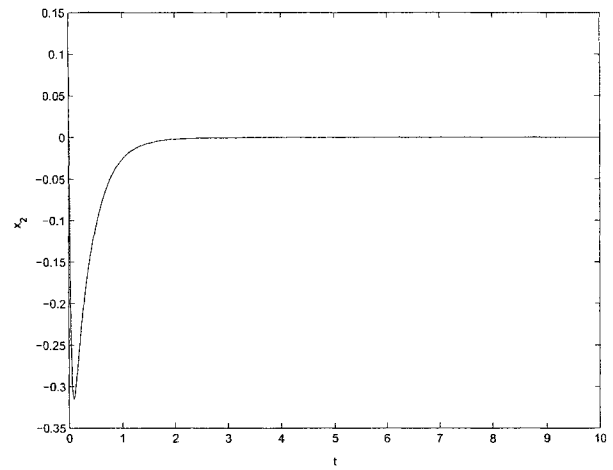


Figure 3.14:  $x_2$ -Nonlinear robust backstepping control -  $\theta_1 = 1, \theta_2 = 1, \theta_3 = 1$

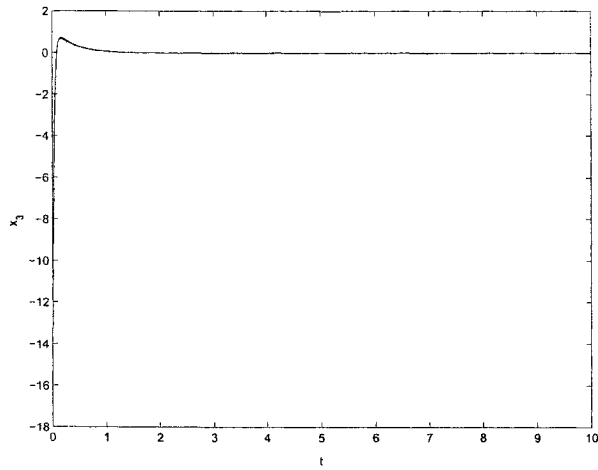


Figure 3.15:  $x_3$ -Nonlinear robust backstepping control -  $\theta_1 = 1, \theta_2 = 1, \theta_3 = 1$

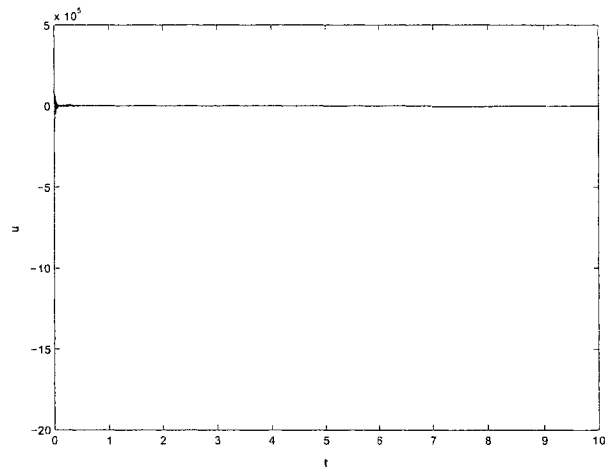


Figure 3.16:  $u$ -Nonlinear robust backstepping control -  $\theta_1 = 1, \theta_2 = 1, \theta_3 = 1$



# Chapter 4

## Adaptive Backstepping Control Design

### 4.1 Theory

Adaptive backstepping is a nonlinear control design technique that has been developed in the last decade. This technique achieves the control of nonlinear systems with parametric uncertainties. These uncertainties consist of unknown constant parameters which appear linearly in the system equations. In this chapter, we will explain the backstepping method for designing an adaptive controller to stabilize the system in the presence of these uncertainties.

In previous chapters, for the robust backstepping control design and the nonlinear

backstepping control design, we used a static feedback control law to stabilize the closed loop system. In addition to the static feedback, the adaptive controller employs nonlinear dynamic feedback.

The underlying idea in the design of this dynamic part of feedback is parameter estimation. Then, the dynamic part of the controller is designed as a parameter update law with which the static part is continuously adapted to new parameter estimates, hence its name: adaptive control law [19].

The adaptive backstepping design employs more than one estimate per unknown parameter. This over parameterization makes the control law complicated and difficult to implement. The tuning functions are introduced to reduce the dynamic order of the adaptive controller to its minimum. The number of parameter estimates is equal to the number of unknown parameters. The benefit from this improvement in the design is not only for implementation, but also because it guarantees the strongest achievable stability and convergence properties.

In the tuning functions procedure, the parameter update law is designed recursively. At each consecutive step we design a tuning function as a potential update law. The controller uses these intermediate update laws to compensate for the effect of parameter estimation transients. Only the final tuning function is used as the parameter update law [19].

The design procedure for a third order system in the lower triangular form is

developed in this chapter.

Consider the following system

$$\begin{aligned}\dot{x}_1 &= x_2 + \phi_1(x_1)\theta \\ \dot{x}_2 &= x_3 + \phi_2(x_1, x_2)\theta \\ \dot{x}_3 &= u + \phi_3(x_1, x_2, x_3)\theta\end{aligned}\tag{4.1}$$

where  $\theta$  is the unknown constant parameter.  $x_1 \in R$ ,  $x_2 \in R$ ,  $x_3 \in R$  are state variables and  $u \in R$  is the control input.  $\phi_{1_0} = 0$ ,  $\phi_{2_0} = 0$ , and  $\phi_{3_0} = 0$ .

We will start the design procedure by assuming that  $x_2$  is the virtual control of the first equation of (4.1). Recursively, we will augment the designed subsystem by one equation and design a stabilizing function  $\alpha_i$  and a tuning function  $\tau_i$ . The update law for the parameter estimate  $\hat{\theta}$  and the adaptive feedback control  $u$  are designed at the final step.

**Step 1:** If  $x_2$  were the control, an adaptive controller for the first equation of (4.1) would be given by

$$x_2 = \alpha_1(x_1, \hat{\theta}) = -c_1 z_1 - \phi_1(x_1)\hat{\theta}\tag{4.2}$$

where  $z_1 = x_1$  and  $\hat{\theta}$  is the estimation of the unknown parameter. Introducing the new error variable  $z_2 = x_2 - \alpha_1$ , the  $\dot{z}_1$ -equation becomes

$$\dot{z}_1 = \alpha_1 + z_2 + \phi_1(x_1)\theta\tag{4.3}$$

our task in this step is to stabilize (4.3) with respect to the Lyapunov function

$$V_1 = \frac{1}{2}z_1^2 + \frac{1}{2\gamma}\tilde{\theta}^2 \quad (4.4)$$

where  $\tilde{\theta} = \theta - \hat{\theta}$  is the parameter estimation error. The derivative of the Lyapunov function is

$$\begin{aligned} \dot{V}_1 &= z_1(\alpha_1 + z_2 + \phi_1\theta) - \frac{1}{\gamma}\tilde{\theta}\dot{\tilde{\theta}} \\ &= z_1(\alpha_1 + z_2 + \phi_1\hat{\theta}) - \frac{1}{\gamma}\tilde{\theta}(\dot{\hat{\theta}} - \gamma\phi_1z_1) \end{aligned} \quad (4.5)$$

We can eliminate  $\tilde{\theta}$  from  $\dot{V}_1$  with the update law  $\dot{\hat{\theta}} = \gamma\tau_1$  where

$$\tau_1(x_1) = \phi_1(x_1)z_1 \quad (4.6)$$

If  $x_2$  were our actual control, we would let  $z_2 \equiv 0$ , that is,  $x_2 \equiv \alpha_1$ . Then,  $\dot{V}_1 = -c_1z_1^2$ . Since  $x_2$  is not our control, we have  $z_2 \neq 0$ , and we do not use  $\dot{\hat{\theta}} = \gamma\tau_1$  as an update law. Instead, we retain  $\tau_1$  as our first tuning function and tolerate the presence of  $\tilde{\theta}$  in  $\dot{V}_1$ :

$$\dot{V}_1 = -c_1z_1^2 + z_1z_2 + \tilde{\theta}\left(-\frac{1}{\gamma}\dot{\tilde{\theta}} + \tau_1\right) \quad (4.7)$$

The second term  $z_1z_2$  in  $\dot{V}_1$  will be canceled at the next step.

**Step 2:** We now consider  $x_3$  as the control variable for the second equation of (4.1). Introducing the new error variable  $z_3 = x_3 - \alpha_2$ , the  $\dot{z}_2$ -equation becomes

$$\begin{aligned}
\dot{z}_2 &= z_3 + \alpha_2 - \frac{\partial \alpha_1}{\partial x_1} \dot{x}_1 - \frac{\partial \alpha_1}{\partial \hat{\theta}} \dot{\hat{\theta}} + \phi_2 \theta \\
&= z_3 + \alpha_2 - \frac{\partial \alpha_1}{\partial x_1} x_2 - \frac{\partial \alpha_1}{\partial \hat{\theta}} \dot{\hat{\theta}} - \frac{\partial \alpha_1}{\partial x_1} \phi_1 \theta + \phi_2 \theta
\end{aligned} \tag{4.8}$$

Our task in this step is to stabilize (4.3), (4.8) with respect to the Lyapunov function

$$V_2 = V_1 + \frac{1}{2} z_2^2 \tag{4.9}$$

The derivative of the Lyapunov function is

$$\begin{aligned}
\dot{V}_2 &= -c_1 z_1^2 + z_2 \left[ z_1 + z_3 + \alpha_2 - \frac{\partial \alpha_1}{\partial x_1} x_2 - \frac{\partial \alpha_1}{\partial \hat{\theta}} \dot{\hat{\theta}} - \frac{\partial \alpha_1}{\partial x_1} \phi_1 \theta + \phi_2 \theta \right] + \tilde{\theta} \left( -\frac{1}{\gamma} \dot{\hat{\theta}} + \tau_1 \right) \\
&= -c_1 z_1^2 + z_2 \left[ z_1 + z_3 + \alpha_2 - \frac{\partial \alpha_1}{\partial x_1} x_2 - \frac{\partial \alpha_1}{\partial \hat{\theta}} \dot{\hat{\theta}} - \frac{\partial \alpha_1}{\partial x_1} \phi_1 \hat{\theta} + \phi_2 \hat{\theta} \right] \\
&\quad + \tilde{\theta} \left( -\frac{1}{\gamma} \dot{\hat{\theta}} + \tau_1 + z_2 \left( -\frac{\partial \alpha_1}{\partial x_1} \phi_1 + \phi_2 \right) \right)
\end{aligned} \tag{4.10}$$

We can eliminate  $\tilde{\theta}$  from  $\dot{V}_2$  with the update law  $\dot{\hat{\theta}} = \gamma \tau_2$ , where

$$\tau_2(x_1, x_2, \hat{\theta}) = \tau_1 + z_2 \left( -\frac{\partial \alpha_1}{\partial x_1} \phi_1 + \phi_2 \right) \tag{4.11}$$

If  $x_3$  were our actual control, we would achieve  $z_3 \equiv 0$ , that is,  $x_3 \equiv \alpha_2$ . Then, to make  $\dot{V}_2 = -c_1 z_1^2 - c_2 z_2^2$ , we would design  $\alpha_2$  as follows

$$\alpha_2(x_1, x_2, \hat{\theta}) = -z_1 - c_2 z_2 + \frac{\partial \alpha_1}{\partial x_1} x_2 + \frac{\partial \alpha_1}{\partial \hat{\theta}} \gamma \tau_2 + \frac{\partial \alpha_1}{\partial x_1} \phi_1 \hat{\theta} - \phi_2 \hat{\theta} \tag{4.12}$$

Since  $x_3$  is not our control, we have  $z_3 \neq 0$ , and we do not use  $\dot{\hat{\theta}} = \gamma \tau_2$  as an update law. Instead, we retain  $\tau_2$  as our second tuning function so that the resulting  $\dot{V}_2$  is:

$$\dot{V}_2 = -c_1 z_1^2 - c_2 z_2^2 + z_2 z_3 + z_2 \frac{\partial \alpha_1}{\partial \hat{\theta}} (\gamma \tau_2 - \dot{\hat{\theta}}) + \tilde{\theta} \left( \tau_2 - \frac{1}{\gamma} \dot{\hat{\theta}} \right) \tag{4.13}$$

The third term  $z_2 z_3$  in  $\dot{V}_2$  will be canceled at the next step.

**Step 3:**The derivative of  $z_3$  is now expressed as

$$\begin{aligned} \dot{z}_3 &= \dot{x}_3 - \dot{\alpha}_2 = u + \phi_3 \theta - \frac{\partial \alpha_2}{\partial x_1} \dot{x}_1 - \frac{\partial \alpha_2}{\partial x_2} \dot{x}_2 - \frac{\partial \alpha_2}{\partial \hat{\theta}} \dot{\hat{\theta}} \\ &= u + \phi_3 \theta - \frac{\partial \alpha_2}{\partial x_1} x_2 - \frac{\partial \alpha_2}{\partial x_1} \phi_1 \theta - \frac{\partial \alpha_2}{\partial x_2} x_3 - \frac{\partial \alpha_2}{\partial x_2} \phi_2 \theta - \frac{\partial \alpha_2}{\partial \hat{\theta}} \dot{\hat{\theta}} \end{aligned} \quad (4.14)$$

We are finally in the position to design our actual update law  $\dot{\hat{\theta}} = \gamma \tau_3$  and feedback control  $u$  to stabilize the system with respect to

$$V_3 = V_2 + \frac{1}{2} z_3^2 \quad (4.15)$$

The derivative of the Lyapunov function

$$\begin{aligned} \dot{V}_3 &= -c_1 z_1^2 - c_2 z_2^2 + z_2 \frac{\partial \alpha_1}{\partial \hat{\theta}} (\gamma \tau_2 - \dot{\hat{\theta}}) \\ &+ z_3 [z_2 + u + \phi_3 \theta - \frac{\partial \alpha_2}{\partial x_1} x_2 - \frac{\partial \alpha_2}{\partial x_1} \phi_1 \theta - \frac{\partial \alpha_2}{\partial x_2} x_3 - \frac{\partial \alpha_2}{\partial x_2} \phi_2 \theta - \frac{\partial \alpha_2}{\partial \hat{\theta}} \dot{\hat{\theta}}] \\ &+ \tilde{\theta} (\tau_2 - \frac{1}{\gamma} \dot{\hat{\theta}}) \\ &= -c_1 z_1^2 - c_2 z_2^2 + z_2 \frac{\partial \alpha_1}{\partial \hat{\theta}} (\gamma \tau_2 - \dot{\hat{\theta}}) \\ &+ z_3 [z_2 + u + \phi_3 \hat{\theta} - \frac{\partial \alpha_2}{\partial x_1} x_2 - \frac{\partial \alpha_2}{\partial x_1} \phi_1 \hat{\theta} - \frac{\partial \alpha_2}{\partial x_2} x_3 - \frac{\partial \alpha_2}{\partial x_2} \phi_2 \hat{\theta} - \frac{\partial \alpha_2}{\partial \hat{\theta}} \dot{\hat{\theta}}] \\ &+ \tilde{\theta} (\tau_2 - \frac{1}{\gamma} \dot{\hat{\theta}} + z_3 (\phi_3 - \frac{\partial \alpha_2}{\partial x_1} \phi_1 - \frac{\partial \alpha_2}{\partial x_2} \phi_2)) \end{aligned} \quad (4.16)$$

we can eliminate  $\tilde{\theta}$  from  $\dot{V}_3$  with the update law  $\dot{\hat{\theta}} = \gamma \tau_3$ , where  $\tau_3$  is our tuning

function

$$\tau_3(x_1, x_2, x_3, \hat{\theta}) = \tau_2 + z_3(\phi_3 - \frac{\partial \alpha_2}{\partial x_1} \phi_1 - \frac{\partial \alpha_2}{\partial x_2} \phi_2) \quad (4.17)$$

We choose the control  $u$  as follows

$$u = -z_2 - c_3 z_3 - \phi_3 \hat{\theta} + \frac{\partial \alpha_2}{\partial x_1} x_2 + \frac{\partial \alpha_2}{\partial x_1} \phi_1 \hat{\theta} + \frac{\partial \alpha_2}{\partial x_2} x_3 + \frac{\partial \alpha_2}{\partial x_2} \phi_2 \hat{\theta} + \frac{\partial \alpha_2}{\partial \hat{\theta}} \gamma \tau_3 + v_3 \quad (4.18)$$

where  $v_3$  is a correction term yet to be chosen.  $\dot{V}_3$  becomes

$$\dot{V}_3 = -c_1 z_1^2 - c_2 z_2^2 - c_3 z_3^2 + z_2 \frac{\partial \alpha_1}{\partial \hat{\theta}} (\gamma \tau_2 - \dot{\hat{\theta}}) + z_3 v_3 \quad (4.19)$$

Then, noting that

$$\dot{\hat{\theta}} - \gamma \tau_2 = \gamma \tau_3 - \gamma \tau_2 = \gamma z_3 (\phi_3 - \frac{\partial \alpha_2}{\partial x_1} \phi_1 - \frac{\partial \alpha_2}{\partial x_2} \phi_2) \quad (4.20)$$

we can rewrite  $\dot{V}_3$  as

$$\dot{V}_3 = -c_1 z_1^2 - c_2 z_2^2 - c_3 z_3^2 + z_3 [v_3 - z_2 \frac{\partial \alpha_1}{\partial \hat{\theta}} \gamma (\phi_3 - \frac{\partial \alpha_2}{\partial x_1} \phi_1 - \frac{\partial \alpha_2}{\partial x_2} \phi_2)] \quad (4.21)$$

Now the correction term  $v_3$  is chosen as

$$v_3 = z_2 \frac{\partial \alpha_1}{\partial \hat{\theta}} \gamma (\phi_3 - \frac{\partial \alpha_2}{\partial x_1} \phi_1 - \frac{\partial \alpha_2}{\partial x_2} \phi_2) \quad (4.22)$$

Finally,  $\dot{V}_3$  can be written as

$$\dot{V}_3 = -c_1 z_1^2 - c_2 z_2^2 - c_3 z_3^2 \quad (4.23)$$

which means that, according to Lyapunov stability theorem, the controller  $u$  associated with the update law  $\dot{\hat{\theta}}$  can stabilize the system.

## 4.2 Example

We will illustrate the design procedure explained in the previous section by the following example

$$\begin{aligned}\dot{x}_1 &= x_2 + x_1\theta \\ \dot{x}_2 &= x_3 + x_2^2x_1\theta \\ \dot{x}_3 &= u + x_1x_2\theta\end{aligned}\tag{4.24}$$

Comparing (4.24) to (4.1):

$$\begin{aligned}\phi_1(x_1) &= x_1 \\ \phi_2(x_1, x_2) &= x_2^2x_1 \\ \phi_3(x_1, x_2, x_3) &= x_1x_2\end{aligned}\tag{4.25}$$

If  $x_2$  were the control, an adaptive controller for the first equation of (4.24) would be given by

$$x_2 = \alpha_1 = -c_1x_1 - x_1\hat{\theta}\tag{4.26}$$

The derivative of the Lyapunov function

$$V_1 = \frac{1}{2}x_1^2 + \frac{1}{2\gamma}\tilde{\theta}^2\tag{4.27}$$

is as follows



$$\begin{aligned}
\dot{V}_1 &= x_1(x_2 + x_1\theta) - \frac{1}{\gamma}\tilde{\theta}\dot{\hat{\theta}} \\
&= x_1(x_2 + \alpha_1 - \alpha_1 + x_1\hat{\theta} + x_1\tilde{\theta}) - \frac{1}{\gamma}\tilde{\theta}\dot{\hat{\theta}} \\
&= -c_1x_1^2 + (x_2 - \alpha_1)x_1 + (x_1^2 - \frac{1}{\gamma}\dot{\hat{\theta}})\tilde{\theta}
\end{aligned} \tag{4.28}$$

The new error variable is  $x_2 - \alpha_1$ . We can choose the Lyapunov function  $V_2$

$$V_2 = V_1 + \frac{1}{2}(x_2 - \alpha_1)^2 \tag{4.29}$$

The derivative of the Lyapunov function is given by

$$\begin{aligned}
\dot{V}_2 &= \dot{V}_1 + (x_2 - \alpha_1)(\dot{x}_2 - \dot{\alpha}_1) \\
&= -c_1x_1^2 + (x_2 - \alpha_1)x_1 + (x_1^2 - \frac{1}{\gamma}\dot{\hat{\theta}})\tilde{\theta} \\
&\quad + (x_2 - \alpha_1)(x_3 + x_2^2x_1\theta - \frac{\partial\alpha_1}{\partial x_1}(x_2 + x_1\theta) - \frac{\partial\alpha_1}{\partial\hat{\theta}}\dot{\hat{\theta}}) \\
&= -c_1x_1^2 + (x_2 - \alpha_1)[x_1 + x_3 + (x_2^2x_1 - \frac{\partial\alpha_1}{\partial x_1}x_1)\hat{\theta} \\
&\quad - \frac{\partial\alpha_1}{\partial x_1}x_2 + (x_2^2x_1 - \frac{\partial\alpha_1}{\partial x_1}x_1)\tilde{\theta}] - (x_2 - \alpha_1)\frac{\partial\alpha_1}{\partial\hat{\theta}}\dot{\hat{\theta}} + (x_1^2 - \frac{1}{\gamma}\dot{\hat{\theta}})\tilde{\theta}
\end{aligned} \tag{4.30}$$

We now consider  $x_3$  as the control variable for the second equation of (4.24). The virtual control

$$x_3 = \alpha_2 = -c_2(x_2 - \alpha_1) - x_1 - (x_2^2x_1 - \frac{\partial\alpha_1}{\partial x_1}x_1)\hat{\theta} + \frac{\partial\alpha_1}{\partial x_1}x_2 + \tau 1 \tag{4.31}$$

can be found to make  $\dot{V}_2$  as

$$\begin{aligned}
\dot{V}_2 &= -c_1 x_1^2 + (x_2 - \alpha_1)[x_1 + x_3 + \alpha_2 - \alpha_2 + (x_2^2 x_1 - \frac{\partial \alpha_1}{\partial x_1} x_1) \hat{\theta}] \\
&\quad - \frac{\partial \alpha_1}{\partial x_1} x_2] + [(x_2 - \alpha_1)(x_2^2 x_1 - \frac{\partial \alpha_1}{\partial x_1} x_1) + x_1^2] \tilde{\theta} - (x_2 - \alpha_1) \frac{\partial \alpha_1}{\partial \hat{\theta}} (\dot{\hat{\theta}} - \beta) \\
&\quad - \frac{1}{\gamma} \tilde{\theta} (\dot{\hat{\theta}} - \beta) - (x_2 - \alpha_1) \frac{\partial \alpha_1}{\partial \hat{\theta}} \beta - \frac{1}{\gamma} \tilde{\theta} \beta \\
&= -c_1 x_1^2 - c_2 (x_2 - \alpha_1)^2 + (x_2 - \alpha_1)(x_3 - \alpha_2) - (x_2 - \alpha_1) \frac{\partial \alpha_1}{\partial \hat{\theta}} (\dot{\hat{\theta}} - \beta) \\
&\quad - \frac{1}{\gamma} \tilde{\theta} (\dot{\hat{\theta}} - \beta)
\end{aligned} \tag{4.32}$$

where  $\beta = \gamma[(x_2 - \alpha_1)(x_2^2 x_1 - \frac{\partial \alpha_1}{\partial x_1} x_1) + x_1^2]$  and  $\tau_1 = \frac{\partial \alpha_1}{\partial \hat{\theta}} \beta = \frac{\partial \alpha_1}{\partial \hat{\theta}} \gamma[(x_2 - \alpha_1)(x_2^2 x_1 - \frac{\partial \alpha_1}{\partial x_1} x_1) + x_1^2]$ .

The new error variable is  $x_3 - \alpha_2$ . We can choose the Lyapunov function  $V_3$

$$V_3 = V_2 + \frac{1}{2} (x_3 - \alpha_2)^2 \tag{4.33}$$

The derivative of the Lyapunov function is given by

$$\begin{aligned}
\dot{V}_3 &= \dot{V}_2 + (x_3 - \alpha_2)(\dot{x}_3 - \dot{\alpha}_2) \\
&= \dot{V}_2 + (x_3 - \alpha_2)(\dot{x}_3 - \frac{\partial \alpha_2}{\partial x_1} \dot{x}_1 - \frac{\partial \alpha_2}{\partial x_2} \dot{x}_2 - \frac{\partial \alpha_2}{\partial \hat{\theta}} \dot{\hat{\theta}} - \frac{\partial \alpha_2}{\partial \alpha_1} \dot{\alpha}_1 - \frac{\partial \alpha_2}{\partial \tau_1} \dot{\tau}_1) \\
&= -c_1 x_1^2 - c_2 (x_2 - \alpha_1)^2 + (x_2 - \alpha_1)(x_3 - \alpha_2) - (x_2 - \alpha_1) \frac{\partial \alpha_1}{\partial \hat{\theta}} (\dot{\hat{\theta}} - \beta) \\
&\quad - \frac{1}{\gamma} \tilde{\theta} (\dot{\hat{\theta}} - \beta) + (x_3 - \alpha_2)(u + x_1 x_2 \theta - \frac{\partial \alpha_2}{\partial x_1} (x_2 + x_1 \theta) - \frac{\partial \alpha_2}{\partial x_2} (x_3 + x_2^2 x_1 \theta) \\
&\quad - \frac{\partial \alpha_2}{\partial \hat{\theta}} \dot{\hat{\theta}} - \frac{\partial \alpha_2}{\partial \alpha_1} (\frac{\partial \alpha_1}{\partial x_1} (x_2 + x_1 \theta) + \frac{\partial \alpha_1}{\partial \hat{\theta}} \dot{\hat{\theta}})) \\
&\quad - \frac{\partial \alpha_2}{\partial \tau_1} (\frac{\partial \tau_1}{\partial x_1} (x_2 + x_1 \theta) + \frac{\partial \tau_1}{\partial x_2} (x_3 + x_2^2 x_1 \theta) + \frac{\partial \tau_1}{\partial \hat{\theta}} \dot{\hat{\theta}} \\
&\quad + \frac{\partial \tau_1}{\partial \alpha_1} (\frac{\partial \alpha_1}{\partial x_1} (x_2 + x_1 \theta) + \frac{\partial \alpha_1}{\partial \hat{\theta}} \dot{\hat{\theta}}))
\end{aligned}$$

$$\begin{aligned}
&= -c_1 x_1^2 - c_2 (x_2 - \alpha_1)^2 - (x_2 - \alpha_1) \frac{\partial \alpha_1}{\partial \hat{\theta}} (\dot{\hat{\theta}} - \beta) - \frac{1}{\gamma} \tilde{\theta} (\dot{\hat{\theta}} - \beta) \\
&+ (x_3 - \alpha_2) (x_2 - \alpha_1 + u - 4 \frac{\partial \alpha_2}{\partial x_1} x_2 - 2 \frac{\partial \alpha_2}{\partial x_2} x_3) \\
&+ (x_1 x_2 - 4 \frac{\partial \alpha_2}{\partial x_1} x_1 - 2 \frac{\partial \alpha_2}{\partial x_2} x_2^2 x_1) \hat{\theta} + (x_1 x_2 - 4 \frac{\partial \alpha_2}{\partial x_1} x_1 - 2 \frac{\partial \alpha_2}{\partial x_2} x_2^2 x_1) \tilde{\theta} \\
&- 4 \frac{\partial \alpha_2}{\partial \hat{\theta}} \dot{\hat{\theta}}
\end{aligned} \tag{4.34}$$

We are finally in the position to design our actual update law  $\dot{\hat{\theta}}$ , second tuning function  $\tau_2$  and feedback control  $u$  to stabilize the system.

$$u = -c_3 (x_3 - \alpha_2) - x_2 + \alpha_1 + 4 \frac{\partial \alpha_2}{\partial x_1} x_2 + 2 \frac{\partial \alpha_2}{\partial x_2} x_3 - (x_1 x_2 - 4 \frac{\partial \alpha_2}{\partial x_1} x_1 - 2 \frac{\partial \alpha_2}{\partial x_2} x_2^2 x_1) \hat{\theta} + \tau_2 \tag{4.35}$$

$$\dot{\hat{\theta}} = \gamma ((x_3 - \alpha_2) (x_1 x_2 - 4 \frac{\partial \alpha_2}{\partial x_1} x_1 - 2 \frac{\partial \alpha_2}{\partial x_2} x_2^2 x_1) + \frac{1}{\gamma} \beta) \tag{4.36}$$

$$\tau_2 = (x_2 - \alpha_1) \frac{\partial \alpha_1}{\partial \hat{\theta}} \gamma (x_1 x_2 - 4 \frac{\partial \alpha_2}{\partial x_1} x_1 - 2 \frac{\partial \alpha_2}{\partial x_2} x_2^2 x_1) + 4 \frac{\partial \alpha_2}{\partial \hat{\theta}} \dot{\hat{\theta}} \tag{4.37}$$

which gives

$$\dot{V}_3 = -c_1 x_1^2 - c_2 (x_2 - \alpha_1)^2 - c_3 (x_3 - \alpha_2)^2 \tag{4.38}$$

The simulation results presented in figures 4.1 - 4.10, which were performed using Matlab, show the system response for adaptive backstepping control.

Figures 4.1, 4.2, 4.3, 4.4, and 4.5 represent the first set of simulations with  $\theta = 1$ . The control parameters are  $c_1 = 1.5$ ,  $c_2 = 4$ ,  $c_3 = 12$ , and  $\gamma = 0.27$ .  $T = 10s$  with initial values  $x_{10} = 0.1$ ,  $x_{20} = 0.1$ ,  $x_{30} = 0$ , and  $\hat{\theta}_0 = 0.1$ .

The second set of simulations is achieved by choosing  $\theta = 2$  and the results are shown in figures 4.6, 4.7, 4.8, 4.9, and 4.10. Control parameters are changed to  $c_1 = 6$ ,

$c_2 = 6$ ,  $c_3 = 14$ , and  $\gamma = 0.03$  to achieve stability with the same initial conditions used for the first set.

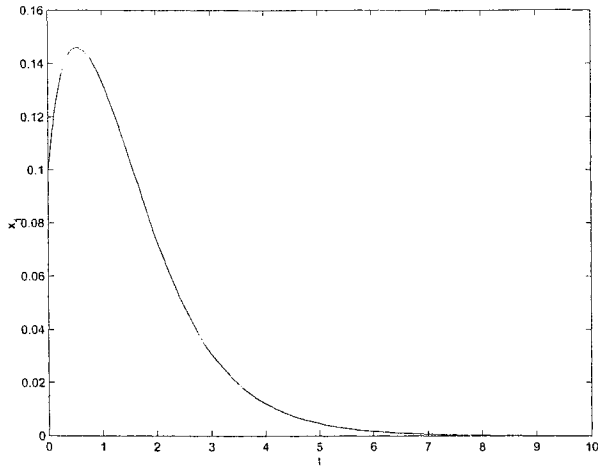


Figure 4.1:  $x_1$ -Nonlinear adaptive backstepping control -  $\theta = 1$

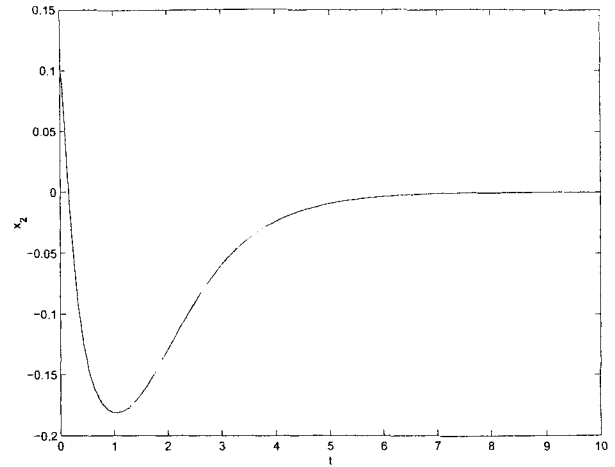


Figure 4.2:  $x_2$ -Nonlinear adaptive backstepping control -  $\theta = 1$

Comparing robust backstepping controller discussed in the last chapter with the adaptive backstepping controller, for the case where  $\theta = 1$ , we conclude that the control effort for the robust controller is much higher than the adaptive controller.

The response of the robust controller is faster. However, the percentage overshoot and/or undershoot is much higher for  $x_2$  and  $x_3$  when the robust controller is applied to the system. Moreover, the control effort for the robust controller is much higher than the adaptive controller.

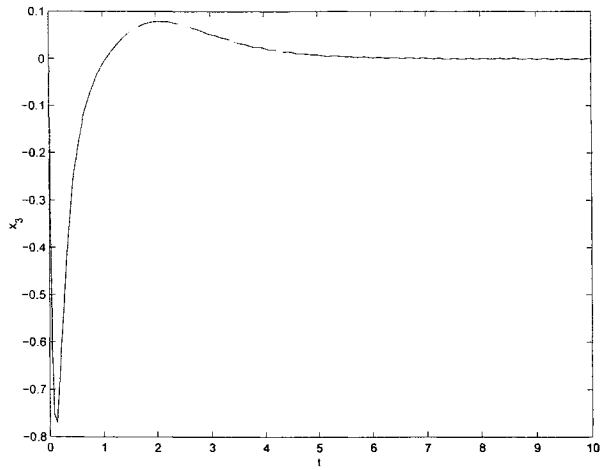


Figure 4.3:  $x_3$ -Nonlinear adaptive  
backstepping control -  $\theta = 1$

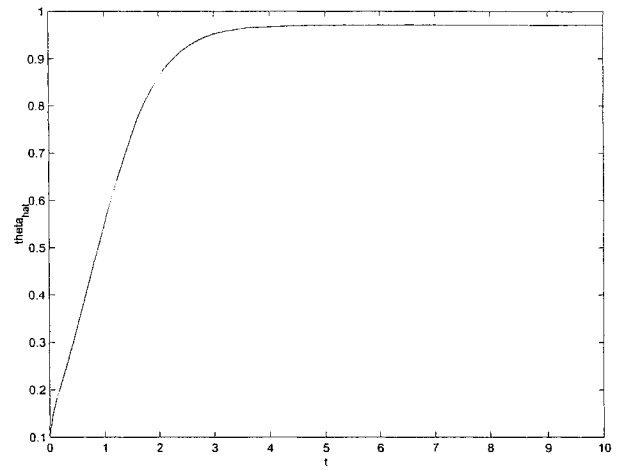


Figure 4.4:  $\hat{\theta}$ -Nonlinear adaptive  
backstepping control -  $\theta = 1$

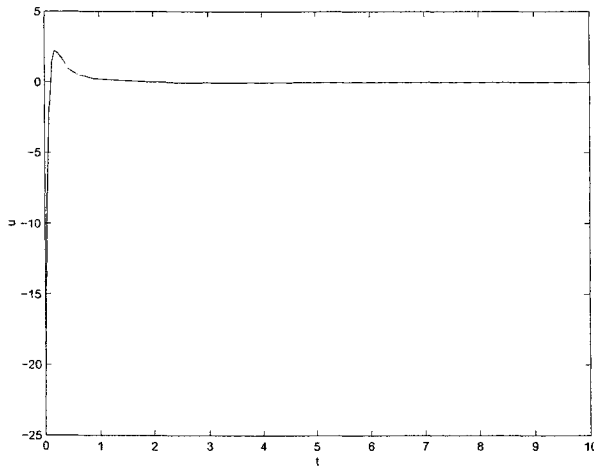


Figure 4.5:  $u$ -Nonlinear adaptive  
backstepping control -  $\theta = 1$

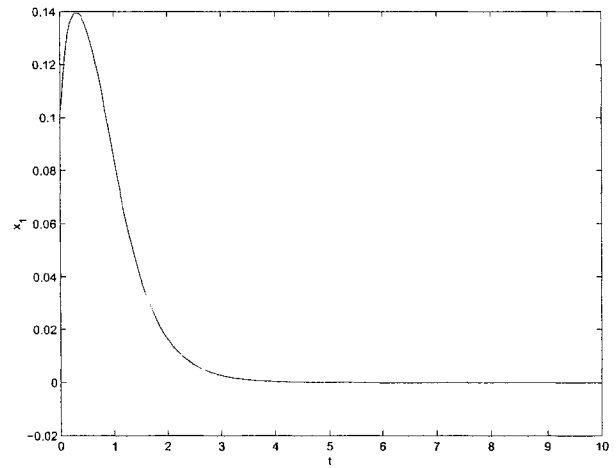


Figure 4.6:  $x_1$ -Nonlinear adaptive  
backstepping control -  $\theta = 2$

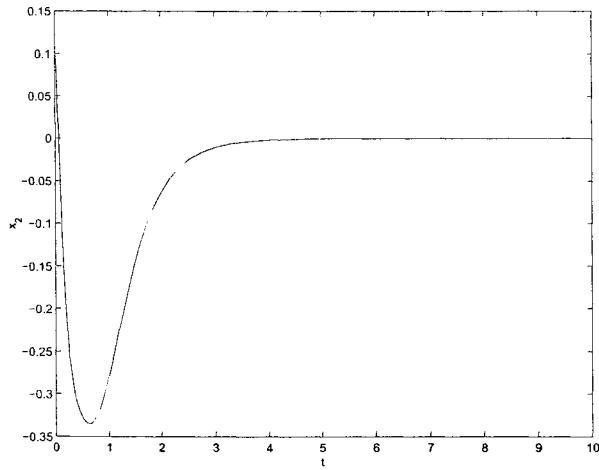


Figure 4.7:  $x_2$ -Nonlinear adaptive  
backstepping control -  $\theta = 2$

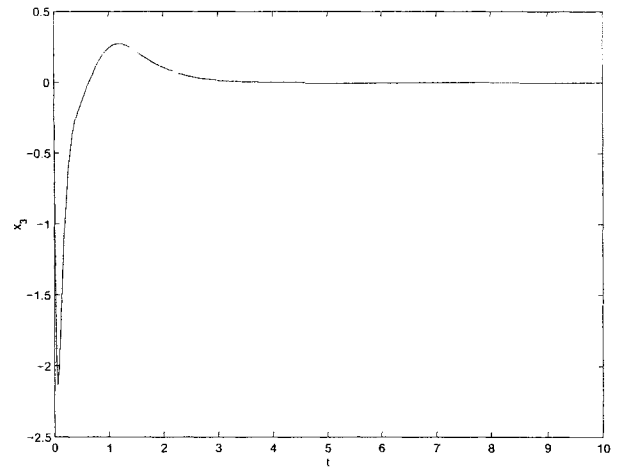


Figure 4.8:  $x_3$ -Nonlinear adaptive  
backstepping control -  $\theta = 2$

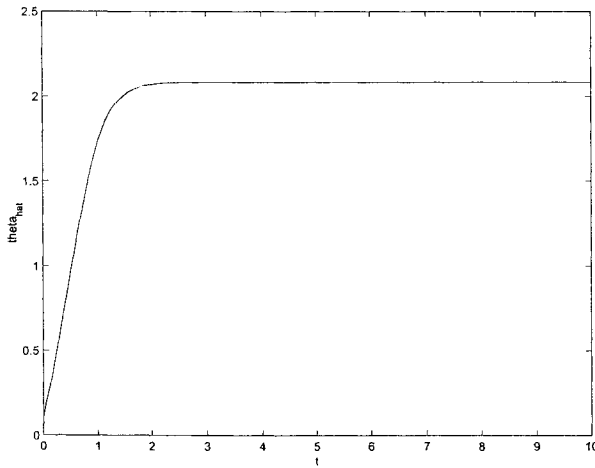


Figure 4.9:  $\hat{\theta}$ -Nonlinear adaptive  
backstepping control -  $\theta = 2$

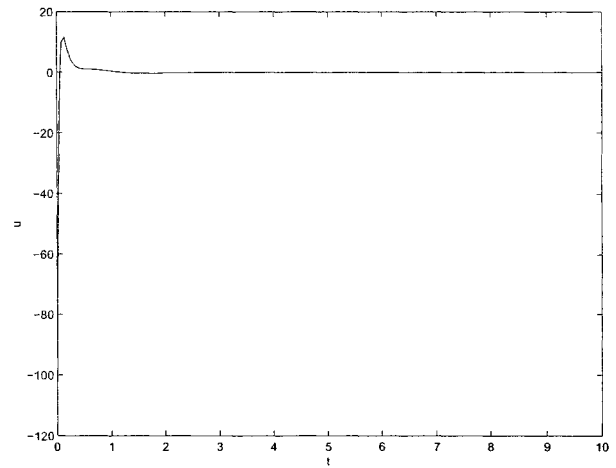


Figure 4.10:  $u$ -Nonlinear adaptive  
backstepping control -  $\theta = 2$

## Part III

# APPLICATION OF DIFFERENT CONTROLLERS ON 2-DOF PLANAR MANIPULATOR

# Chapter 5

## System and Experimental Setup

### 5.1 Robotics Background

Robotics technology is likely to become the high technology field of the 21st century. Developments in fields such as microprocessors, vision, and artificial intelligence are used to fulfill the needs of a competitive worldwide manufacturing industry. Robotics technology is finding applications in many other fields as well, such as medicine, health care, space exploration, and transportation. Today, robots are used in many ways, from lawn mowing to auto manufacturing. Scientists see practical uses for robots in performing socially undesirable, hazardous or even "impossible" tasks such as trash collection, toxic waste clean-up, desert and space exploration, and more.

Robot manipulators are composed of links connected by joints. The joints of



the manipulator may be electrically, hydraulically, or pneumatically actuated. The number of joints determines the degrees of freedom (DOF) of the manipulator. The workspace of a manipulator is the total volume swept out by the end-effector as the manipulator executes all possible motions [21].

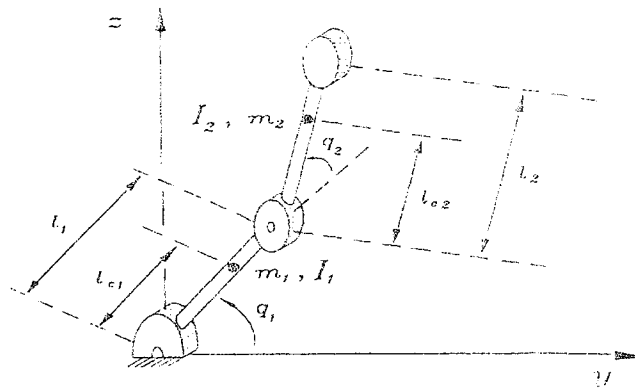


Figure 5.1: 2 DOF robot manipulator

Robots are usually equipped with internal position sensors (e.g. joint encoders) in order to measure the relative position of two neighboring links.

With increasing number of joints not only the mobility of the manipulator is enhanced, but also the mechanical and electrical problems become difficult to solve, and the development of a motion controller becomes a more complex and more expensive task.

For many simple handling tasks in robotics, 4 joints are already sufficient. For some specific welding and painting applications 5 joints are necessary, and for general-

purpose applications, a manipulator with 6 joints has to be chosen, which is the standard type of an industrial robot. A 6 joints robot offers solutions to a variety of advanced handling problems, because it provides 6 degrees of freedom in its workspace.

To apply different types of nonlinear controllers experimentally, a two-link planar manipulator system is used. The dynamics for the robot can be written as follows

$$M(q)\ddot{q} + C(q, \dot{q})\dot{q} + g(q) = \tau \quad (5.1)$$

where  $q$  is the  $2 \times 1$  vector of joint positions,  $\tau$  is the  $2 \times 1$  vector of applied torques,  $M(q)$  is the  $2 \times 2$  symmetric positive definite manipulator inertia matrix,  $C(q, \dot{q})\dot{q}$  is the  $2 \times 1$  vector of centrifugal and Coriolis torques, and  $g(q)$  is the  $2 \times 1$  vector of gravitational torques. Gravitational torques can be eliminated from our model since it's a planar (horizontal) model [17][22].

Equation (5.1) can be written as follows

$$M(q)\ddot{q} + C(q, \dot{q})\dot{q} = \tau \quad (5.2)$$

The elements of the inertia matrix  $M(q)$  are given by

$$\begin{aligned} M_{11}(q) &= m_1 l_{c1}^2 + m_2(l_1^2 + l_{c2}^2 + 2l_1 l_{c2} \cos(q_2)) + I_1 + I_2 \\ M_{12}(q) &= m_2(l_{c2}^2 + l_1 l_{c2} \cos(q_2)) + I_2 \\ M_{21}(q) &= m_2(l_{c2}^2 + l_1 l_{c2} \cos(q_2)) + I_2 \\ M_{22}(q) &= m_2 l_{c2}^2 + I_2 \end{aligned} \quad (5.3)$$

The elements of the centrifugal and Coriolis matrix  $C(q, \dot{q})$  are given by

$$\begin{aligned}C_{11}(q, \dot{q}) &= -m_2 l_1 l_{c2} \sin(q_2) \dot{q}_2 \\C_{12}(q, \dot{q}) &= -m_2 l_1 l_{c2} \sin(q_2) (\dot{q}_1 + \dot{q}_2) \\C_{21}(q, \dot{q}) &= m_2 l_1 l_{c2} \sin(q_2) \dot{q}_1 \\C_{22}(q, \dot{q}) &= 0\end{aligned}\tag{5.4}$$

The meaning of the symbols and their numerical values for the 2-DOF robot manipulator shown in figure 5.1 and used in the experiment are as follows

$l_1$  : length of link 1 = 0.74m

$l_2$  : length of link 2 = 0.475m

$m_1$  : mass of link 1 = 5.106kg

$m_2$  : mass of link 2 = 1.1317kg

$l_{c1}$  : distance to the centre of gravity of the link 1 = 0.2293m

$l_{c2}$  : distance to the centre of gravity of the link 2 = 0.171m

$I_1$  : moment of inertia of link 1 = 0.2158kg.m<sup>2</sup>

$I_2$  : moment of inertia of link 2 = 0.0137kg.m<sup>2</sup>

## 5.2 Experimental Setup

The experimental setup consists of three main parts.

### 5.2.1 Mechanical Assembly

The mechanical setup consists of two links made of aluminum connected through gear trains. The joints are actuated by DC motors, Pittman GM9434H187, via gear trains with the optical encoders providing motors position measurements. Each motor has a built-in gearbox with a transmission ratio of 1:5.9 and with a no load speed of 6151rpm. The mechanical assembly has a further gear ratio of 22:64 for the first link and 30:86 for the second link.

The voltage equation of the motor can be derived as follows

$$\begin{aligned}v_a &= R_a i_a + L \frac{\partial i_a}{\partial t} + v \\ \tau_m &= k_m i_a \\ v &= k_e \dot{q}_m\end{aligned}\tag{5.5}$$

where  $v_a$  is the armature voltage,  $R_a$  is the armature resistance,  $i_a$  is the armature current,  $L$  is the armature inductance,  $v$  is the back emf,  $\tau_m$  is the motor torque,  $k_m$  is the torque constant,  $k_e$  is the back emf constant,  $\dot{q}_m$  is the angular velocity of the motor.

The gear ratio  $G$  causes an increase in the torque seen at the load and a reduction in the speed of the load.

$$\begin{aligned}\tau &= G \tau_m \\ \dot{q} &= \frac{1}{G} \dot{q}_m\end{aligned}\tag{5.6}$$

The value of the gear ratio should reflect the gear ratio of the link and the motor gearbox transmission ratio.  $G \geq 1$

Finally, neglecting the change in the motor current, the voltage equation of each motor link is measured by the following equation

$$\begin{aligned} v_1 &= R_a \frac{1}{G_1} \frac{1}{k_m} u_1 + k_e G_1 \dot{q}_1 \\ v_2 &= R_a \frac{1}{G_2} \frac{1}{k_m} u_2 + k_e G_2 \dot{q}_2 \end{aligned} \quad (5.7)$$

where  $G_1$  is the gear ratio for link 1,  $G_2$  is the gear ratio for link 2,  $v_1$  is the armature voltage for the motor of link 1,  $v_2$  is the armature voltage for the motor of link 2, and

$$\tau = u = \begin{bmatrix} u_1 \\ u_2 \end{bmatrix}$$

$$\dot{q} = \begin{bmatrix} \dot{q}_1 \\ \dot{q}_2 \end{bmatrix}$$

The values used in the simulation and the experiments for (5.7) are as follows

$$R_a = 2.96 \text{ohms}$$

$$G_1 = 64/22 * 5.9$$

$$G_2 = 86/30 * 5.9$$

$$k_m = 0.0365 \text{N.m/A}$$

$$k_e = 0.0365 \text{V/rad/s}$$

The motor is driven by the driver circuitry explained in the following section.

### **5.2.2 Circuitry**

To better understand the controller circuit, we will explain briefly two main concepts, which are H-bridge and PWM signal.

#### **H-Bridge Module**

A microprocessor cannot drive a motor directly, since it cannot supply enough current. Instead, there must be some interface circuitry so that the motor power is supplied from another power source and only the control signals are provided by the microprocessor. This interface circuitry can be implemented by a circuit known as the H-bridge [23]. An H-bridge merely consists of 4 switches connected in topology of an H, where the motor terminals form the crossbar of the H. In an H-bridge, the switches are opened and closed in a manner so as to put a voltage of one polarity across the motor for current to flow through it in one direction or a voltage of the opposite polarity, causing current to flow through the motor in the opposite direction for reverse direction.

#### **Pulse-Width-Modulation Control**

In pulse-width-modulation (PWM) control [24] [25], the converter switches are turned on and off during a half-cycle and the output voltage is controlled by varying the width of the pulses. The gate signals are generated by comparing a triangular wave with

a dc signal. The PWM circuit requires a steadily running oscillator to operate. The main disadvantages of PWM circuits are the added complexity and the possibility of generating radio frequency interference (RFI). RFI may be minimized by locating the controller near the load, using short leads, and in some cases, using additional filtering on the power supply leads.

### **Controller Circuit Description**

The driver board is divided into two main circuits. Each circuit deals with different types of input, analog and digital. The driver board consists of 4 chips: JWD-107-1, LMD18200, TL494, and MOC5007.

The LMD18200 is made by National Semiconductor. It is an H-bridge, which can supply up to 3 amps continuously at 55 volts. The motor and the LMD18200 are in series with an electromechanical relay. The relay must be enabled by the DAQ device. This prevents unwanted motor motion.

In this circuit, the LMD18200 is configured to accept a PWM signal. This type of signal encodes both direction and speed information. A PWM signal of 50% means motor off. A PWM signal less than 50% makes the motor rotate at ever increasing speed as the PWM signal approaches 0%. A PWM signal greater than 50% makes the motor rotate at ever increasing speed in the opposite direction as the PWM signal approaches 100%.

The circuit will also accept a 0 to +5 volt analog signal. The 3-pin header to the immediate right of the relay selects whether the PWM signal comes from the DAQ or from the TL494. The DAQ - PWM line is optically isolated from the LMD18200 to prevent 12 volts from reaching DAQ 5-volt logic devices.

For a given control input, the motor rotation can be reversed by configuring the 3-pin header to the immediate left of the TL494.

### 5.2.3 Data Acquisition Module

Traditionally, measurements are done on stand-alone instruments of various types-oscilloscopes, multi meters, counters etc. However, the need to record the measurements and process the collected data for visualization has become increasingly important.

There are several ways in which the data can be exchanged between instruments and a computer. A popular way to measure signals and transfer the data into a computer is by using a data acquisition board. A typical commercial DAQ card contains analog to digital converter (ADC) and digital to analog converter (DAC) that allow input and output of analog and digital signals in addition to digital input/output channels.

The Data Acquisition (DAQ) board used for the experiment is DS1102 from dSpace. ControlDesk (dSPACE) is used to interface between Matlab/Simulink and



DS1102. DS1102 is a single board system, specifically designed for development of high-speed digital controllers and real-time simulations. The DS1102 board is based on Texas Instruments TMS320C31 third generation floating-point digital signal processor, which builds the main processing unit

# Chapter 6

## PD Controller

### 6.1 Theory

Most of the present industrial robots are controlled through local PID controllers. The PID controller has been shown in practice to be effective for set-point control of robot manipulators. The PID controller structure consists of three components, the Proportional, Integral, and Derivative part.

Proportional control is the primary alternative to on-off control. If the difference between the output signal and its desired value is large, the software should change the drive signal a lot. If the error is small, it should change it only a little. If the proportional gain is well chosen, the time the system takes to reach a new set-point will be as short as possible, with overshoot (or undershoot) and oscillation minimized.

The control signal in a P controller is given by [26]:

$$u = u_0 + k_c e, \quad (6.1)$$

where  $u_0$  is the level of the control signal when we have no control error,  $e$  is the error signal, and  $K_c$  is the proportional gain of the controller.  $K_c$  indicates the change in the control signal per unit change in the error signal.

Unfortunately, proportional control alone is not sufficient in all control applications. One or more of the requirements for response time, overshoot, and oscillation may be impossible to fulfill at any proportional gain setting. The biggest problem with proportional control alone is that you want to reach new desired outputs quickly and avoid overshoot and minimize ripple once you get there. Responding quickly suggests a high proportional gain; minimizing overshoot and oscillation suggests a small proportional gain. Achieving both at the same time may not be possible in all systems.

With derivative action, the controller output is proportional to the rate of change of the measurement or error. The controller output is calculated by the rate of change of the measurement with time. If the output is changing rapidly, overshoot or undershoot may lie ahead. In that case, we can reduce the size of the change suggested by the proportional controller.

In practice, proportional-derivative (PD) controllers work well. The net effect is a slower response time with far less overshoot and ripple than a proportional controller

alone. The derivative action may also result in difficulties if high frequency measurement noise is present. These difficulties are normally resolved using additional filtering techniques.

The control signal in a PD controller is given by [26]:

$$u = k_c(e + T_d \frac{de}{dt}) \quad (6.2)$$

where  $T_d$  is the derivative time of the controller.

With integral action, the controller output is proportional to the integration of the error over the time. Integral action eliminates offset.

The control law of the PID controller is [26]:

$$u = k_c(e + \frac{1}{T_i} \int edt + T_d \frac{de}{dt}), \quad (6.3)$$

where  $T_i$  is the integral time of the controller.

Each of the three components of the PID controller has its own distinctive function to fulfill certain control objectives. In actual applications, different permutations of the P, I and D components may be used depending mainly on the process and the control requirements.

The PD control is able to vanish position error when used for set-point control of robot having zero gravitational torques into its dynamic model. The integral term has been suggested to eliminate the offset, which appears when robot dynamics having gravitational torques is under PD control. We will study in the following section the

application of PD control on the 2-DOF planar manipulator.

## 6.2 Control Design

In this section, we will show the application of PD controller on the 2-DOF robot manipulator. The main goal is to compare the simulation and the experimental results with other nonlinear controllers applications as will be shown in the following chapters.

The dynamical equation of the robot manipulator is given by

$$M(q)\ddot{q} + C(q, \dot{q})\dot{q} + g(q) = \tau \quad (6.4)$$

The term  $g(q)$  is eliminated due to the absence of the gravitational torques as the experimental setup is horizontal. The dynamical equation of the robot manipulator is now,

$$M(q)\ddot{q} + C(q, \dot{q})\dot{q} = \tau \quad (6.5)$$

An independent joint PD-control scheme can be written in vector form as

$$\tau = -K_p\tilde{q} - K_v\dot{\tilde{q}} \quad (6.6)$$

where  $\tilde{q} = q - q_d = e$  is the error between the desired joint displacements  $q_d$  and the actual joint displacements  $q$ .  $K_p$  and  $K_v$  are diagonal matrices of (positive) proportional and derivative gains, respectively. In the absence of gravity, the PD

control law achieves asymptotic tracking of the desired joint positions. To show that the above control law achieves zero steady error, consider the Lyapunov function candidate

$$V = \frac{1}{2}\tilde{q}^T K_p \tilde{q} + \frac{1}{2}\dot{q}^T M(q)\dot{q} \quad (6.7)$$

V is a positive definite function. The time derivative of V is given by

$$\begin{aligned} \dot{V} &= \frac{1}{2}\dot{\tilde{q}}^T K_p \dot{q} + \frac{1}{2}\dot{q}^T K_p \tilde{q} + \frac{1}{2}\ddot{q}^T M\dot{q} + \frac{1}{2}\dot{q}^T M\ddot{q} + \frac{1}{2}\dot{q}^T \dot{M}\dot{q} \\ &= \dot{q}^T K_p \tilde{q} + \dot{q}^T M\ddot{q} + \frac{1}{2}\dot{q}^T \dot{M}\dot{q} \\ &= \dot{q}^T K_p \tilde{q} + \dot{q}^T (\tau - C\dot{q}) + \frac{1}{2}\dot{q}^T \dot{M}\dot{q} \\ &= \dot{q}^T K_p \tilde{q} + \dot{q}^T \tau + \frac{1}{2}\dot{q}^T (\dot{M} - 2C)\dot{q} \\ &= \dot{q}^T (\tau + K_p \tilde{q}) \end{aligned} \quad (6.8)$$

where the last equality results from the fact that, for any robot manipulator, the matrix  $(\dot{M}(q) - 2C(q, \dot{q}))$  is skew symmetric. Substituting the PD control law for  $\tau$  into the above yields

$$\begin{aligned} \dot{V} &= \dot{q}^T (-K_p \tilde{q} - K_v \dot{\tilde{q}} + K_p \tilde{q}) \\ &= -\dot{q}^T K_v \dot{q} \end{aligned} \quad (6.9)$$

which is negative definite.

It is possible that the manipulator can reach a position where  $\dot{q} = 0$  but  $q \neq q_d$ . To show that this cannot happen we can use LaSalle's theorem. Suppose  $\dot{V} \equiv 0$ . Then (6.9) implies that  $\dot{q} \equiv 0$  and hence  $\ddot{q} \equiv 0$  [21]. From (6.6) and (6.5)

$$M(q)\ddot{q} + C(q, \dot{q})\dot{q} = -K_p\tilde{q} - K_v\dot{\tilde{q}} \quad (6.10)$$

then

$$0 = -K_p\tilde{q} \quad (6.11)$$

which implies that  $\tilde{q} = 0$ . LaSalle's Theorem then implies that the system is asymptotically stable. This means that  $q \rightarrow q_d$  when  $t \rightarrow \infty$  for any initial condition  $q(0)$ .

Figures 6.1, 6.2, 6.3, 6.4, 6.5, 6.6, 6.7, and 6.8 are the simulation results when applying PD controller on the 2-DOF robot manipulator using Matlab with control parameters

$$K_p = \begin{bmatrix} 2 & 0 \\ 0 & 1.5 \end{bmatrix} \quad K_v = \begin{bmatrix} 4 & 0 \\ 0 & 2 \end{bmatrix}$$

Time ( $t$ ) is in sec and motors voltages for link 1  $v_1$  and link 2  $v_2$  are in Volts.

$$q_d = \begin{bmatrix} q_{d_1} \\ q_{d_2} \end{bmatrix} = \begin{bmatrix} \pi/2 \\ \pi/2 \end{bmatrix}$$

Initial values are  $q_{1_0} = 0$ ,  $q_{2_0} = 0$ ,  $\dot{q}_{1_0} = 0$ , and  $\dot{q}_{2_0} = 0$ . For clearness, the figures for  $q_1$ ,  $q_2$ ,  $\tilde{q}_1$ , and  $\tilde{q}_2$  are shown in deg.  $\dot{q}_1$  and  $\dot{q}_2$  are in deg/sec.

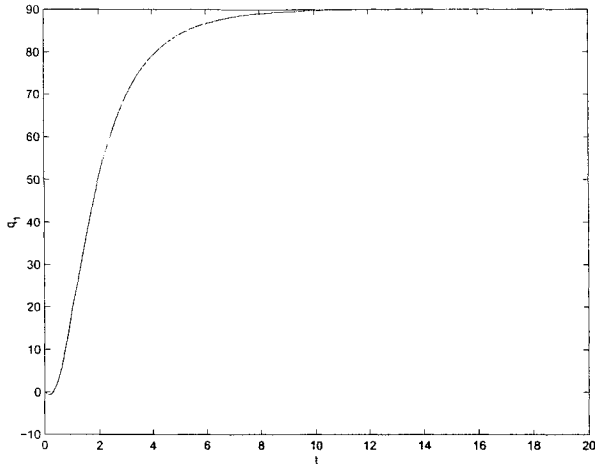


Figure 6.1:  $q_1$  - Simulation result with PD control

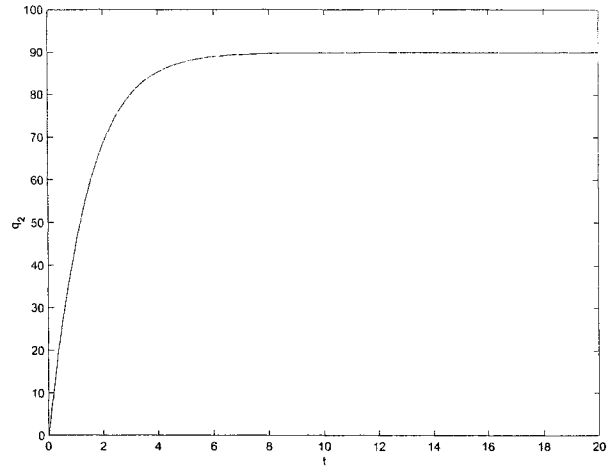


Figure 6.2:  $q_2$  - Simulation result with PD control

### 6.3 Experimental Results

The experimental results on the 2-DOF planar manipulator shown in figures 6.9, 6.10, 6.11, 6.12, 6.13, 6.14, 6.15, and 6.16 were realized using Simulink/dSpace environment with a sampling period of 0.05sec and with the same units, desired angles, and initial values used in the simulation part. To achieve the best results, the control parameters are chosen as follows

$$K_p = \begin{bmatrix} 2 & 0 \\ 0 & 1.5 \end{bmatrix} \quad K_v = \begin{bmatrix} 0.5 & 0 \\ 0 & 0.3 \end{bmatrix}$$

The PD controller is able to stabilize the system, which means that  $q \rightarrow q_d$  when  $t \rightarrow \infty$ . PD control was simulated and experimentally implemented on the robot to be compared with other nonlinear controllers as will be further discussed in the



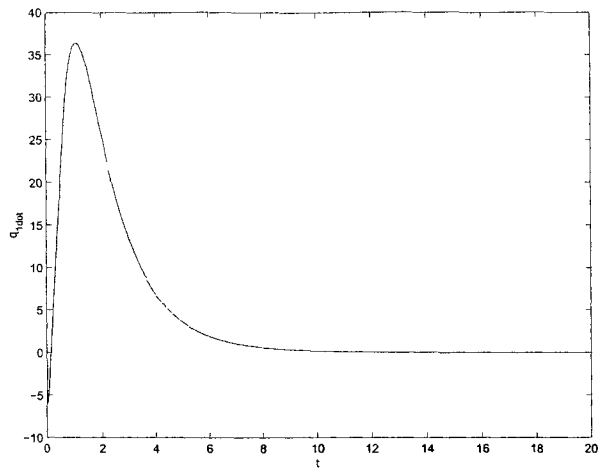


Figure 6.3:  $q_1$  - Simulation result with PD control conclusion.

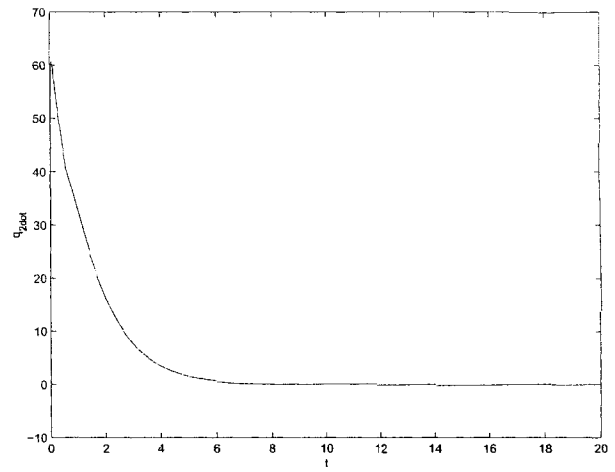


Figure 6.4:  $q_2$  - Simulation result with PD control

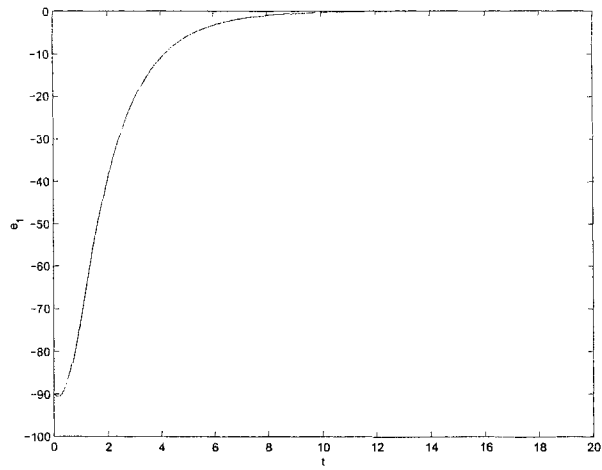


Figure 6.5:  $e_1$  - Simulation result with PD control

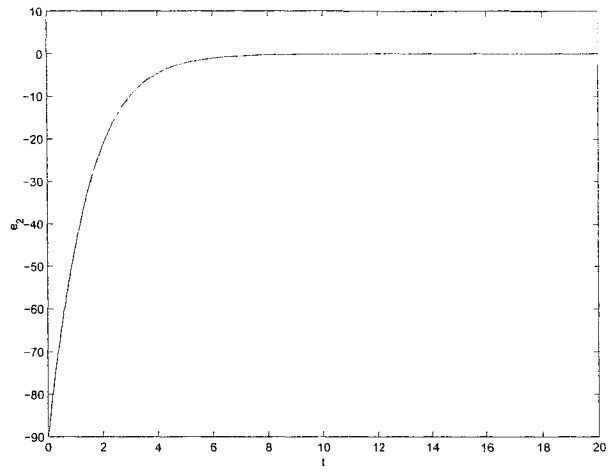


Figure 6.6:  $e_2$  - Simulation result with PD control

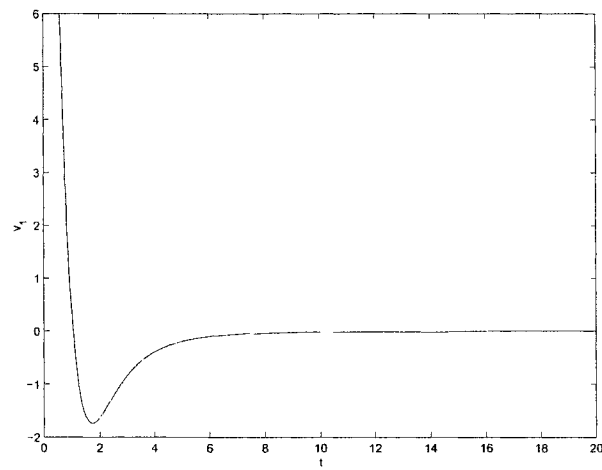


Figure 6.7:  $v_1$  - Simulation result with PD control

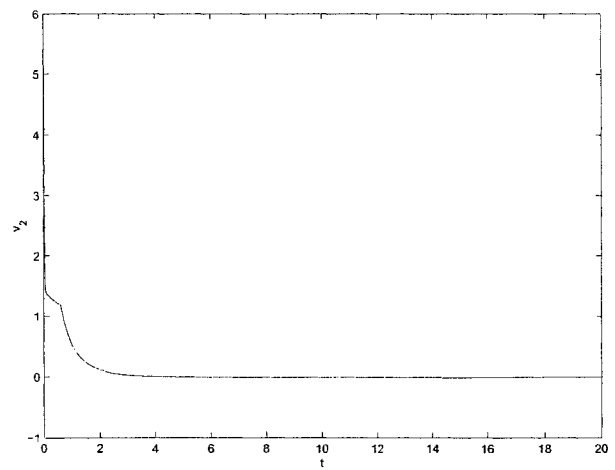


Figure 6.8:  $v_2$  - Simulation result with PD control

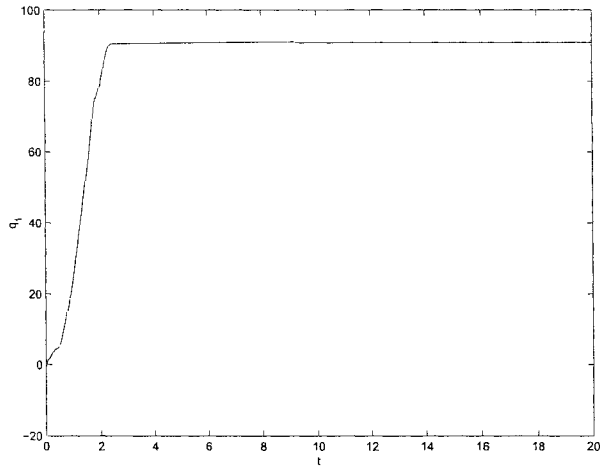


Figure 6.9:  $q_1$  - Experimental result  
with PD control

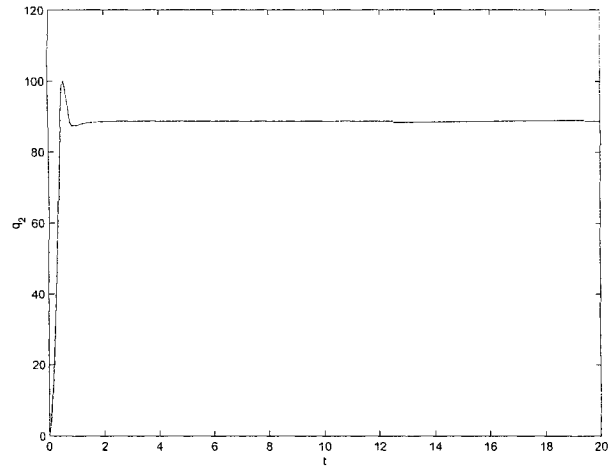


Figure 6.10:  $q_2$  - Experimental result  
with PD control

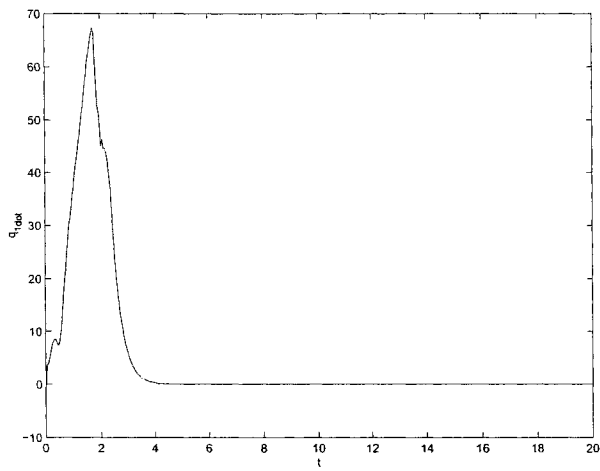


Figure 6.11:  $\dot{q}_1$  - Experimental result  
with PD control

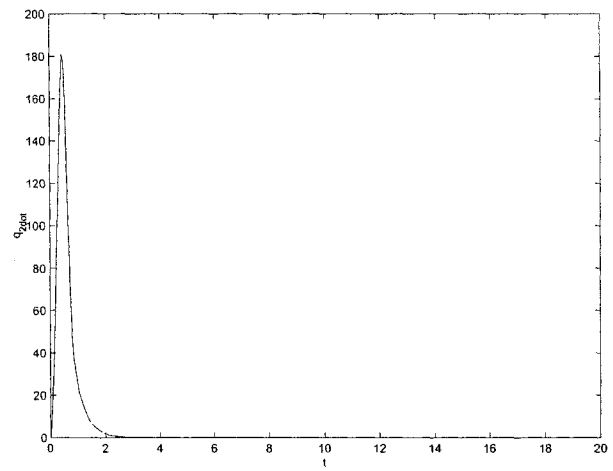


Figure 6.12:  $\dot{q}_2$  - Experimental result  
with PD control

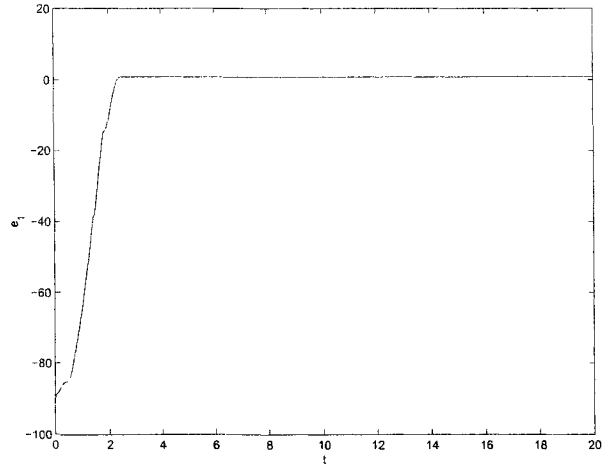


Figure 6.13:  $e_1$  - Experimental result  
with PD control

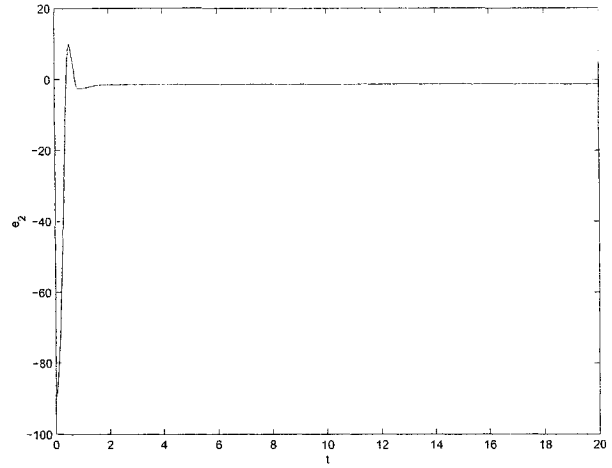


Figure 6.14:  $e_2$  - Experimental result  
with PD control

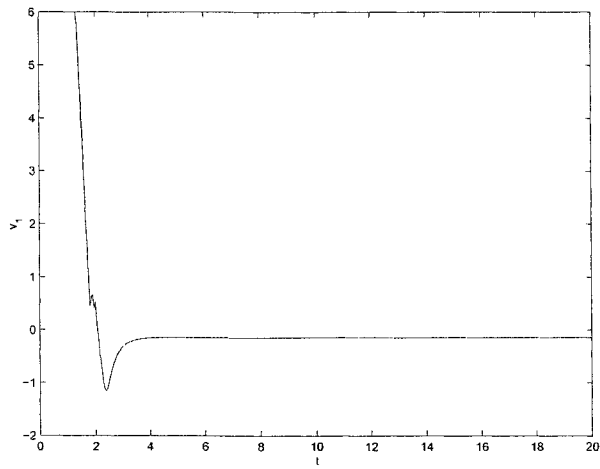


Figure 6.15:  $v_1$  - Experimental result  
with PD control

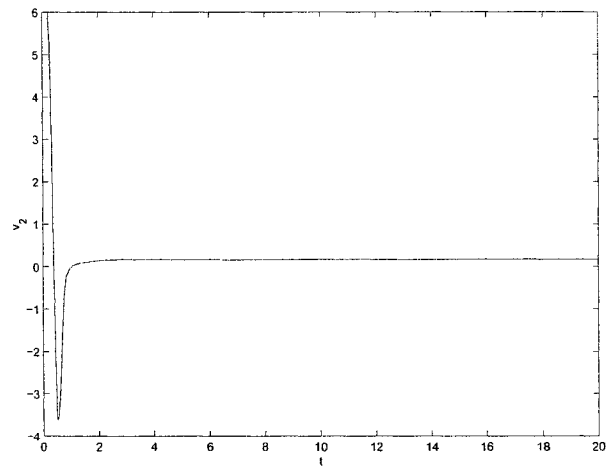


Figure 6.16:  $v_2$  - Experimental result  
with PD control

# Chapter 7

## Nonlinear Controller

### 7.1 Control Design

In the previous chapter, PD controller was applied on the 2-DOF robot manipulator and a Lyapunov function was found to show the global asymptotic convergence of the closed loop system. This is considered the first technique for using Lyapunov's direct method for control design. The second technique is shown in this chapter, which requires hypothesizing a Lyapunov function candidate and then finding a control law to make this candidate a real Lyapunov function.

The controller designed by the second technique is simulated and implemented on the 2-DOF robot manipulator. Comparison among these controllers and also other controllers discussed in the next chapters will be made.

To start the design technique, let's consider the dynamical equation of the robot manipulator without the gravitational torques

$$M(q)\ddot{q} + C(q, \dot{q})\dot{q} = \tau \quad (7.1)$$

$\tilde{q} = q - q_d = e$  is the error between the desired joint displacements  $q_d$  and the actual joint displacements  $q$ . The goal is to design  $\tau$  such that  $q \rightarrow q_d$  as  $t \rightarrow \infty$ .  $q_d$  is a constant vector.

Let's choose

$$V = \frac{1}{2}\dot{q}^T \dot{q} + \frac{1}{2}\tilde{q}^T K_1 \tilde{q} \quad (7.2)$$

$K_1$  is chosen to be diagonal positive definite.

$$\begin{aligned} \dot{V} &= \frac{1}{2}\dot{q}^T \dot{q} + \frac{1}{2}\dot{q}^T \ddot{q} + \frac{1}{2}\tilde{q}^T K_1 \dot{q} + \frac{1}{2}\dot{q}^T K_1 \tilde{q} \\ &= \frac{1}{2}\dot{q}^T \ddot{q} + \frac{1}{2}\dot{q}^T \ddot{q} + \frac{1}{2}\dot{q}^T K_1 \tilde{q} + \frac{1}{2}\dot{q}^T K_1 \tilde{q} \\ &= \dot{q}^T \ddot{q} + \dot{q}^T K_1 \tilde{q} \\ &= \dot{q}^T (M^{-1}(\tau - C\dot{q}) + K_1 \tilde{q}) \end{aligned} \quad (7.3)$$

Let's choose  $\tau$

$$\tau = C\dot{q} - MK_1 \tilde{q} - MK_2 \dot{q} \quad (7.4)$$

$K_2$  is chosen to be diagonal positive definite. Finally, we obtain

$$\dot{V} = -\dot{q}^T K_2 \dot{q} \quad (7.5)$$

which is negative definite.

Using LaSalle's theorem,  $\dot{V} = 0 \Rightarrow \dot{q} = 0 \Rightarrow \ddot{q} = 0$ , then

$$\tau = -MK_1\tilde{q} \quad (7.6)$$

$M(q)$  is symmetric positive definite for any robot manipulator.

$$\begin{aligned} \tau &= 0 \\ \Rightarrow \tilde{q} &= 0 \end{aligned}$$

This means that  $q \rightarrow q_d$  when  $t \rightarrow \infty$  for any initial condition  $q(0)$ .

By choosing the control parameters

$$K_1 = \begin{bmatrix} 1 & 0 \\ 0 & 2.5 \end{bmatrix} \quad K_2 = \begin{bmatrix} 3 & 0 \\ 0 & 3 \end{bmatrix}$$

the simulation results in figures 7.1, 7.2, 7.3, 7.4, 7.5, 7.6, 7.7, and 7.8 obtained by Matlab show the system response for the nonlinear stabilizing control based on Lyapunov's direct method.

Time ( $t$ ) is in sec and motors voltages for link 1  $v_1$  and link 2  $v_2$  are in Volts. In order to compare the results with other controllers, same initial values and same desired angles are used.  $q_{1_0} = 0$ ,  $q_{2_0} = 0$ ,  $\dot{q}_{1_0} = 0$ ,  $\dot{q}_{2_0} = 0$ ,  $q_{d_1} = \pi/2$ , and  $q_{d_2} = \pi/2$ .

The figures for  $q_1$ ,  $q_2$ ,  $\tilde{q}_1$ , and  $\tilde{q}_2$  are shown in deg.  $\dot{q}_1$  and  $\dot{q}_2$  are in deg/sec.

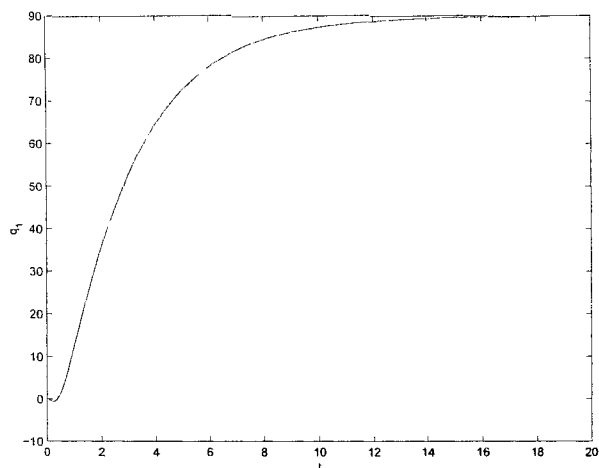


Figure 7.1:  $q_1$  - Simulation result with nonlinear stabilizing control based on Lyapunov method

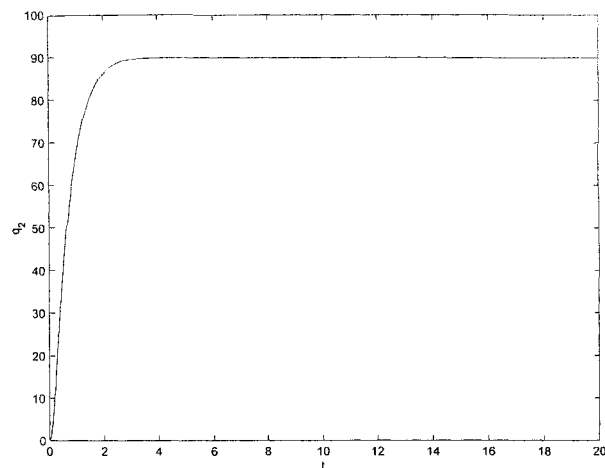


Figure 7.2:  $q_2$  - Simulation result with nonlinear stabilizing control based on Lyapunov method

## 7.2 Experimental Results

Simulink/dSpace environment with a sampling period of 0.05sec was used to obtain the experimental results on the 2-DOF planar manipulator shown in figures 7.9, 7.10, 7.11, 7.12, 7.13, 7.14, 7.15, and 7.16. These figures show the system response for nonlinear stabilizing controller based on Lyapunov's direct method with the same units, desired angles, and initial values used in the simulation part.

The control parameters are chosen as follows

$$K_1 = \begin{bmatrix} 2.2 & 0 \\ 0 & 2.5 \end{bmatrix} \quad K_2 = \begin{bmatrix} 0.5 & 0 \\ 0 & 4 \end{bmatrix}$$

We can conclude from the experimental and simulation results that both PD



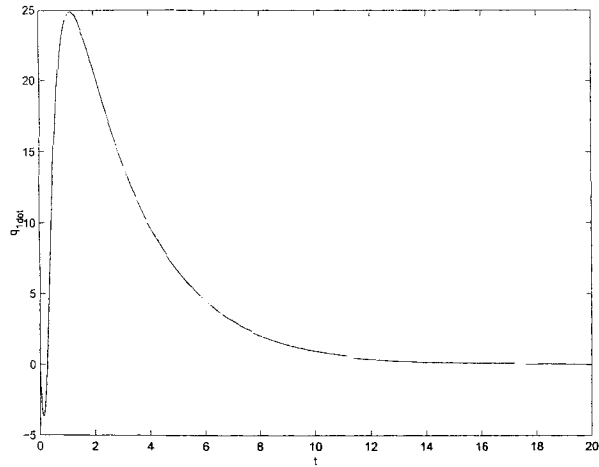


Figure 7.3:  $q_1$  - Simulation result with nonlinear stabilizing control based on Lyapunov method

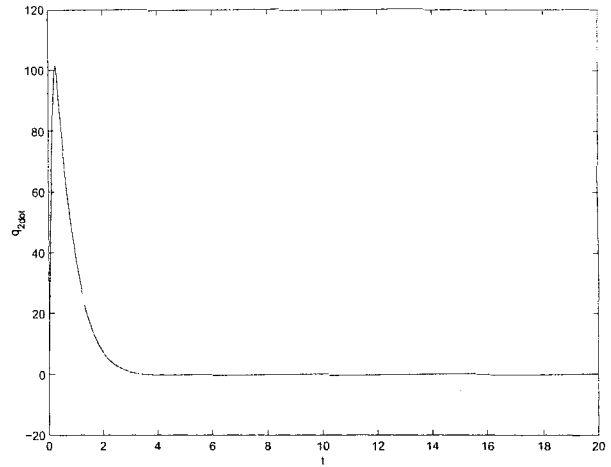


Figure 7.4:  $q_2$  - Simulation result with nonlinear stabilizing control based on Lyapunov method

controller and nonlinear controller based on Lyapunov's direct method can stabilize the system. There is no big difference between the figures of the two controllers for both simulations and experiments. Any small difference can result from the fact that different control parameters are used. However,  $v_2$  is higher when using PD control for both simulation and experimental results. Further comparison will be done after introducing the robust and adaptive backstepping control for the 2-DOF robot manipulator.

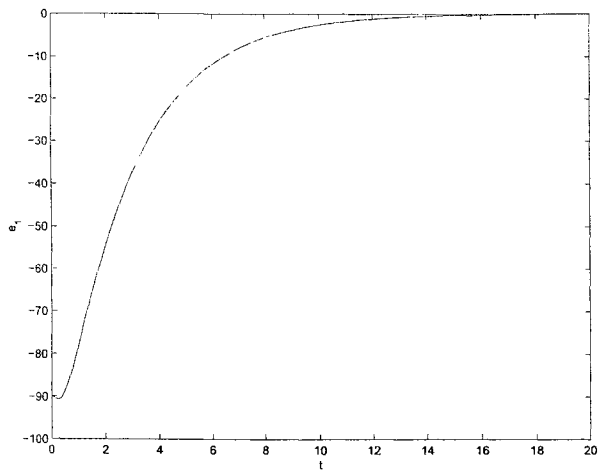


Figure 7.5:  $e_1$  - Simulation result with nonlinear stabilizing control based on Lyapunov method

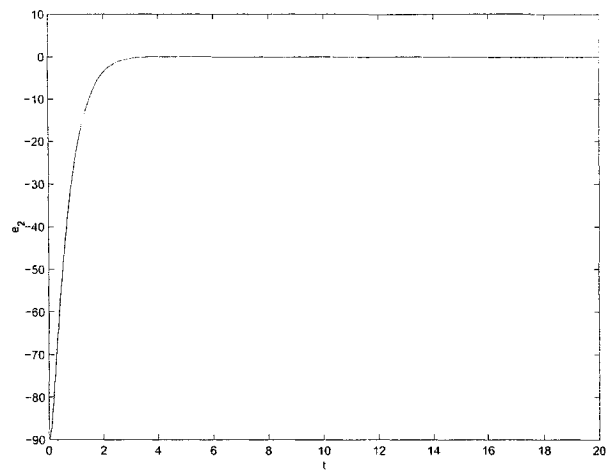


Figure 7.6:  $e_2$  - Simulation result with nonlinear stabilizing control based on Lyapunov method

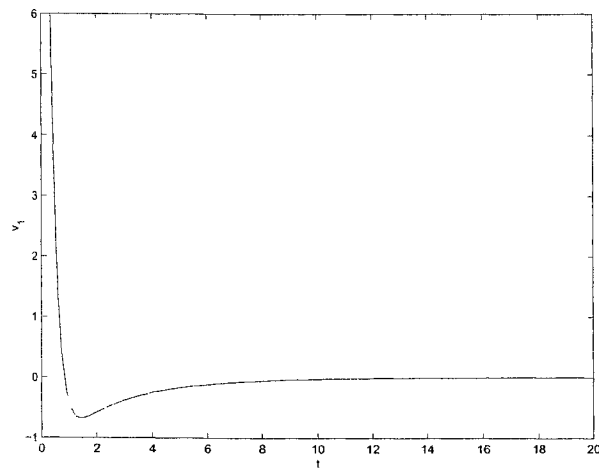


Figure 7.7:  $v_1$  - Simulation result with nonlinear stabilizing control based on Lyapunov method

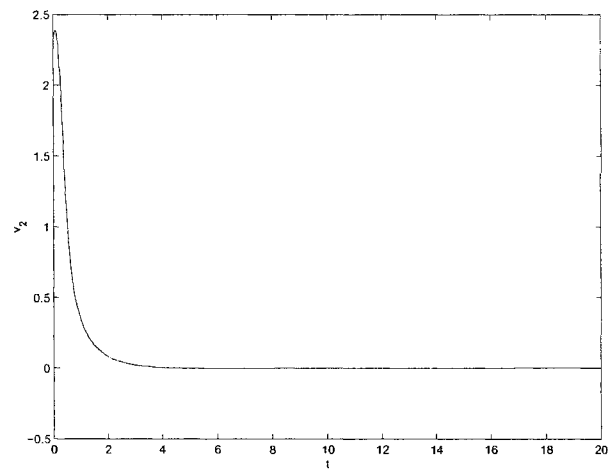


Figure 7.8:  $v_2$  - Simulation result with nonlinear stabilizing control based on Lyapunov method

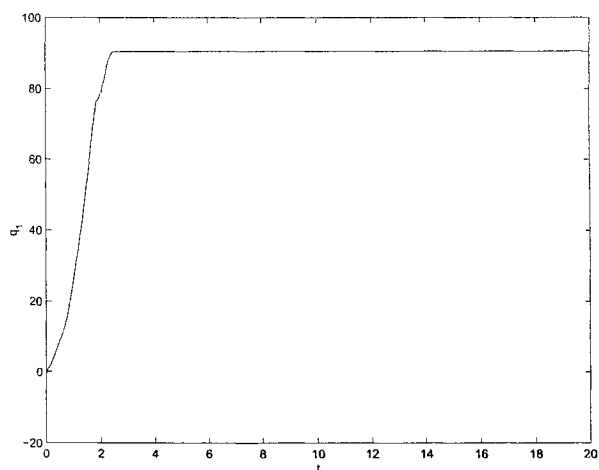


Figure 7.9:  $q_1$  - Experimental result with nonlinear stabilizing control based on Lyapunov method

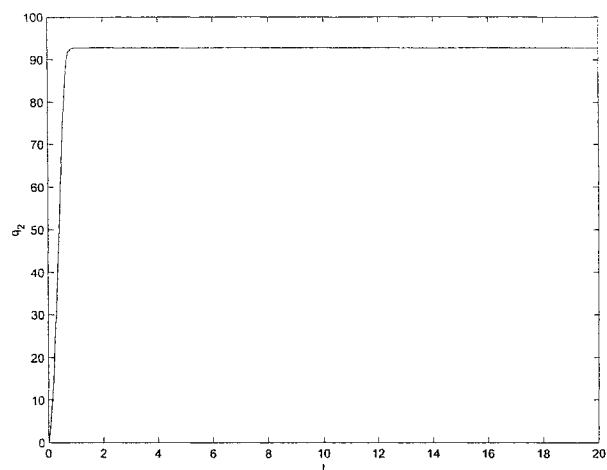


Figure 7.10:  $q_2$  - Experimental result with nonlinear stabilizing control based on Lyapunov method

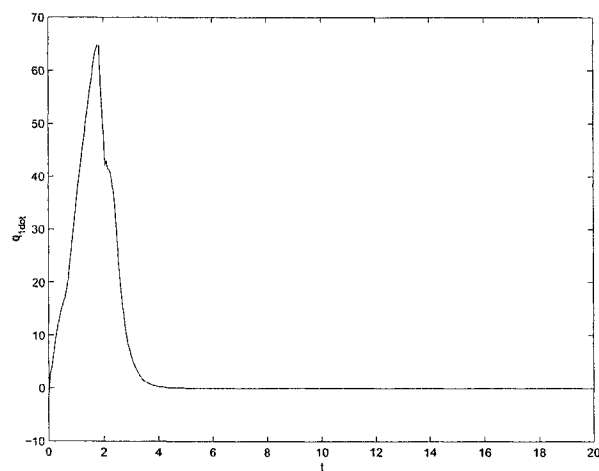


Figure 7.11:  $\dot{q}_1$  - Experimental result with nonlinear stabilizing control based on Lyapunov method

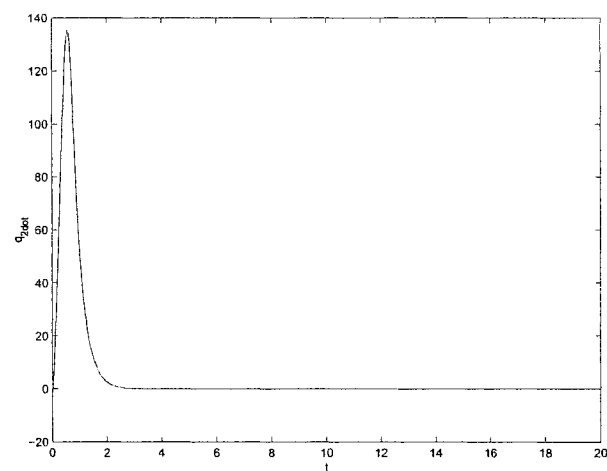


Figure 7.12:  $\dot{q}_2$  - Experimental result with nonlinear stabilizing control based on Lyapunov method

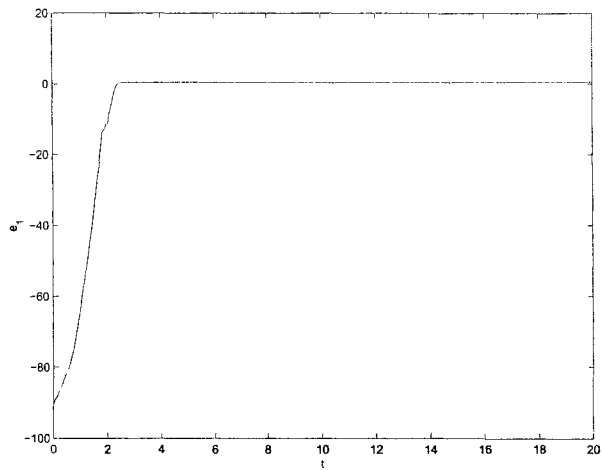


Figure 7.13:  $e_1$  - Experimental result with nonlinear stabilizing control based on Lyapunov method

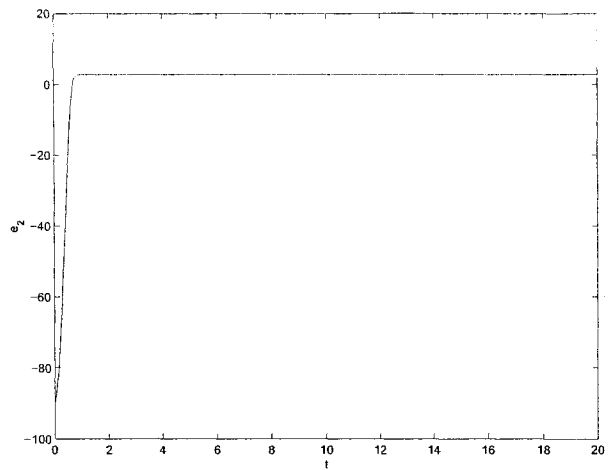


Figure 7.14:  $e_2$  - Experimental result with nonlinear stabilizing control based on Lyapunov method

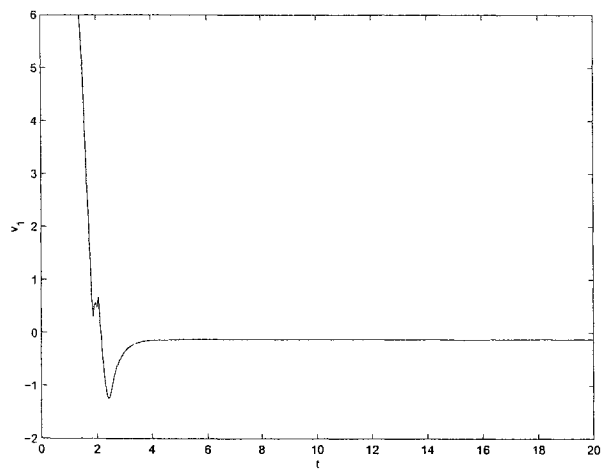


Figure 7.15:  $v_1$  - Experimental result with nonlinear stabilizing control based on Lyapunov method

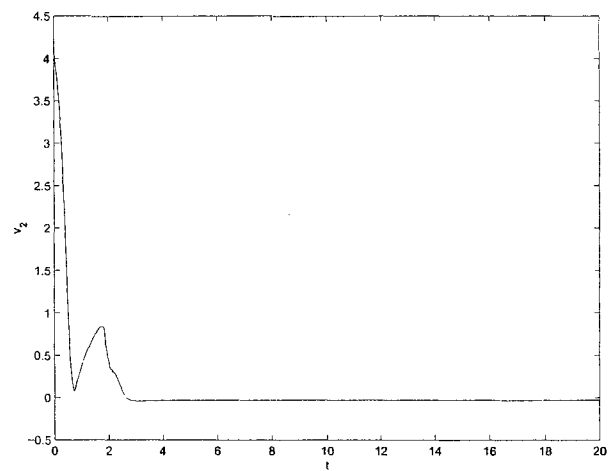


Figure 7.16:  $v_2$  - Experimental result with nonlinear stabilizing control based on Lyapunov method

# Chapter 8

## Robust Controller

### 8.1 Control Design

In a previous chapter, robust backstepping control design technique was discussed with an example. In this chapter, the objective is to stabilize the 2-DOF planar manipulator using the robust backstepping technique in the presence of bounded uncertainties in the dynamical equation of the robot. Simulation and experimental results will be shown. Let's start with the dynamical equation of the robot

$$M(q)\ddot{q} + C(q, \dot{q})\dot{q} + D(\dot{q}) = \tau \quad (8.1)$$

$\tau = u$  is the control input.  $D(\dot{q})$  is the dynamic friction term in the dynamical equation of the robot, which can be expressed as [17]

$$D(\dot{q}) = \begin{bmatrix} d_1 \dot{q}_1 \\ d_2 \dot{q}_2 \end{bmatrix} = \begin{bmatrix} d_1 & 0 \\ 0 & d_2 \end{bmatrix} \begin{bmatrix} \dot{q}_1 \\ \dot{q}_2 \end{bmatrix}$$

$$D_1 = \begin{bmatrix} d_1 & 0 \\ 0 & d_2 \end{bmatrix}$$

There exists a positive constant  $k_{c_1}$  which satisfies the following inequality

$$\| D_1 \dot{q} \| \leq k_{c_1} \| \dot{q} \| \quad (8.2)$$

We can rewrite the dynamical equation of the robot as follows

$$\ddot{q} = M(q)^{-1}(\tau - C(q, \dot{q})\dot{q} - D_1 \dot{q}) \quad (8.3)$$

$\tilde{q} = q - q_d = e$  is the error between the desired joint displacements  $q_d$  and the actual joint displacements  $q$ . Let  $x_1 = q_1 - q_{d1} = \tilde{q}_1 = e_1$  and  $x_2 = q_2 - q_{d2} = \tilde{q}_2 = e_2$ .

The vector A is introduced as

$$A = \begin{bmatrix} x_1 \\ x_2 \end{bmatrix}$$

Let  $q_1 = x_3$  and  $q_2 = x_4$ . The vector B is introduced as

$$B = \begin{bmatrix} x_3 \\ x_4 \end{bmatrix}$$

then

$$\dot{A} = B = \begin{bmatrix} x_3 \\ x_4 \end{bmatrix} = \begin{bmatrix} \dot{x}_1 \\ \dot{x}_2 \end{bmatrix}$$

$$\dot{B} = \begin{bmatrix} \dot{x}_3 \\ \dot{x}_4 \end{bmatrix} = \begin{bmatrix} \ddot{q}_1 \\ \ddot{q}_2 \end{bmatrix} = M^{-1}(u - CB - D_1B)$$

$$\dot{A} = B \quad (8.4)$$

First step in the design is by choosing  $V_1 = \frac{1}{2}A^T A$  to obtain

$$\begin{aligned} \dot{V}_1 &= \frac{1}{2}\dot{A}^T A + \frac{1}{2}A^T \dot{A} \\ &= A^T B \end{aligned} \quad (8.5)$$

If  $B$  were the control, a virtual controller  $\alpha_1$  would be chosen such that

$$B = \alpha_1 = -\lambda_1 A \quad (8.6)$$

$\dot{V}_1$  can be written as follows

$$\dot{V}_1 = A^T(B + \alpha_1 - \alpha_1) = A^T \alpha_1 + A^T(B - \alpha_1) \quad (8.7)$$

Second step is by choosing  $V_2$

$$V_2 = V_1 + \frac{1}{2}(B - \alpha_1)^T M(B - \alpha_1) \quad (8.8)$$

to obtain the derivative of the Lyapunov function  $V_2$  as follows

$$\begin{aligned} \dot{V}_2 &= \dot{V}_1 + \frac{1}{2}(B - \alpha_1)^T \dot{M}(B - \alpha_1) + (B - \alpha_1)^T M(\dot{B} - \dot{\alpha}_1) \\ &= -A^T \lambda_1 A + A^T(B - \alpha_1) + \frac{1}{2}(B - \alpha_1)^T \dot{M}(B - \alpha_1) \\ &\quad + (B - \alpha_1)^T M\left(\dot{B} - \frac{\partial \alpha_1}{\partial A} \dot{A}\right) \\ &= -A^T \lambda_1 A + (B - \alpha_1)^T \left(A + M\left(\dot{B} - \frac{\partial \alpha_1}{\partial A} \dot{A}\right) + \frac{1}{2}\dot{M}(B - \alpha_1)\right) \end{aligned} \quad (8.9)$$

The matrix  $(\dot{M}(q) - 2C(q, \dot{q}))$  is skew symmetric. This implies  $\dot{M}(q) = C(q, \dot{q}) + C^T(q, \dot{q})$  [22], then

$$\begin{aligned}
\dot{V}_2 &= -A^T \lambda_1 A + (B - \alpha_1)^T (A + M(M^{-1}u - M^{-1}CB - M^{-1}D_1B - \frac{\partial \alpha_1}{\partial A}B)) \\
&+ \frac{1}{2}(C + C^T)(B - \alpha_1) \\
&= -A^T \lambda_1 A + (B - \alpha_1)^T (A + u - \frac{1}{2}CB - D_1B - M \frac{\partial \alpha_1}{\partial A}B) \\
&- \frac{1}{2}(C + C^T)\alpha_1 + \frac{1}{2}C^T B
\end{aligned} \tag{8.10}$$

From equation (8.2),  $\dot{V}_2$  can be written as follows

$$\begin{aligned}
\dot{V}_2 &\leq -A^T \lambda_1 A + (B - \alpha_1)^T (A + u - \frac{1}{2}CB - M \frac{\partial \alpha_1}{\partial A}B) \\
&- \frac{1}{2}(C + C^T)\alpha_1 + \frac{1}{2}C^T B \\
&+ \|(B - \alpha_1)^T\| k_{c_1} \|B\|
\end{aligned} \tag{8.11}$$

Let

$$\begin{aligned}
B &= B - \alpha_1 + \alpha_1 \\
\|B\| &\leq \|(B - \alpha_1)\| + \|\alpha_1\| \\
&\leq \|(B - \alpha_1)\| + \|\lambda_1\| \|A\|
\end{aligned} \tag{8.12}$$

We can rewrite  $\dot{V}_2$  as follows

$$\begin{aligned}
\dot{V}_2 &\leq -A^T \lambda_1 A + (B - \alpha_1)^T (A + u - \frac{1}{2}CB - M \frac{\partial \alpha_1}{\partial A}B) \\
&- \frac{1}{2}(C + C^T)\alpha_1 + \frac{1}{2}C^T B
\end{aligned}$$



$$\begin{aligned}
& + \| (B - \alpha_1) \| k_{c_1} [\| (B - \alpha_1) \| + \| \lambda_1 \| \| A \|] \\
& \leq -A^T \lambda_1 A + (B - \alpha_1)^T (A + u - M \frac{\partial \alpha_1}{\partial A} B) \\
& - \frac{1}{2} (C + C^T) \alpha_1 + \frac{1}{2} (C^T - C) B \\
& + \| (B - \alpha_1) \| k_{c_1} \| (B - \alpha_1) \| \\
& + \| (B - \alpha_1) \| k_{c_1} \| \lambda_1 \| \| A \| \\
& \leq -A^T \lambda_1 A + (B - \alpha_1)^T (A + u - M \frac{\partial \alpha_1}{\partial A} B) \\
& - \frac{1}{2} (C + C^T) \alpha_1 + \frac{1}{2} (C^T - C) B \\
& + (B - \alpha_1)^T k_{c_1} (B - \alpha_1) \\
& + \frac{1}{2} k_{c_1}^2 \| \lambda_1 \|^2 (B - \alpha_1)^T (B - \alpha_1) + \frac{1}{2} A^T A \\
& \leq -A^T \lambda_1 A + \frac{1}{2} A^T A + (B - \alpha_1)^T (A + u - M \frac{\partial \alpha_1}{\partial A} B) \\
& - \frac{1}{2} (C + C^T) \alpha_1 + \frac{1}{2} (C^T - C) B \\
& + (B - \alpha_1) k_{c_1} (1 + \frac{1}{2} k_{c_1} \| \lambda_1 \|^2) \tag{8.13}
\end{aligned}$$

We are in the position to design our actual feedback control  $u$  to stabilize the system.

$$\begin{aligned}
u & = -\lambda_2 (B - \alpha_1) - A + M \frac{\partial \alpha_1}{\partial A} B \\
& + \frac{1}{2} (C + C^T) \alpha_1 - \frac{1}{2} (C^T - C) B \\
& - (B - \alpha_1) k_{c_1} (1 + \frac{1}{2} k_{c_1} \| \lambda_1 \|^2) \tag{8.14}
\end{aligned}$$

The controller  $u$  can stabilize the system by causing  $\dot{V}_2$  to be negative

$$\dot{V}_2 \leq -A^T \lambda_1 A + \frac{1}{2} A^T A - (B - \alpha_1)^T \lambda_2 (B - \alpha_1) \tag{8.15}$$

The simulation results in figures 8.1, 8.2, 8.3, 8.4, 8.5, 8.6, 8.7, and 8.8, which were carried out on Matlab, show that the robust backstepping controller is able to stabilize the system in the presence of uncertainties.

Time ( $t$ ) is in sec and motors voltages for link 1  $v_1$  and link 2  $v_2$  are in Volts.

Initial values and desired angles are chosen like the one used for other controllers.

$q_{1_0} = 0$ ,  $q_{2_0} = 0$ ,  $\dot{q}_{1_0} = 0$ ,  $\dot{q}_{2_0} = 0$ ,  $q_{d_1} = \pi/2$ , and  $q_{d_2} = \pi/2$ .

The figures show the results by choosing  $k_{c_1} = 0.05$ . By changing the value of  $D_1$ , the robust controller can stabilize the system as long as equation (8.2) is satisfied.

Control parameters are chosen as follows

$$\lambda_1 = \begin{bmatrix} 0.6 & 0 \\ 0 & 0.9 \end{bmatrix} \quad \lambda_2 = \begin{bmatrix} 2 & 0 \\ 0 & 1.5 \end{bmatrix}$$

The figures for  $q_1$ ,  $q_2$ ,  $\tilde{q}_1$ , and  $\tilde{q}_2$  are shown in deg.  $\dot{q}_1$  and  $\dot{q}_2$  are in deg/sec.

## 8.2 Experimental Results

In the same environment (Simulink/dSpace) with the same sampling period (0.05sec) of the controllers discussed in the previous chapters, robust controller was implemented on the 2-DOF robot manipulator. Experimental results are shown in figures 8.9, 8.10, 8.11, 8.12, 8.13, 8.14, 8.15, and 8.16.

The same initial values, units, and same desired angles of the simulation part are used for the experimental part. To achieve stability, control parameters for the

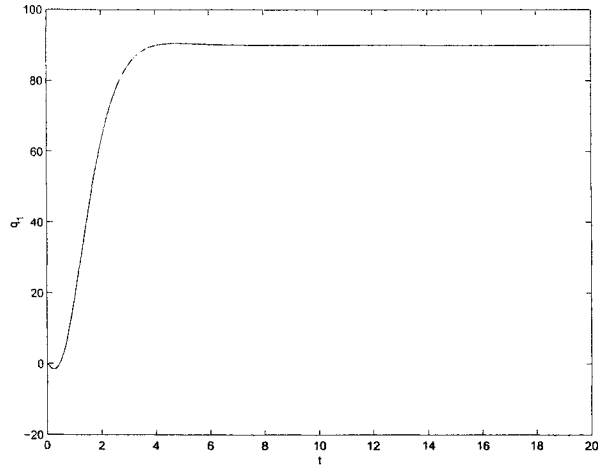


Figure 8.1:  $q_1$  - Simulation result with robust control

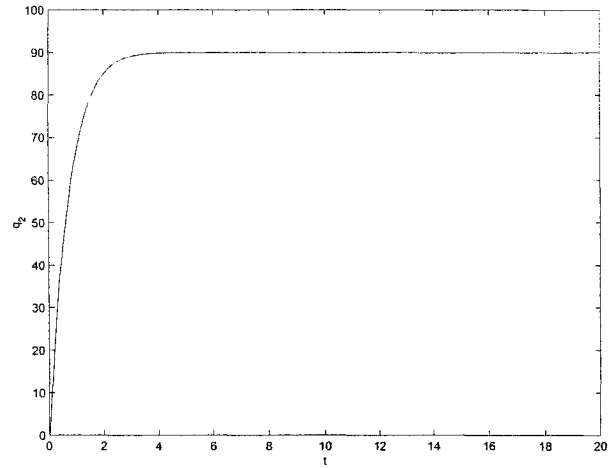


Figure 8.2:  $q_2$  - Simulation result with robust control

experiment are:

$$\lambda_1 = \begin{bmatrix} 0.01 & 0 \\ 0 & 0.9 \end{bmatrix} \quad \lambda_2 = \begin{bmatrix} 0.01 & 0 \\ 0 & 0.2 \end{bmatrix}$$

$k_{c1} = 0.05$ . The figures for  $q_1$ ,  $q_2$ ,  $\dot{q}_1$ , and  $\dot{q}_2$  are shown in deg.  $\dot{q}_1$  and  $\dot{q}_2$  are in deg/sec.

In practical system, modeling error is unavoidable. A control scheme is needed that guarantees robustness in the presence of the modeling error. Experimental works were carried out to evaluate the performance of the robust backstepping controller. The controller can stabilize the system in spite of the presence of model inaccuracy. This means that  $q \rightarrow q_d$  when  $t \rightarrow \infty$ . Hence, the effectiveness of the proposed controller is verified. More comparison with other controllers will be discussed in the conclusion.

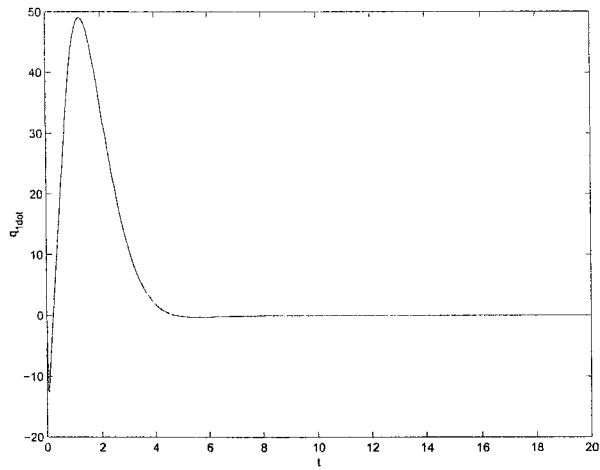


Figure 8.3:  $\dot{q}_1$  - Simulation result with robust control

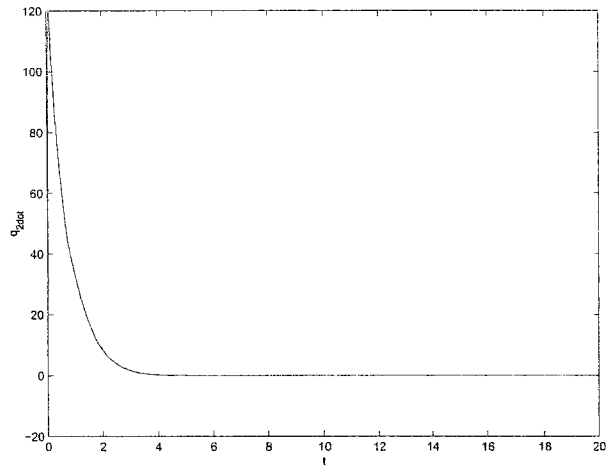


Figure 8.4:  $\dot{q}_2$  - Simulation result with robust control

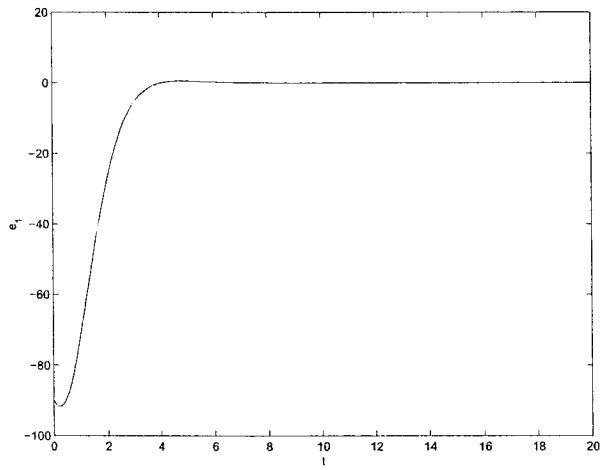


Figure 8.5:  $e_1$  - Simulation result with robust control

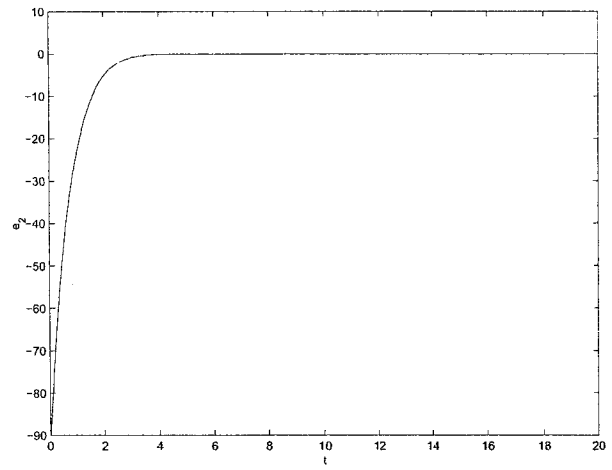


Figure 8.6:  $e_2$  - Simulation result with robust control

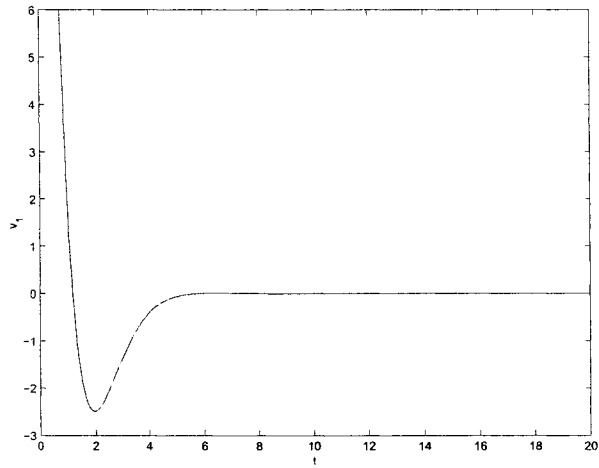


Figure 8.7:  $v_1$  - Simulation result with robust control

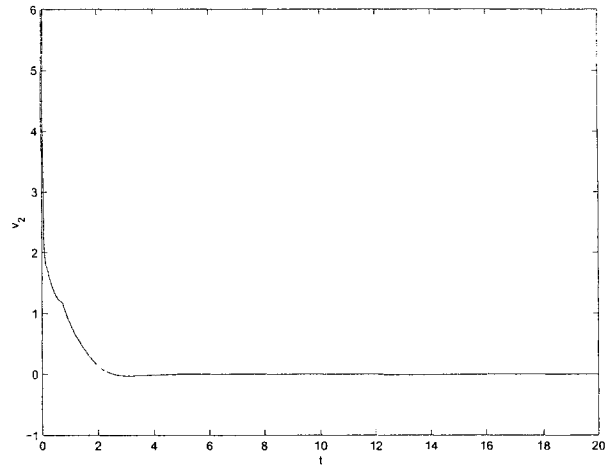


Figure 8.8:  $v_2$  - Simulation result with robust control

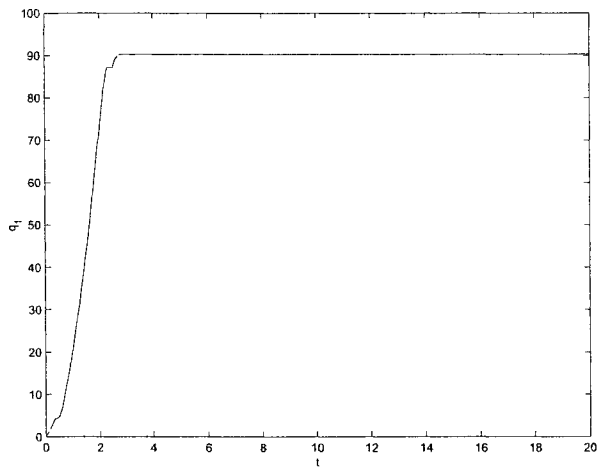


Figure 8.9:  $q_1$  - Experimental result with robust control

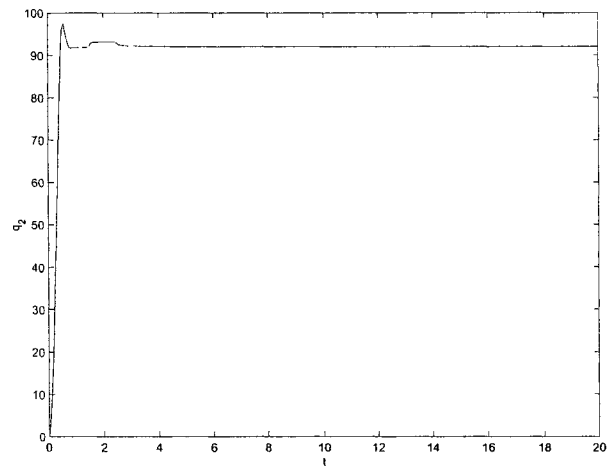


Figure 8.10:  $q_2$  - Experimental result with robust control

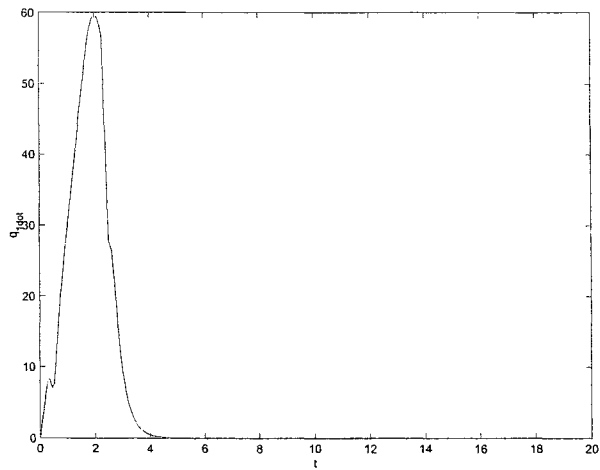


Figure 8.11:  $\dot{q}_1$  - Experimental result  
with robust control

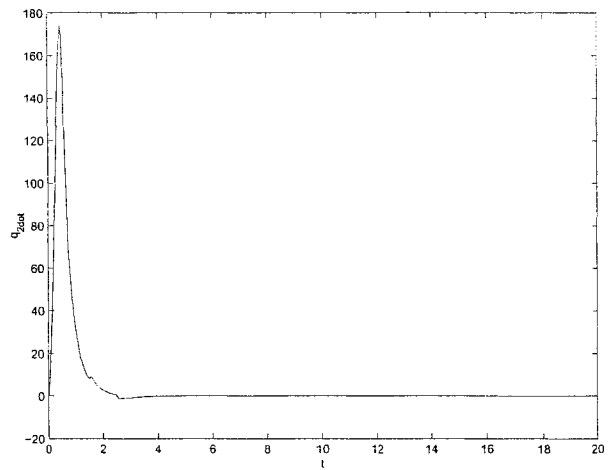


Figure 8.12:  $\dot{q}_2$  - Experimental result  
with robust control

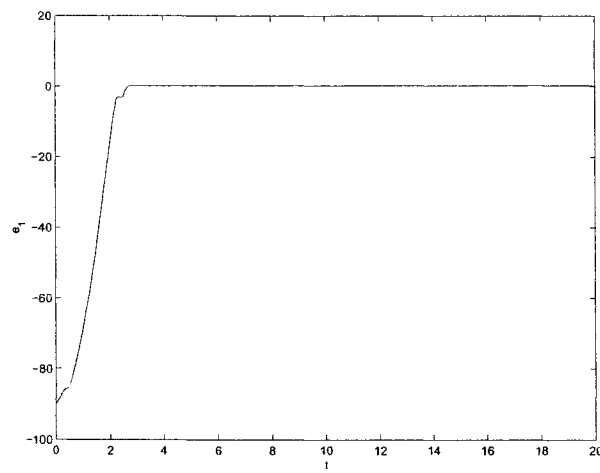


Figure 8.13:  $e_1$  - Experimental result  
with robust control

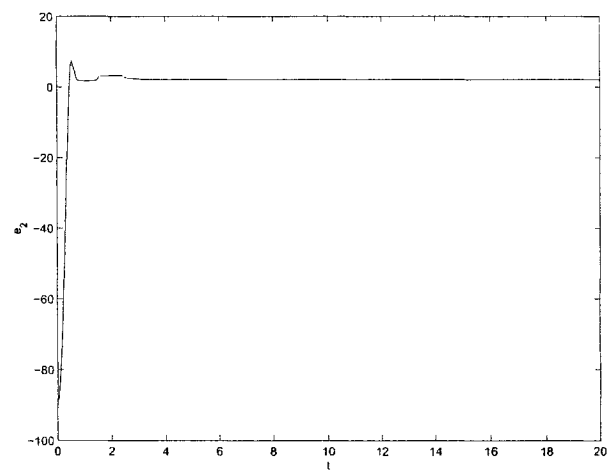


Figure 8.14:  $e_2$  - Experimental result  
with robust control

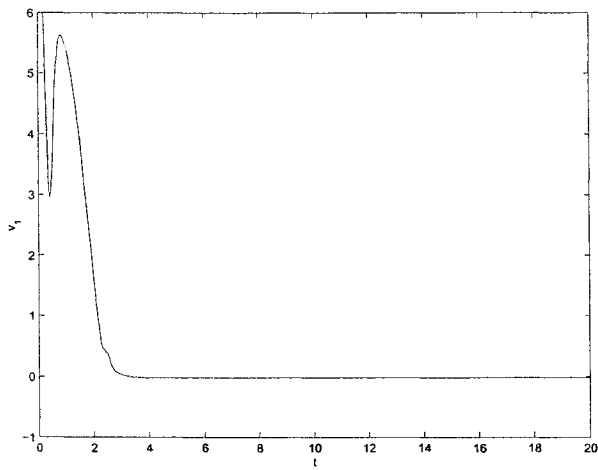


Figure 8.15:  $v_1$  - Experimental result  
with robust control

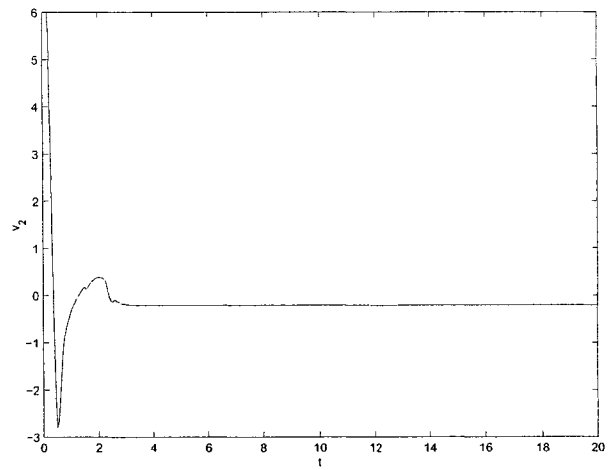


Figure 8.16:  $v_2$  - Experimental result  
with robust control

# Chapter 9

## Adaptive Controller

### 9.1 Control Design

In this chapter, we will assume that the inertia for the robot is an unknown parameter. The objective of this chapter is to prove by simulations and experiments that the adaptive controller can stabilize the system in the presence of this unknown parameter using the backstepping technique. The dynamical equation of the robot is given by

$$M(q)\ddot{q} + C(q, \dot{q})\dot{q} = \tau \quad (9.1)$$

$\tau = u$  is the control input. We can rewrite the dynamical equation of the robot as follows

$$\ddot{q} = M(q)^{-1}(\tau - C(q, \dot{q})\dot{q}) \quad (9.2)$$



The elements of the inertia matrix  $M(q)$  are given by

$$\begin{aligned}
M_{11}(q) &= m_1 l_{c1}^2 + m_2(l_1^2 + l_{c2}^2 + 2l_1 l_{c2} \cos(q_2)) + I_1 + I_2 \\
M_{12}(q) &= m_2(l_{c2}^2 + l_1 l_{c2} \cos(q_2)) + I_2 \\
M_{21}(q) &= m_2(l_{c2}^2 + l_1 l_{c2} \cos(q_2)) + I_2 \\
M_{22}(q) &= m_2 l_{c2}^2 + I_2
\end{aligned} \tag{9.3}$$

We will assume that the inertia of link 1,  $I_1$ , and the inertia of link 2,  $I_2$ , are the unknown parameters. The inertia matrix  $M$  can be written as follows

$$\begin{aligned}
M_{11}(q) &= m_1 l_{c1}^2 + m_2(l_1^2 + l_{c2}^2 + 2l_1 l_{c2} \cos(q_2)) + \theta_1 + \theta_2 \\
M_{12}(q) &= m_2(l_{c2}^2 + l_1 l_{c2} \cos(q_2)) + \theta_2 \\
M_{21}(q) &= m_2(l_{c2}^2 + l_1 l_{c2} \cos(q_2)) + \theta_2 \\
M_{22}(q) &= m_2 l_{c2}^2 + \theta_2
\end{aligned} \tag{9.4}$$

$$M = \begin{bmatrix} m_1 l_{c1}^2 + m_2(l_1^2 + l_{c2}^2 + 2l_1 l_{c2} \cos(q_2)) & m_2(l_{c2}^2 + l_1 l_{c2} \cos(q_2)) \\ m_2(l_{c2}^2 + l_1 l_{c2} \cos(q_2)) & m_2 l_{c2}^2 \end{bmatrix} + \begin{bmatrix} 1 & 0 \\ 0 & 0 \end{bmatrix} \theta_1 + \begin{bmatrix} 1 & 1 \\ 1 & 1 \end{bmatrix} \theta_2$$

Let

$$M_n = \begin{bmatrix} m_1 l_{c1}^2 + m_2(l_1^2 + l_{c2}^2 + 2l_1 l_{c2} \cos(q_2)) & m_2(l_{c2}^2 + l_1 l_{c2} \cos(q_2)) \\ m_2(l_{c2}^2 + l_1 l_{c2} \cos(q_2)) & m_2 l_{c2}^2 \end{bmatrix}$$

$$M_1 = \begin{bmatrix} 1 & 0 \\ 0 & 0 \end{bmatrix}$$

$$M_2 = \begin{bmatrix} 1 & 1 \\ 1 & 1 \end{bmatrix}$$

Let's introduce the change of variables  $x_1 = q_1 - q_{d1} = \tilde{q}_1 = e_1$  and  $x_2 = q_2 - q_{d2} = \tilde{q}_2 = e_2$ .

$$A = \begin{bmatrix} x_1 \\ x_2 \end{bmatrix}$$

$\dot{q}_1 = x_3$  and  $\dot{q}_2 = x_4$ .

$$B = \begin{bmatrix} x_3 \\ x_4 \end{bmatrix}$$

$$\dot{A} = B = \begin{bmatrix} x_3 \\ x_4 \end{bmatrix} = \begin{bmatrix} \dot{x}_1 \\ \dot{x}_2 \end{bmatrix}$$

$$\dot{B} = \begin{bmatrix} \dot{x}_3 \\ \dot{x}_4 \end{bmatrix} = \begin{bmatrix} \ddot{q}_1 \\ \ddot{q}_2 \end{bmatrix} = M^{-1}(u - CB)$$

$$\dot{A} = B \tag{9.5}$$

First step is to take  $V_1 = \frac{1}{2}A^T A$  to obtain

$$\begin{aligned} \dot{V}_1 &= \frac{1}{2}\dot{A}^T A + \frac{1}{2}A^T \dot{A} \\ &= A^T B \end{aligned} \tag{9.6}$$

If  $B$  were the control, a virtual controller  $\alpha_1$  would be chosen such that

$$B = \alpha_1 = -\lambda_1 A \tag{9.7}$$

We can rewrite  $\dot{V}_1$  as follows

$$\dot{V}_1 = A^T(B + \alpha_1 - \alpha_1) = A^T\alpha_1 + A^T(B - \alpha_1) \quad (9.8)$$

Second step is to choose  $V_2$  as follows

$$V_2 = V_1 + \frac{1}{2}(B - \alpha_1)^T M(B - \alpha_1) + \frac{1}{2}(\theta - \hat{\theta})^T \Gamma(\theta - \hat{\theta}) \quad (9.9)$$

where  $\theta$  is the unknown constant parameter which appears in the system equations.

$$\theta = \begin{bmatrix} \theta_1 \\ \theta_2 \end{bmatrix}$$

The parameter estimate is  $\hat{\theta}$ .

$$\hat{\theta} = \begin{bmatrix} \hat{\theta}_1 \\ \hat{\theta}_2 \end{bmatrix}$$

The derivative of the Lyapunov function is as follows

$$\begin{aligned} \dot{V}_2 &= -A^T\lambda_1 A + A^T(B - \alpha_1) + \frac{1}{2}(B - \alpha_1)^T \dot{M}(B - \alpha_1) \\ &+ (B - \alpha_1)^T M(\dot{B} - \dot{\alpha}_1) + (\theta - \hat{\theta})^T \Gamma(-\dot{\hat{\theta}}) \\ &= -A^T\lambda_1 A + (B - \alpha_1)^T \left( A + \frac{1}{2}(C + C^T)(B - \alpha_1) \right. \\ &\left. + u - CB - M\dot{\alpha}_1 \right) + (\theta - \hat{\theta})^T \Gamma(-\dot{\hat{\theta}}) \end{aligned} \quad (9.10)$$

Let

$$\Gamma = \begin{bmatrix} \Gamma_1 & 0 \\ 0 & \Gamma_2 \end{bmatrix}$$

We can rewrite  $\dot{V}_2$  as follows

$$\dot{V}_2 = -A^T\lambda_1 A + (B - \alpha_1)^T \left( A + \frac{1}{2}(C + C^T)(B - \alpha_1) + u - CB \right)$$

$$\begin{aligned}
& - M_n \dot{\alpha}_1 - M_1 \hat{\theta}_1 \dot{\alpha}_1 - M_2 \hat{\theta}_2 \dot{\alpha}_1 - M_1(\theta_1 - \hat{\theta}_1) \dot{\alpha}_1 - M_2(\theta_2 - \hat{\theta}_2) \dot{\alpha}_1 \\
& + (\theta_1 - \hat{\theta}_1) \Gamma_1(-\dot{\hat{\theta}}_1) + (\theta_2 - \hat{\theta}_2) \Gamma_2(-\dot{\hat{\theta}}_2)
\end{aligned} \tag{9.11}$$

We are finally in the position to design our actual update law  $\dot{\hat{\theta}}$  and feedback control  $u$  to stabilize the system as follows

$$\begin{aligned}
\dot{\hat{\theta}}_1 &= -\frac{1}{\Gamma_1}(B - \alpha_1)^T M_1 \dot{\alpha}_1 \\
\dot{\hat{\theta}}_2 &= -\frac{1}{\Gamma_2}(B - \alpha_1)^T M_2 \dot{\alpha}_1
\end{aligned} \tag{9.12}$$

$$\begin{aligned}
u &= -\lambda_2(B - \alpha_1) - A - \frac{1}{2}(C + C^T)(B - \alpha_1) + CB \\
&+ M_n \dot{\alpha}_1 + M_1 \hat{\theta}_1 \dot{\alpha}_1 + M_2 \hat{\theta}_2 \dot{\alpha}_1
\end{aligned} \tag{9.13}$$

such that

$$\dot{V}_2 = -A^T \lambda_1 A - (B - \alpha_1)^T \lambda_2 (B - \alpha_1) \tag{9.14}$$

We are then proving that the controller  $u$  and the update law  $\dot{\hat{\theta}}$  can stabilize the system by making  $\dot{V}_2$  negative definite. This is proved by the simulation results shown in figures 9.1, 9.2, 9.3, 9.4, 9.5, 9.6, 9.7, and 9.8, which were performed on Matlab.

Time ( $t$ ) is in sec and motors voltages for link 1  $v_1$  and link 2  $v_2$  are in Volts.

Initial values and desired angles are  $q_{1_0} = 0$ ,  $q_{2_0} = 0$ ,  $\dot{q}_{1_0} = 0$ ,  $\dot{q}_{2_0} = 0$ ,  $q_{d_1} = \pi/2$ , and  $q_{d_2} = \pi/2$ .

$\theta_1 = I_1 = 0.2158$  and  $\theta_2 = I_2 = 0.0137$ .

Control parameters are chosen as follows

$$\lambda_1 = \begin{bmatrix} 0.05 & 0 \\ 0 & 0.01 \end{bmatrix} \quad \lambda_2 = \begin{bmatrix} 1.5 & 0 \\ 0 & 1.5 \end{bmatrix}$$

$$\Gamma = \begin{bmatrix} 10 & 0 \\ 0 & 55 \end{bmatrix}$$

The figures for  $q_1$ ,  $q_2$ ,  $\tilde{q}_1$ , and  $\tilde{q}_2$  are shown in deg.  $\dot{q}_1$  and  $\dot{q}_2$  are in deg/sec.

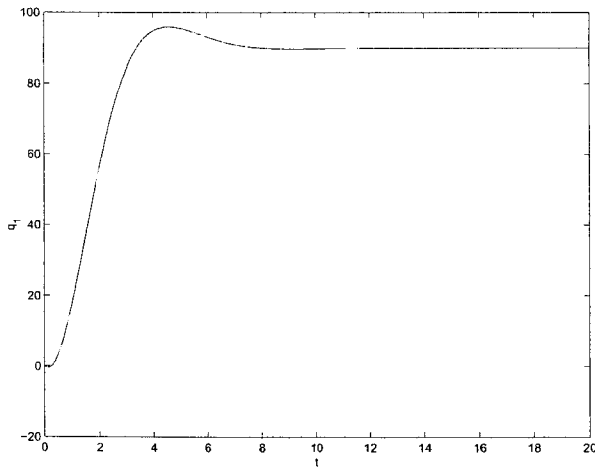


Figure 9.1:  $q_1$  - Simulation result with adaptive control

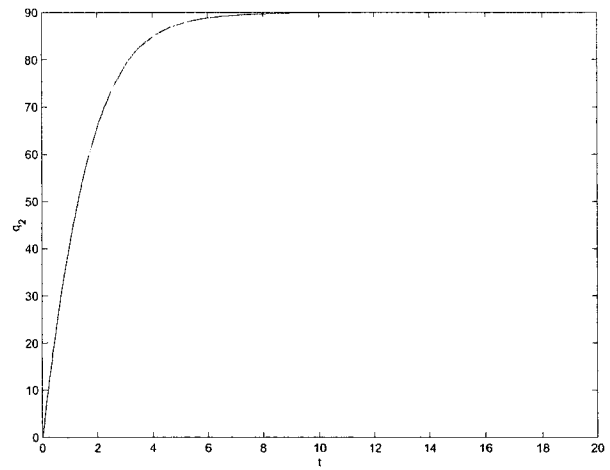


Figure 9.2:  $q_2$  - Simulation result with adaptive control

## 9.2 Experimental Results

Simulink/dSpace environment with a sampling period of 0.05sec is used to obtain the experimental results on the 2-DOF planar manipulator shown in figures 9.11, 9.12, 9.13, 9.14, 9.15, 9.16, 9.17, and 9.18.

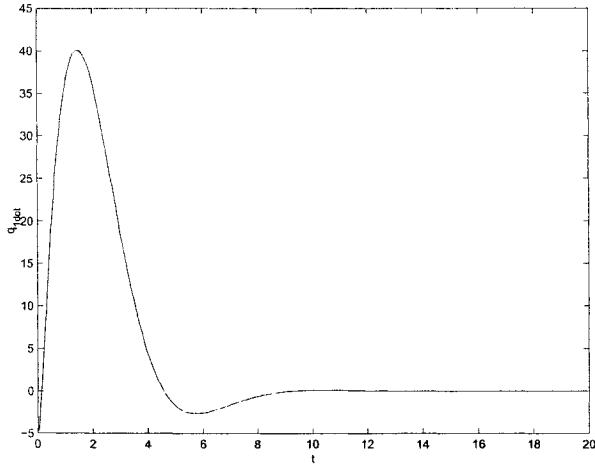


Figure 9.3:  $q_1$  - Simulation result with adaptive control

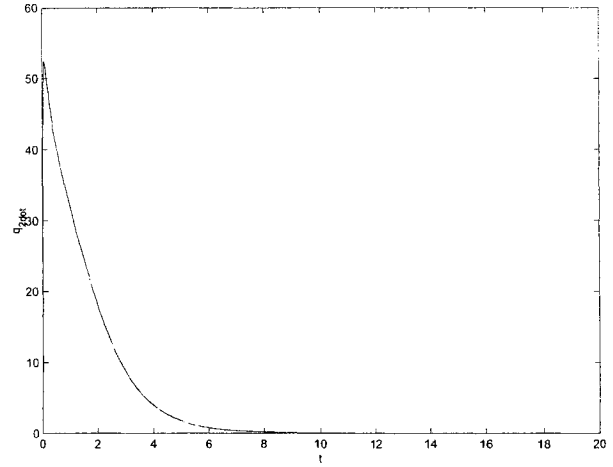


Figure 9.4:  $q_2$  - Simulation result with adaptive control

With the same initial values, units, and same desired angles of the simulation part, stability is reached by choosing the control parameters as follows:

$$\lambda_1 = \begin{bmatrix} 0.05 & 0 \\ 0 & 0.01 \end{bmatrix} \quad \lambda_2 = \begin{bmatrix} 0.1 & 0 \\ 0 & 0.3 \end{bmatrix}$$

$$\Gamma = \begin{bmatrix} 10 & 0 \\ 0 & 55 \end{bmatrix}$$

By assuming that the inertia is unknown, the adaptive backstepping control proved its ability to stabilize the system under this condition. Convergence of the estimated parameters to the real values is not guaranteed. However, simulations and experimental results show that the estimated parameters are bounded. A more general comparison will be discussed in the conclusion to compare the effectiveness of the four type of controllers tested on the 2-DOF robot manipulator.

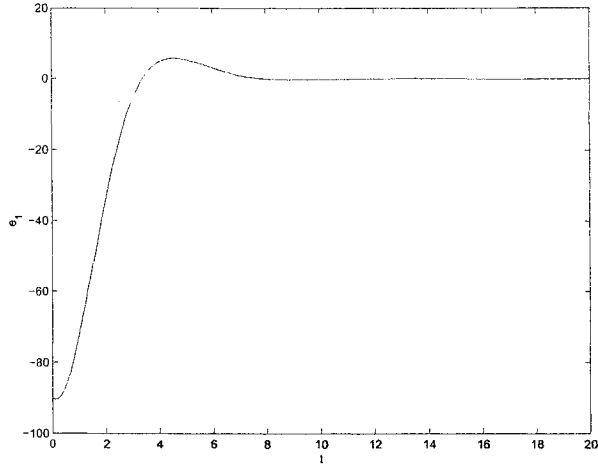


Figure 9.5:  $e_1$  - Simulation result with adaptive control

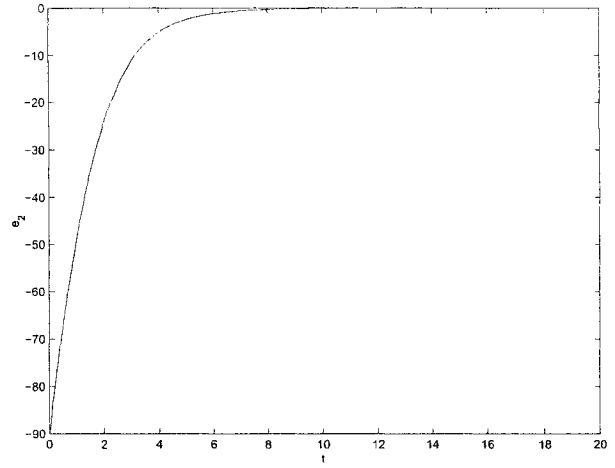


Figure 9.6:  $e_2$  - Simulation result with adaptive control

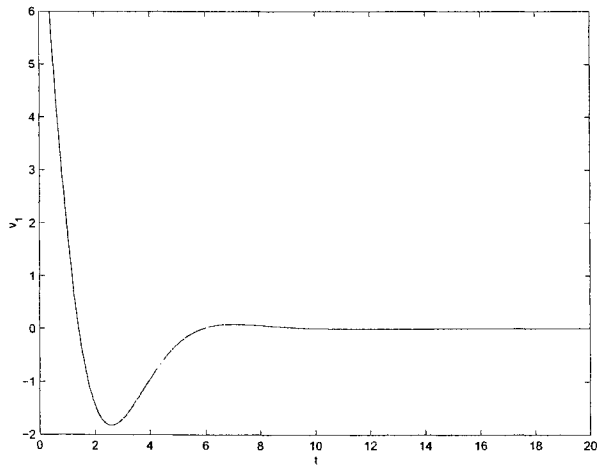


Figure 9.7:  $v_1$  - Simulation result with adaptive control

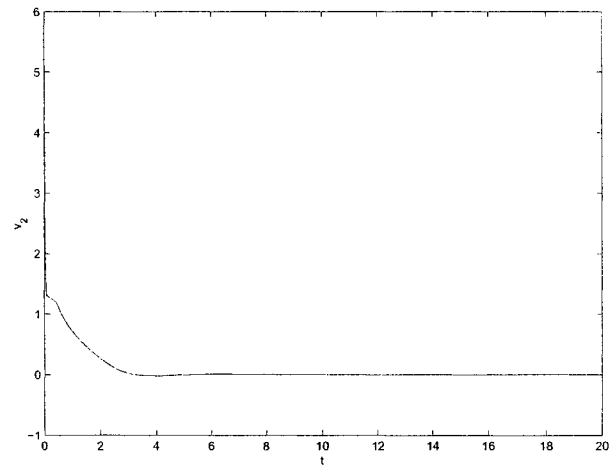


Figure 9.8:  $v_2$  - Simulation result with adaptive control

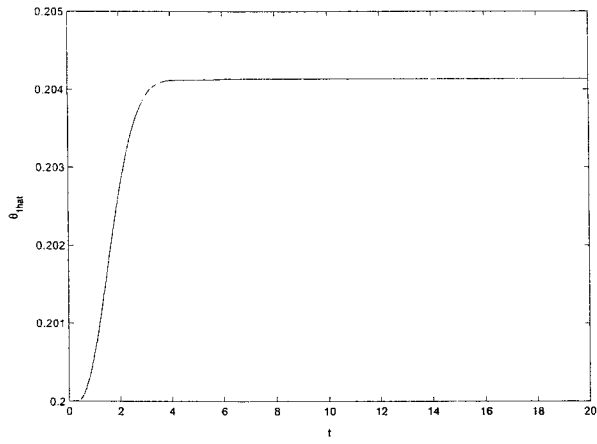


Figure 9.9:  $\hat{\theta}_1$  - Simulation result with adaptive control

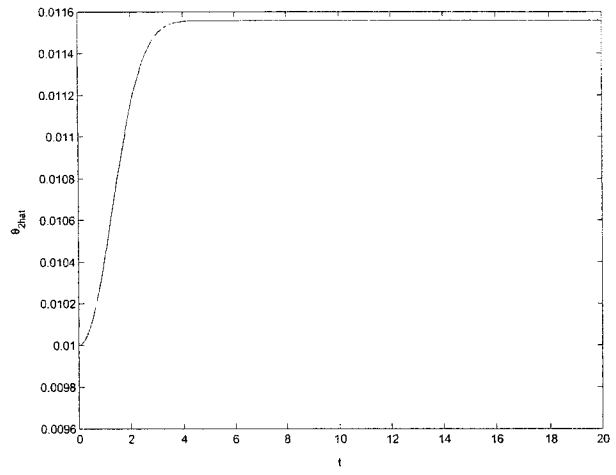


Figure 9.10:  $\hat{\theta}_2$  - Simulation result with adaptive control

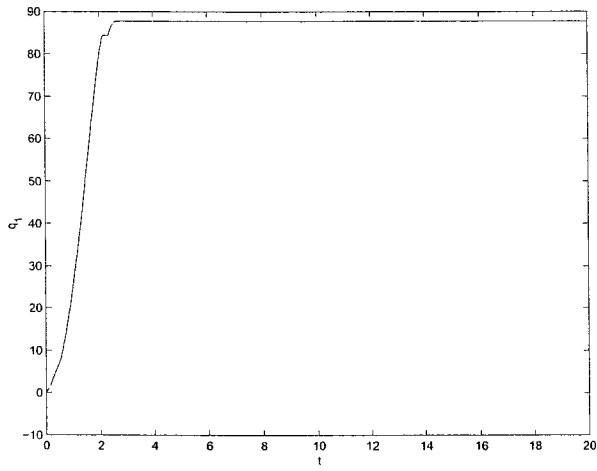


Figure 9.11:  $q_1$  - Experimental result with adaptive control

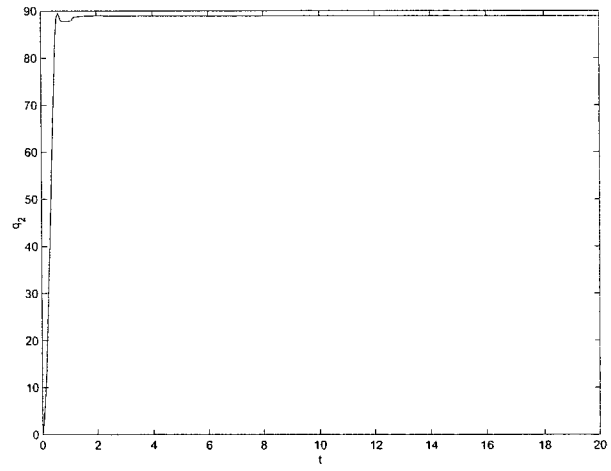


Figure 9.12:  $q_2$  - Experimental result with adaptive control



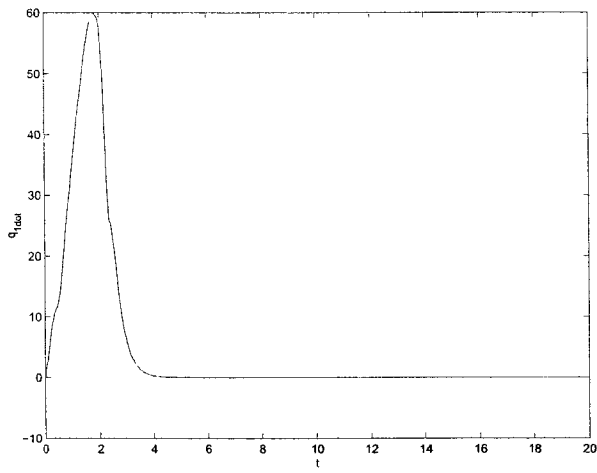


Figure 9.13:  $\hat{q}_1$  - Experimental result  
with adaptive control

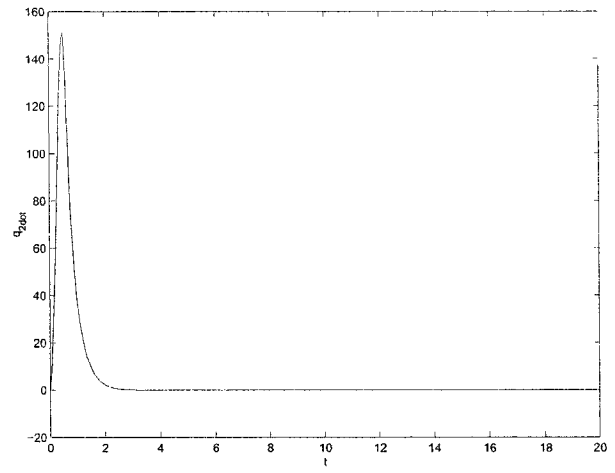


Figure 9.14:  $\hat{q}_2$  - Experimental result  
with adaptive control

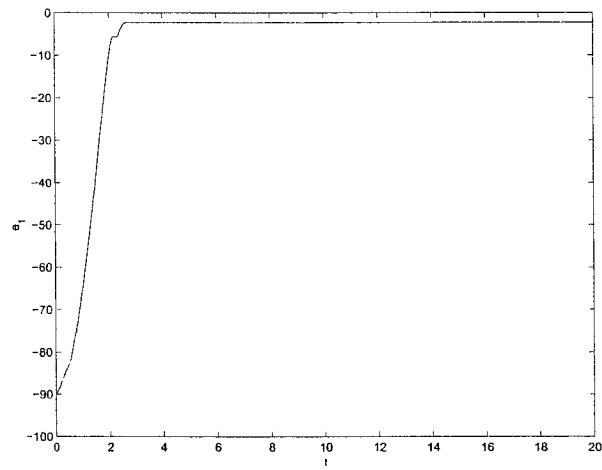


Figure 9.15:  $e_1$  - Experimental result  
with adaptive control

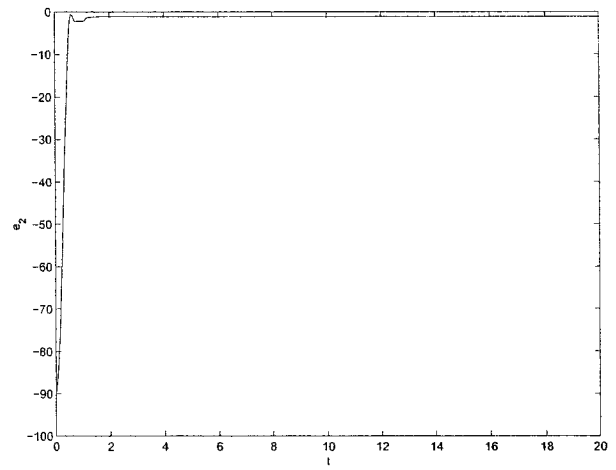


Figure 9.16:  $e_2$  - Experimental result  
with adaptive control

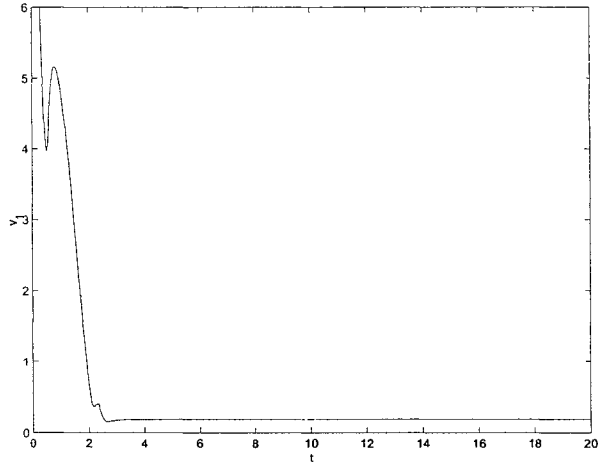


Figure 9.17:  $v_1$  - Experimental result with adaptive control

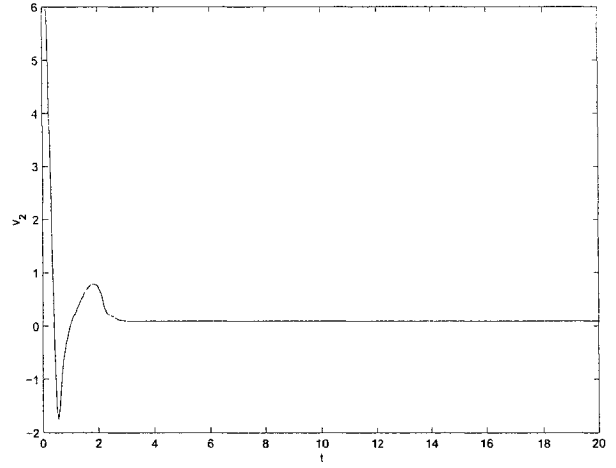


Figure 9.18:  $v_2$  - Experimental result with adaptive control

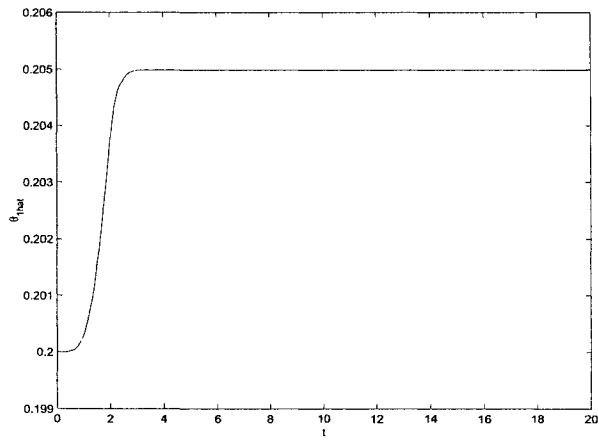


Figure 9.19:  $\hat{\theta}_1$  - Experimental result with adaptive control

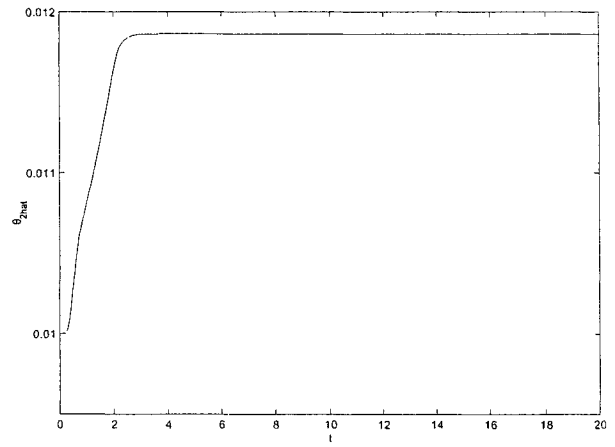


Figure 9.20:  $\hat{\theta}_2$  - Experimental result with adaptive control

## Part IV

### CONCLUSION

# Chapter 10

## Conclusion and future work

### 10.1 Conclusion

Comparing different controllers discussed in this thesis report leads us to the following conclusions:

- Adaptive backstepping controller and robust backstepping controller were effective when applied on a third order system. However, high overshoot is one of the disadvantages of nonlinear control techniques.
- When the system gets more complicated, adaptive backstepping controller and robust backstepping controller require powerful tools to be implemented experimentally because of the complexity of the control laws.

- Adaptive backstepping controller has shown very good performance when applied on a practical system (2 DOF robot manipulator). However, if the number of unknown parameters increases, then the controller will be more complicated and it will affect negatively the implementation of the controller experimentally.
- The effectiveness of the robust backstepping controller is verified. However, if the uncertainty model becomes more complicated, the controller may be difficult to implement.
- Better results can be achieved experimentally with smaller sampling periods than the one used (0.05 sec). This couldn't be achieved because of the speed of the data acquisition board.
- The performance on the 2-DOF robot is quite similar for the four controllers. All control parameters were tuned by trial-and-error until the best result was achieved.
- The work done proves that adaptive and robust controllers are able to stabilize the system in spite of model uncertainties or unknown parameters, which are unavoidable problems in practical systems. Moreover, the results are quite similar to the PD controller, which is widely used to control the 2-DOF robot manipulator. Hence, the effectiveness of the proposed controllers is verified.

## 10.2 Future work

Experimental work was successful. However, we can achieve more accurate results with a better mechanical system. The figures showing the experimental results are the best readings after many trials. Repeating the experiment with the same parameters may sometimes give different results.

Consequently, our recommendation for future work is to update the mechanical system to accomplish the following:

- Obtain better experimental results for stabilizing controllers.
- Approach the tracking control problem.

Moreover, better data acquisition system and other programming languages (C-language) can be used to overcome some of the difficulties in the experimental work and to realize better performance.

# Bibliography

- [1] K.Ogata, Modern control engineering, Prentice-Hall, 1990.
- [2] J.J.Slotine and W.Li, Applied nonlinear control, Prentice-Hall, 1991.
- [3] M.J.Grimble, Robust industrial control optimal design approach for polynomial systems, Prentice-Hall, 1994.
- [4] P.Kokotovic and M.Arcak, Constructive nonlinear control: a historical perspective, Automatica, Vol. 37, 2001, pp. 637-662.
- [5] D.Nganga-Kouya, M.Saad, L.Lamarche, and C.Khairallah, Backstepping adaptive position control for robotic manipulators, Proceedings of the American Control Conference, Vol. 1, 2001, pp. 636-640.
- [6] V.Manosa, F.Ikhouane, and J.Rodellar, Control of uncertain non-linear systems via adaptive backstepping, Journal of Sound and Vibration, Vol. 280, No. 3-5, 2005, pp. 657-680.

- [7] R.A.Freeman and P.V.Kokotovic, Backstepping design of robust controllers for a class of nonlinear systems, IFAC Symposia Series, No. 7, 1993, pp. 431-436.
- [8] S.T.Glad and O.Hakegard, Backstepping control of a rigid body, Proceedings of the IEEE Conference on Decision and Control, Vol. 4, 2002, pp. 3944-3945.
- [9] C.Tsai, M.Cheng, and C.Chan, Adaptive backstepping position control for a linear DC brushless motor, IECON Proceedings, Vol. 1, IECON 2004 - 30th Annual Conference of IEEE Industrial Electronics Society, 2004, pp. 365-370.
- [10] C.Huang, K.Chen, H.Lee, and L.Fu, Nonlinear adaptive backstepping motion control of linear induction motor, Proceedings of the American Control Conference, Vol. 4, 2002, pp. 3099-3104.
- [11] G.Li, Guang and A.Khajepour, Application of backstepping technique to robust control of a hydraulically driven flexible arm, Proceedings of the Tenth International Congress on Sound and Vibration, 2003, pp. 4101-4108.
- [12] H.Sira-Ramirez, Hebertt and O.Llanes-Santiago, Adaptive dynamical sliding mode control via backstepping, Proceedings of the IEEE Conference on Decision and Control, Vol. 2, 1993, pp. 1422-1427.
- [13] H.K.Khalil, Nonlinear Systems, Prentice-Hall, 2002.



- [14] C.M.Kwan and F.L.Lewis, Robust backstepping control of nonlinear systems using neural networks, IEEE Transactions on Systems, Man, and Cybernetics Part A:Systems and Humans, Vol. 30, No. 6, 2000, pp. 753-766.
- [15] M.Sharma and A.J.Calise, Adaptive backstepping control for a class of nonlinear systems via multilayered neural networks, Proceedings of the American Control Conference, Vol. 4, 2002, pp. 2683-2688.
- [16] H.G.Sage, M.F.De Mathelin, and E.Ostertag, Robust control of robot manipulators: a survey , International Journal of Control, Vol. 72, No. 16, 1999, pp. 1498-1522.
- [17] C.Ishii, T.Shen, and Z.Qu, Lyapunov recursive design of robust adaptive tracking control with  $L_2$ -gain performance for electrically-driven robot manipulators, International Journal of Control, Vol. 74, No. 8, 2001, pp. 811-828.
- [18] D.Nganga-Kouya, M.Saad, and L.Lamarche, Backstepping passivity adaptive position control for robotic manipulators, Proceedings of the American Control Conference, Vol. 6, 2002, pp. 4607-4611.
- [19] M.Krstic, I.Kanellakopoulos, and P.Kokotovic, Nonlinear and adaptive control design, Wiley, 1995.

- [20] R.S.Sanchez-Pena and M.Sznaier, Robust systems theory and applications, Wiley, 1998.
- [21] M.W.Spong and M.Vidyasagar, Robot dynamics and control, Wiley, 1989.
- [22] R.Kelly, A tuning procedure for stable PID control of robot manipulators , Robotica, Vol. 13, 1995, pp. 141-148.
- [23] N.Mohan, T.M.Undeland, and W.P.Robbins, Power electronics: converters, applications and design, Wiley, 1989.
- [24] M.H.Rashid, Power electronics, circuits, devices, and applications, Prentice-Hall, 1993.
- [25] R.E.Tarter, Solid-state power conversion handbook, Wiley, 1993.
- [26] T.K.Kiong, W.Quing-Guo, and H.C.Chieh with T.J.Hagglund, Advances in PID control, Springer, 1999.

# Appendix A

## Block Diagrams

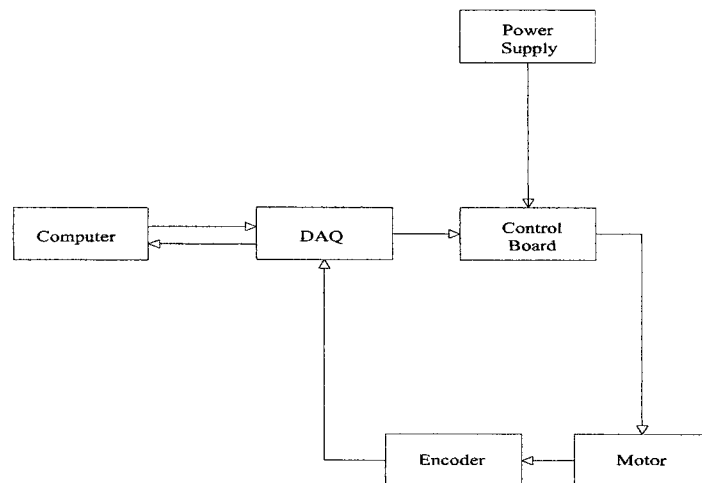


Figure A.1: Experimental Block Diagram

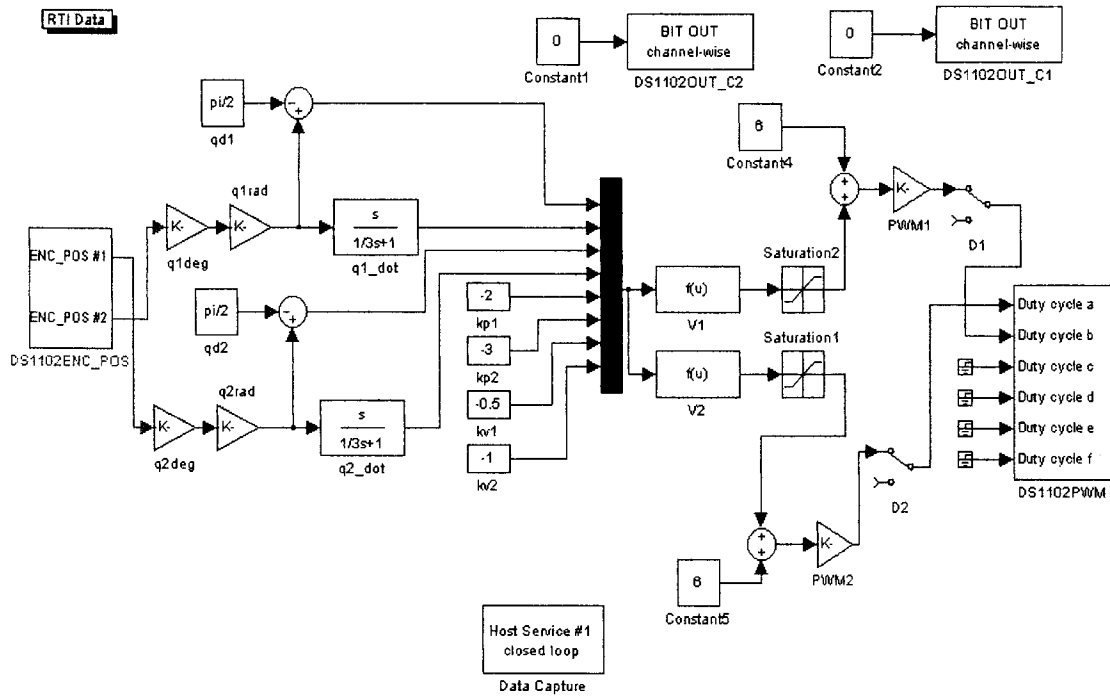


Figure A.2: PD Controller - Simulink Block

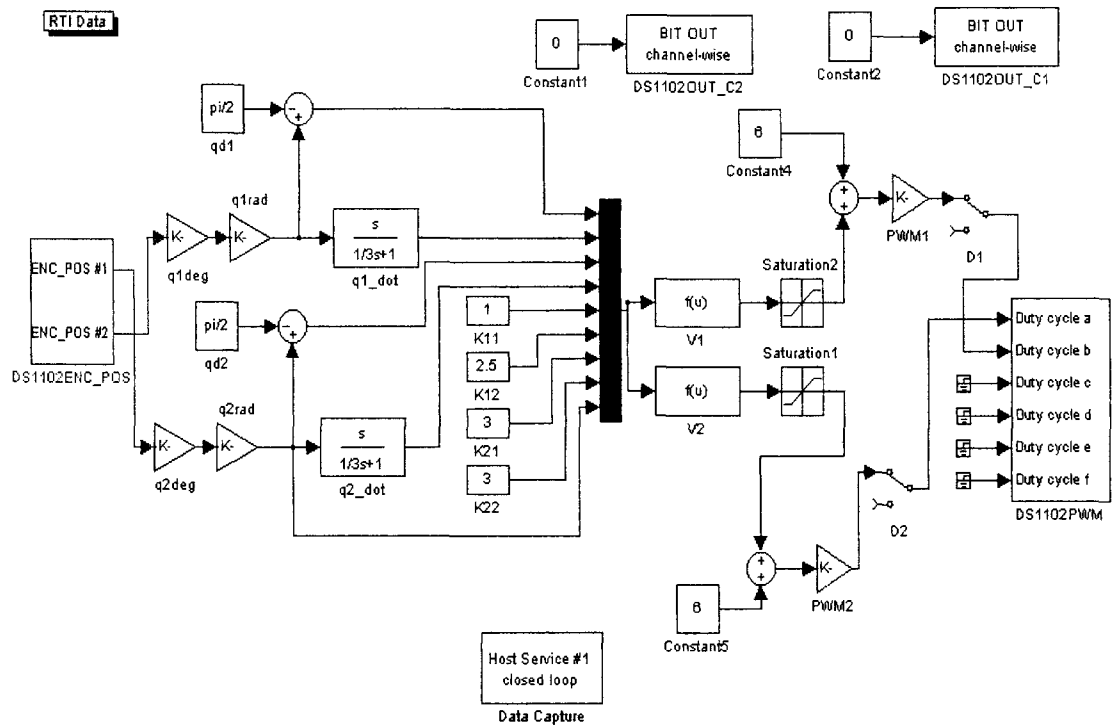


Figure A.3: Nonlinear Controller - Simulink Block

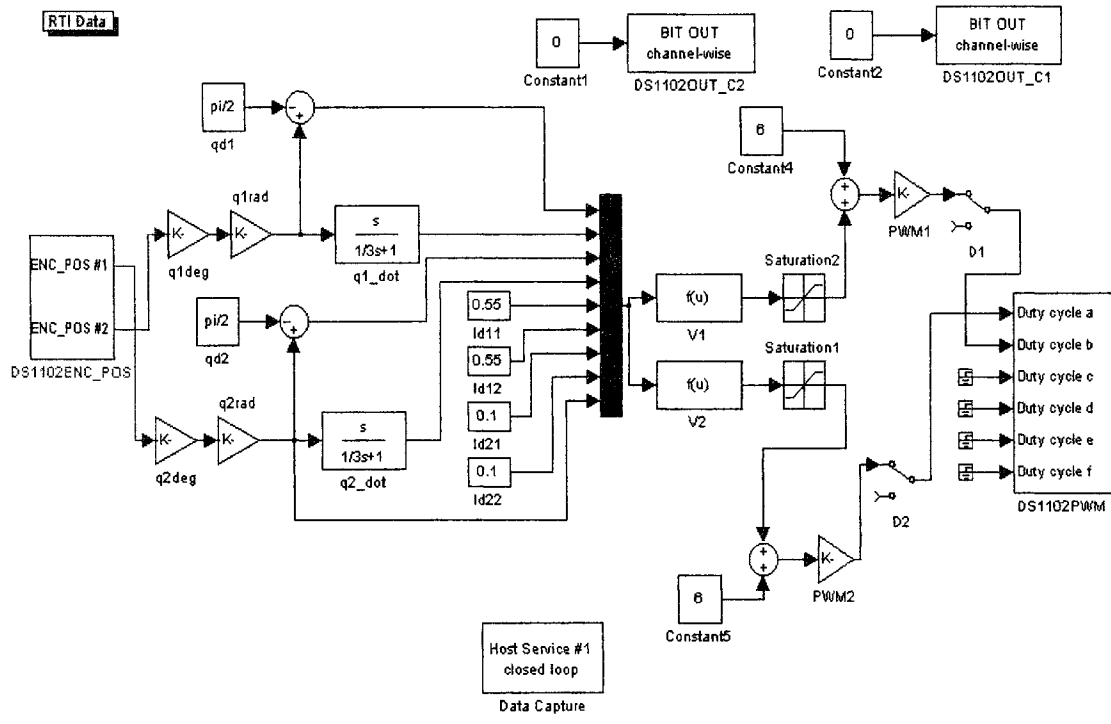


Figure A.4: Robust Controller - Simulink Block

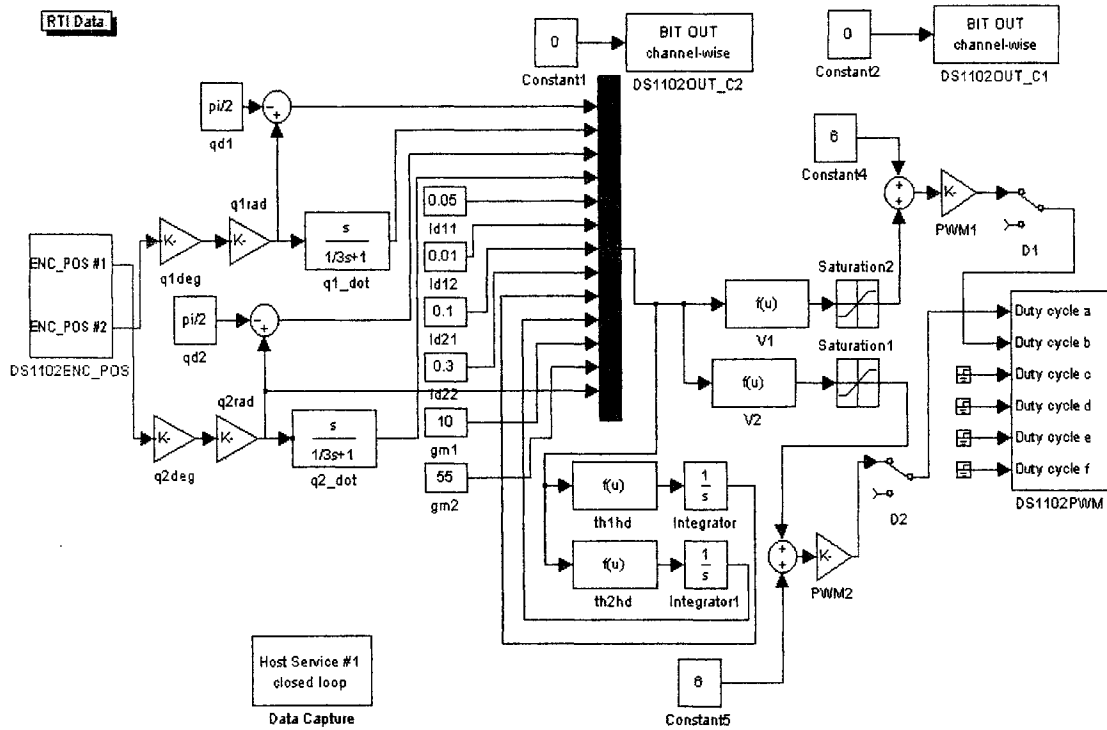


Figure A.5: Adaptive Controller - Simulink Block

# Appendix B

## Cut Sheets - LMD18200, 55V H-bridge



### LMD18200 3A, 55V H-Bridge

#### General Description

The LMD18200 is a 3A H-Bridge designed for motion control applications. The device is built using a multi-technology process which combines bipolar and CMOS control circuitry with CMOS power devices on the same monolithic structure. Ideal for driving DC and stepper motors, the LMD18200 accommodates peak output currents up to 6A. An innovative circuit which facilitates low-loss sensing of the output current has been implemented.

#### Features

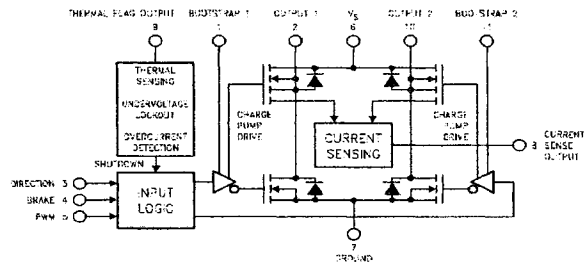
- Delivers up to 3A continuous output
- Operates at supply voltages up to 55V
- Low  $R_{DS(ON)}$  typically 0.3 $\Omega$  per switch

- TTL and CMOS compatible inputs
- No "shoot-through" current
- Thermal warning flag output at 145°C
- Thermal shutdown (outputs off) at 170°C
- Internal clamp diodes
- Shorted load protection
- Internal charge pump with external bootstrap capability

#### Applications

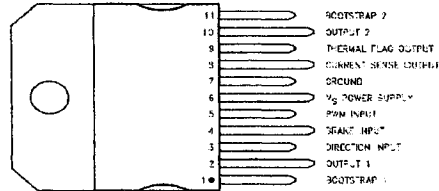
- DC and stepper motor drives
- Position and velocity servomechanisms
- Factory automation robots
- Numerically controlled machinery
- Computer printers and plotters

#### Functional Diagram



TL/H/10568-1

#### Connection Diagram and Ordering Information



Order Number LMD18200T  
See NS Package TA11B

Top View

TL/H/10568-2

Figure B.1: LMD18200, 55V H-bridge - Page1

Symbol	Parameter	Conditions	Typ	Limit	Units
$R_{DS(ON)}$	Switch ON Resistance	Output Current = 3A (Note 6)	0.33	0.4/ <b>0.6</b>	$\Omega$ (max)
$R_{DS(OFF)}$	Switch OFF Resistance	Output Current = 6A (Note 6)	0.33	0.4/ <b>0.6</b>	$\Omega$ (max)
$V_{CLAMP}$	Clamp Diode Forward Drop	Clamp Current = 3A (Note 6)	1.2	1.6	V (max)
$V_{IL}$	Logic Low Input Voltage	Pins 3, 4, 5		-0.1 0.8	V (min) V (max)
$I_{IL}$	Logic Low Input Current	$V_{IN} = -0.1V$ , Pins = 3, 4, 5		-10	$\mu A$ (max)
$V_{IH}$	Logic High Input Voltage	Pins 3, 4, 5		2 12	V (min) V (max)
$I_{IH}$	Logic High Input Current	$V_{IN} = 12V$ , Pins = 3, 4, 5		10	$\mu A$ (max)
	Current Sense Output	$I_{OUT} = 1A$ (Note 8)	377	325/ <b>300</b> 425/ <b>450</b>	$\mu A$ (min) $\mu A$ (max)
	Current Sense Linearity	$1A \leq I_{OUT} \leq 3A$ (Note 7)	$\pm 6$	$\pm 9$	%
	Undervoltage Lockout	Outputs turn OFF		9 11	V (min) V (max)
$T_{JW}$	Warning Flag Temperature	Pin 9 $\leq 0.8V$ , $I_L = 2mA$	145		$^{\circ}C$
$V_F(ON)$	Flag Output Saturation Voltage	$T_J = T_{JW}$ , $I_L = 2mA$	0.15		V
$I_F(OFF)$	Flag Output Leakage	$V_F = 12V$	0.2	10	$\mu A$ (max)
$T_{JSD}$	Shutdown Temperature	Outputs Turn OFF	170		$^{\circ}C$
$I_S$	Quiescent Supply Current	All Logic Inputs Low	13	26	mA (max)
$t_{Don}$	Output Turn-On Delay Time	Sourcing Outputs, $I_{OUT} = 3A$ Sinking Outputs, $I_{OUT} = 3A$	300 300		ns
$t_{on}$	Output Turn-On Switching Time	Bootstrap Capacitor = 10 nF Sourcing Outputs, $I_{OUT} = 3A$ Sinking Outputs, $I_{OUT} = 3A$	100 80		ns
$t_{Doff}$	Output Turn-Off Delay Times	Sourcing Outputs, $I_{OUT} = 3A$ Sinking Outputs, $I_{OUT} = 3A$	200 200		ns
$t_{off}$	Output Turn-Off Switching Times	Bootstrap Capacitor = 10 nF Sourcing Outputs, $I_{OUT} = 3A$ Sinking Outputs, $I_{OUT} = 3A$	75 70		ns
$t_{pw}$	Minimum Input Pulse Width	Pins 3, 4 and 5	1		$\mu s$
$t_{cor}$	Charge Pump Rise Time	No Bootstrap Capacitor	20		$\mu s$

Figure B.2: LMD18200, 55V H-bridge - Page2

### Electrical Characteristics Notes

Note 1: Absolute Maximum Ratings indicate limits beyond which damage to the device may occur. DC and AC electrical specifications do not apply when operating the device beyond its rated operating conditions.

Note 2: See Application Information for details regarding current limiting.

Note 3: The maximum power dissipation must be derated at elevated temperatures and is a function of  $T_{J(max)}$ ,  $\theta_{JA}$ , and  $T_A$ . The maximum allowable power dissipation at any temperature is  $P_{D(max)} = (T_{J(max)} - T_A) / \theta_{JA}$ , or the number given in the Absolute Ratings, whichever is lower. The typical thermal resistance from junction to case ( $\theta_{JC}$ ) is 1.0°C/W and from junction to ambient ( $\theta_{JA}$ ) is 30°C/W. For guaranteed operation  $T_{J(max)} = 125^\circ\text{C}$ .

Note 4: Human-body model, 100 pF discharged through a 1.5 k $\Omega$  resistor. Except Bootstrap pins (pins 1 and 11) which are protected to 1000V of ESD.

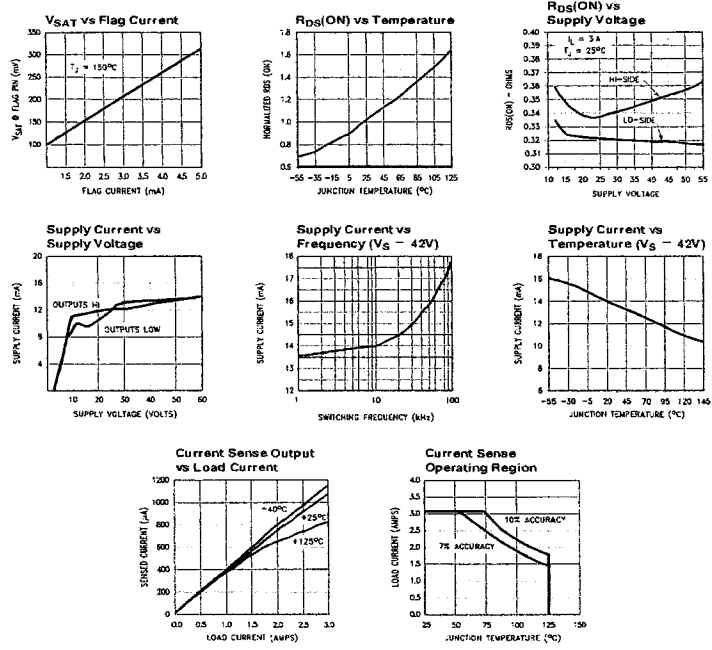
Note 5: All limits are 100% production tested at 25°C. Temperature extreme limits are guaranteed via correlation using accepted SQC (Statistical Quality Control) methods. All limits are used to calculate AOCQ, (Average Outgoing Quality Level).

Note 6: Output currents are pulsed ( $t_w < 2$  ms, Duty Cycle  $< 5\%$ ).

Note 7: Regulation is calculated relative to the current sense output value with a 1A load.

Note 8: Selections for tighter tolerance are available. Contact factory.

### Typical Performance Characteristics



TL/H/10568-3

Figure B.3: LMD18200, 55V H-bridge - Page3

### Pinout Description (See Connection Diagram)

**Pin 1, BOOTSTRAP 1 Input:** Bootstrap capacitor pin for half H-bridge number 1. The recommended capacitor (10 nF) is connected between pins 1 and 2.

**Pin 2, OUTPUT 1:** Half H-bridge number 1 output.

**Pin 3, DIRECTION Input:** See Table 1. This input controls the direction of current flow between OUTPUT 1 and OUTPUT 2 (pins 2 and 10) and, therefore, the direction of rotation of a motor load.

**Pin 4, BRAKE Input:** See Table 1. This input is used to brake a motor by effectively shorting its terminals. When braking is desired, this input is taken to a logic high level and it is also necessary to apply logic high to PWM input, pin 5. The drivers that short the motor are determined by the logic level at the DIRECTION input (Pin 3): with Pin 3 logic high, both current sourcing output transistors are ON; with Pin 3 logic low, both current sinking output transistors are ON. All output transistors can be turned OFF by applying a logic high to Pin 4 and a logic low to PWM input Pin 5; in this case only a small bias current (approximately -1.5 mA) exists at each output pin.

**Pin 5, PWM Input:** See Table 1. How this input (and DIRECTION input, Pin 3) is used is determined by the format of the PWM Signal.

**Pin 6, Vs Power Supply**

**Pin 7, GROUND Connection:** This pin is the ground return, and is internally connected to the mounting tab.

**Pin 8, CURRENT SENSE Output:** This pin provides the sourcing current sensing output signal, which is typically 377  $\mu$ A/A.

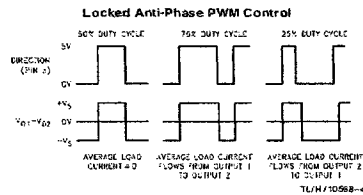
**Pin 9, THERMAL FLAG Output:** This pin provides the thermal warning flag output signal. Pin 9 becomes active-low at 145°C (junction temperature). However the chip will not shut itself down until 170°C is reached at the junction.

**Pin 10, OUTPUT 2:** Half H-bridge number 2 output.

**Pin 11, BOOTSTRAP 2 Input:** Bootstrap capacitor pin for Half H-bridge number 2. The recommended capacitor (10 nF) is connected between pins 10 and 11.

TABLE 1. Logic Truth Table

PWM	Dir	Brake	Active Output Drivers
H	H	L	Source 1, Sink 2
H	L	L	Sink 1, Source 2
L	X	L	Source 1, Source 2
H	H	H	Source 1, Source 2
H	L	H	Sink 1, Sink 2
L	X	H	NONE



### Application Information

#### TYPES OF PWM SIGNALS

The LMD18200 readily interfaces with different forms of PWM signals. Use of the part with two of the more popular forms of PWM is described in the following paragraphs.

**Simple, locked anti-phase PWM** consists of a single, variable duty-cycle signal in which is encoded both direction and amplitude information. A 50% duty-cycle PWM signal represents zero drive, since the net value of voltage (integrated over one period) delivered to the load is zero. For the LMD18200, the PWM signal drives the direction input (pin 3) and the PWM input (pin 5) is tied to logic high.

**Sign/magnitude PWM** consists of separate direction (sign) and amplitude (magnitude) signals. The (absolute) magnitude signal is duty-cycle modulated, and the absence of a pulse signal (a continuous logic low level) represents zero drive. Current delivered to the load is proportional to pulse width. For the LMD18200, the DIRECTION input (pin 3) is driven by the sign signal and the PWM input (pin 5) is driven by the magnitude signal.

#### USING THE CURRENT SENSE OUTPUT

The CURRENT SENSE output (pin 8) has a sensitivity of 377  $\mu$ A per ampere of output current. For optimal accuracy and linearity of this signal, the value of voltage generating resistor between pin 8 and ground should be chosen to limit the maximum voltage developed at pin 8 to 5V, or less. The maximum voltage compliance is 12V.

It should be noted that the recirculating currents (free wheeling currents) are ignored by the current sense circuitry. Therefore, only the currents in the upper sourcing outputs are sensed.

#### USING THE THERMAL WARNING FLAG

The THERMAL FLAG output (pin 9) is an open collector transistor. This permits a wired OR connection of thermal warning flag outputs from multiple LMD18200's, and allows the user to set the logic high level of the output signal swing to match system requirements. This output typically drives the interrupt input of a system controller. The interrupt service routine would then be designed to take appropriate steps, such as reducing load currents or initiating an orderly system shutdown. The maximum voltage compliance on the flag pin is 12V.

#### SUPPLY BYPASSING

During switching transitions the levels of fast current changes experienced may cause troublesome voltage transients across system stray inductance.

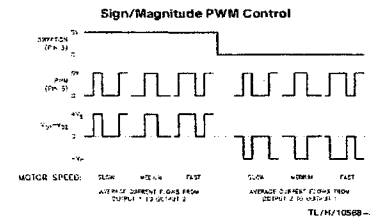


Figure B.4: LMD18200, 55V H-bridge - Page4

### Application Information (Continued)

It is normally necessary to bypass the supply rail with a high quality capacitor(s) connected as close as possible to the  $V_S$  Power Supply (Pin 6) and GROUND (Pin 7). A 1  $\mu\text{F}$  high-frequency ceramic capacitor is recommended. Care should be taken to limit the transients on the supply pin below the Absolute Maximum Rating of the device. When operating the chip at supply voltages above 40V a voltage suppressor (transorb) such as P6KE82A is recommended from supply to ground. Typically the ceramic capacitor can be eliminated in the presence of the voltage suppressor. Note that when driving high load currents a greater amount of supply bypass capacitance (in general at least 100  $\mu\text{F}$  per Amp of load current) is required to absorb the recirculating currents of the inductive loads.

#### CURRENT LIMITING

Current limiting protection circuitry has been incorporated into the design of the LMD18200. With any power device it is important to consider the effects of the substantial surge currents through the device that may occur as a result of shorted loads. The protection circuitry monitors this increase in current (the threshold is set to approximately 10 Amps) and shuts off the power device as quickly as possible in the event of an overload condition. In a typical motor driving application the most common overload faults are caused by shorted motor windings and locked rotors. Under these conditions the inductance of the motor (as well as any series inductance in the  $V_{CC}$  supply line) serves to reduce the magnitude of a current surge to a safe level for the LMD18200. Once the device is shut down, the control circuitry will periodically try to turn the power device back on. This feature allows the immediate return to normal operation in the event that the fault condition has been removed. While the fault remains however, the device will cycle in and out of thermal shutdown. This can create voltage transients on the  $V_{CC}$  supply line and therefore proper supply bypassing techniques are required.

The most severe condition for any power device is a direct, hard-wired ("screwdriver") long term short from an output to ground. This condition can generate a surge of current through the power device on the order of 15 Amps and require the die and package to dissipate up to 500 Watts of power for the short time required for the protection circuitry to shut off the power device. This energy can be destructive, particularly at higher operating voltages (> 30V) so

some precautions are in order. Proper heat sink design is essential and it is normally necessary to heat sink the  $V_{CC}$  supply pin (pin 6) with 1 square inch of copper on the PCB.

#### INTERNAL CHARGE PUMP AND USE OF BOOTSTRAP CAPACITORS

To turn on the high-side (sourcing) DMOS power devices, the gate of each device must be driven approximately 8V more positive than the supply voltage. To achieve this an internal charge pump is used to provide the gate drive voltage. As shown in Figure 1, an internal capacitor is alternately switched to ground and charged to about 14V, then switched to  $V_S$  supply thereby providing a gate drive voltage greater than  $V_S$  supply. This switching action is controlled by a continuously running internal 300 kHz oscillator. The rise time of this drive voltage is typically 20  $\mu\text{s}$  which is suitable for operating frequencies up to 1 kHz.

For higher switching frequencies, the LMD18200 provides for the use of external bootstrap capacitors. The bootstrap principle is in essence a second charge pump whereby a large value capacitor is used which has enough energy to quickly charge the parasitic gate input capacitance of the power device resulting in much faster rise times. The switching action is accomplished by the power switches themselves (Figure 2). External 10 nF capacitors, connected from the outputs to the bootstrap pins of each high-side switch provide typically less than 100 ns rise times allowing switching frequencies up to 500 kHz.

#### INTERNAL PROTECTION DIODES

A major consideration when switching current through inductive loads is protection of the switching power devices from the large voltage transients that occur. Each of the four switches in the LMD18200 have a built-in protection diode to clamp transient voltages exceeding the positive supply or ground to a safe diode voltage drop across the switch.

The reverse recovery characteristics of these diodes, once the transient has subsided, is important. These diodes must come out of conduction quickly and the power switches must be able to conduct the additional reverse recovery current of the diodes. The reverse recovery time of the diodes protecting the sourcing power devices is typically only 70 ns with a reverse recovery current of 1A when tested with a full 8A of forward current through the diode. For the sinking devices the recovery time is typically 100 ns with 4A of reverse current under the same conditions.

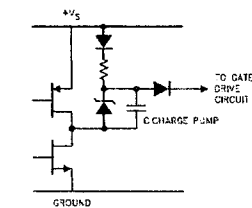


FIGURE 1. Internal Charge Pump Circuitry

TL/N/10568-6

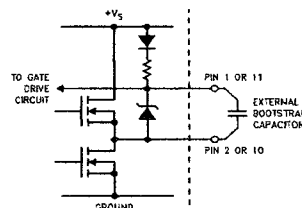


FIGURE 2. Bootstrap Circuitry

TL/N/10568-7

Figure B.5: LMD18200, 55V H-bridge - Page5

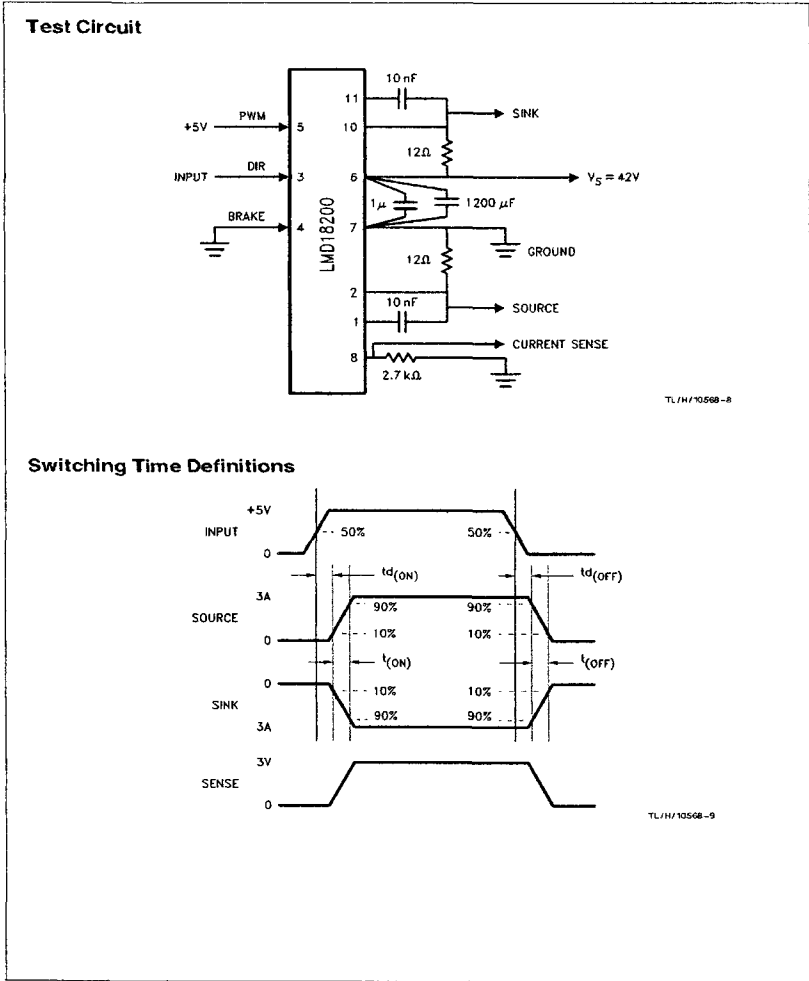
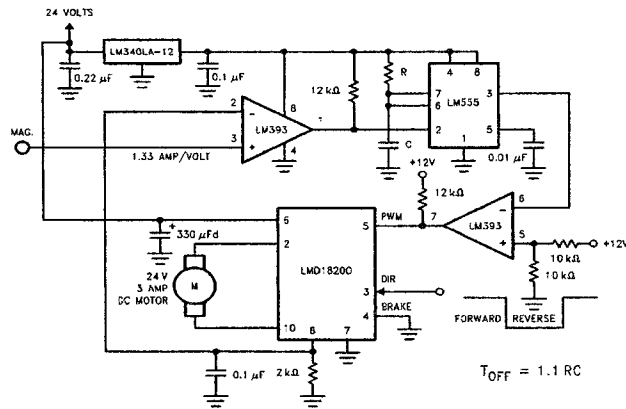


Figure B.6: LMD18200, 55V H-bridge - Page6

### Typical Applications

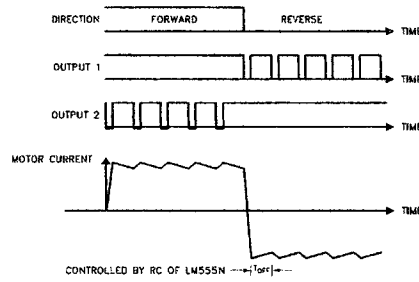
**Fixed Off-Time Control:** This circuit controls the current through the motor by applying an average voltage equal to zero to the motor terminals for a fixed period of time, whenever the current through the motor exceeds the commanded current. This action causes the motor current to vary

slightly about an externally controlled average level. The duration of the Off-period is adjusted by the resistor and capacitor combination of the LM555. In this circuit the Sign/Magnitude mode of operation is implemented (see Types of PWM Signals).



TL/H/10568-10

### Switching Waveforms



TL/H/10568-11

Figure B.7: LMD18200, 55V H-bridge - Page7

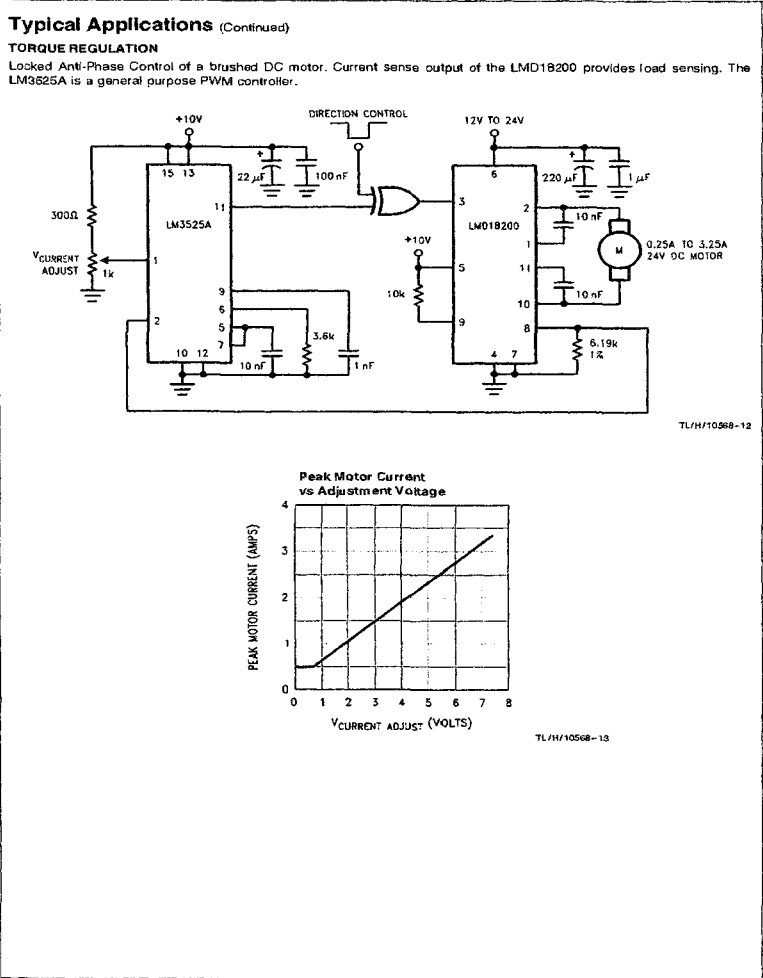


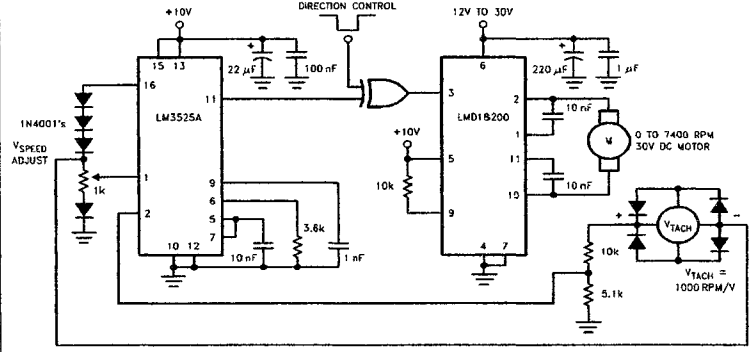
Figure B.8: LMD18200, 55V H-bridge - Page8



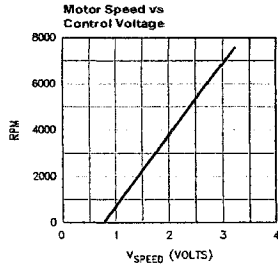
**Typical Applications (Continued)**

**VELOCITY REGULATION**

Utilizes tachometer output from the motor to sense motor speed for a locked anti-phase control loop.



TL/H/1056B-14



TL/H/1056B-15

Figure B.9: LMD18200, 55V H-bridge - Page9

LMD18200 3A, 55V H-Bridge

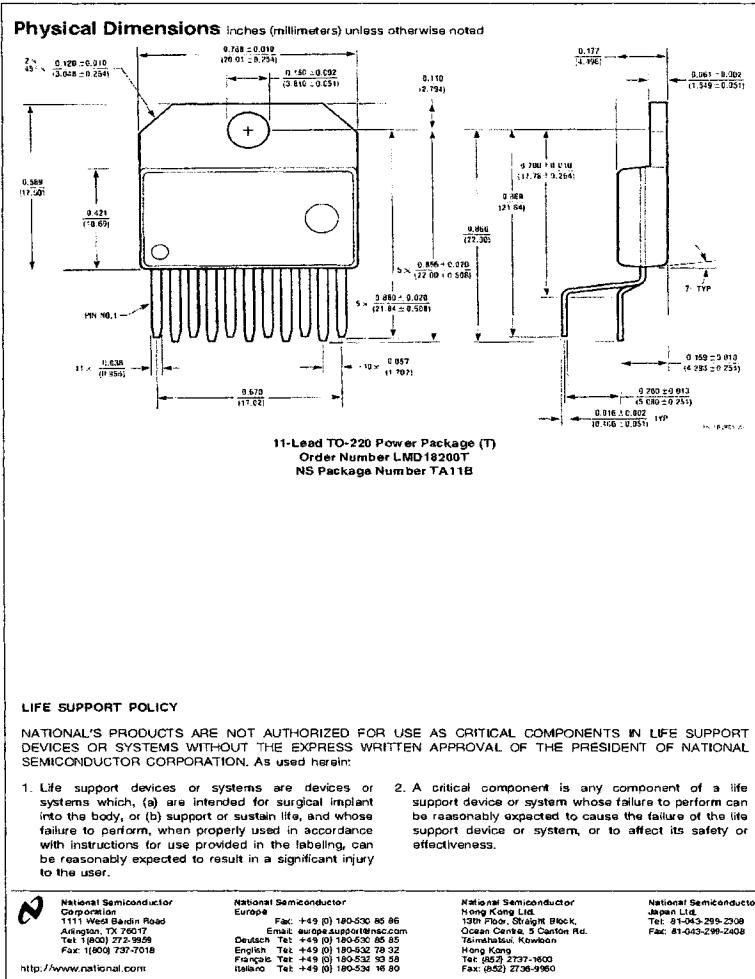


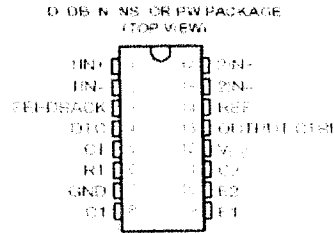
Figure B.10: LMD18200, 55V H-bridge - Page 10

# Appendix C

## Cut Sheets - TL494, PWM Control Circuit

TL494  
PULSE-WIDTH-MODULATION CONTROL CIRCUITS

- Complete PWM Power-Control Circuitry
- Uncommitted Outputs for 200 mA Sink or Source Current
- Output Control Selects Single Ended or Push-Pull Operation
- Internal Circuitry Prohibits Double Pulse at Either Output
- Variable Dead Time Provides Control Over Total Range
- Internal Regulator Provides a Stable 5-V Reference Supply With 5% Tolerance
- Circuit Architecture Allows Easy Synchronization



**description**

The TL494 incorporates all the functions required in the construction of a pulse-width modulation (PWM) control circuit on a single chip. Designed primarily for power-supply control, this device offers the flexibility to tailor the power-supply control circuitry to a specific application.

The TL494 contains two error amplifiers, an on-chip adjustable oscillator, a dead-time control (DTC) comparator, a pulse-skewing control flip-flop, a 5-V, 5%-precision regulator, and output control circuits.

The error amplifiers exhibit a common-mode voltage range from  $-0.3\text{ V}$  to  $V_{CC} - 2\text{ V}$ . The dead-time control comparator has a fixed offset that provides approximately 5% dead time. The on-chip oscillator can be bypassed by terminating R1 to the reference output and providing a sawtooth input to CT, or it can drive the common outputs in synchronous multiple-lead power supplies.

The uncommitted output transistors provide either common-emitter or emitter-follower output capability. The TL494 provides for push-pull or single-ended output operation, which can be selected through the output control function. The architecture of this device prohibits the possibility of either output being pulsed twice during push-pull operation.

The TL494C is characterized for operation from  $0^\circ\text{C}$  to  $70^\circ\text{C}$ . The TL494 is characterized for operation from  $-40^\circ\text{C}$  to  $85^\circ\text{C}$ .

AVAILABLE OPTIONS

TA	PACKAGED DEVICES				
	SMALL OUTLINE (DB)	PLASTIC DIP (N)	SMALL OUTLINE (NS)	SHRINK SMALL OUTLINE (DB)	THIN SHRINK SMALL OUTLINE (PW)
TL494C (DB)	TL494CDB	TL494CN	TL494CNS	TL494CDB	TL494CPW
TL494 (NS)	TL494NS	TL494N	—	—	—

The D, DB, N, NS, and PW packages are available in leaded and leadless. Add the suffix "R" to denote RoHS-compliant (TL494CDBR).



Be sure to check that you are getting the right product, standard warranty, and use of control applications of Texas Instruments. Please refer to our website for more information on our products and services.

Reproduction of this document is prohibited without the written permission of Texas Instruments. Please refer to our website for more information on our products and services.



Copyright © 2004 Texas Instruments Incorporated

Figure C.1: TL494, PWM Control Circuit - Page1

TL494  
PULSE-WIDTH-MODULATION CONTROL CIRCUITS

FIGURE C.2. TL494, PWM CONTROL CIRCUIT

FUNCTION TABLE	
INPUT TO OUTPUT CTRL	OUTPUT FUNCTION
0000	ENABLES THE CONTROL CIRCUIT
0001	ENABLES THE CONTROL CIRCUIT

functional block diagram

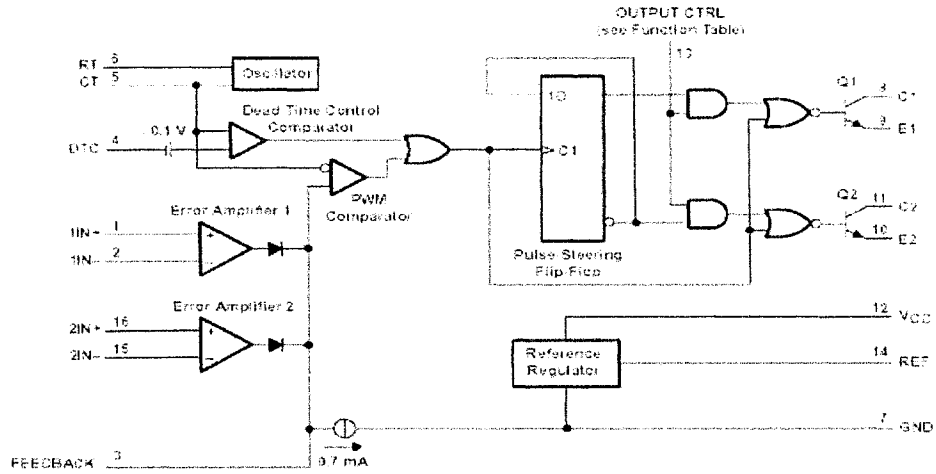


Figure C.2: TL494, PWM Control Circuit - Page2

**TL494**  
**PULSE-WIDTH-MODULATION CONTROL CIRCUITS**

(continued from page 1)

**absolute maximum ratings over operating free-air temperature range (unless otherwise noted)<sup>†</sup>**

Supply voltage, $V_{CC}$ (see Note 1)	41 V
Amplifier input voltage, $V_i$	$V_{CC} + 0.3$ V
Collector output voltage, $V_{CO}$	41 V
Collector output current, $I_C$	250 mA
Package thermal impedance, $\theta_{JA}$ (see Note 2 and 3)	
D package	73 °C/W
DB package	82 °C/W
N package	87 °C/W
NS package	84 °C/W
PW package	116 °C/W
Lead temperature: 1.6 mm (1/16 inch) from case for 10 seconds	260 °C
Storage temperature range, $T_{STG}$	-65°C to 150 °C

<sup>†</sup> These ratings apply only when the device is being operated at its rated power level and package temperature. The device may be operated at higher power levels at lower ambient temperatures, but the maximum power dissipation must be limited to the maximum power dissipation at the highest ambient temperature. For more information on absolute maximum ratings, see the Absolute Maximum Ratings section of the TL494 data sheet.

- NOTES: 1. All voltages are with respect to the reference pin 2 terminal.  
 2. Maximum power dissipation is a function of  $\theta_{JA}$ ,  $\theta_{JC}$ , and  $T_{JC}$ . The maximum allowable power dissipation at any allowable ambient temperature  $T_A$  and package  $T_{JC}$  is calculated in the Absolute Maximum Ratings section of the TL494 data sheet.  
 3. The package thermal impedance  $\theta_{JA}$  is listed in accordance with JEDEC 91-7.

**recommended operating conditions**

		MIN	MAX	UNIT
$V_{CC}$	Supply voltage	7	40	V
$V_i$	Amplifier input voltage	$V_{CC} - 0.3$	$V_{CC} + 1$	V
$V_{CO}$	Collector output voltage		40	V
	Collector output current (at 25°C temperature)		250	mA
	Collector output current (at 100°C temperature)		80	mA
$f_{osc}$	Oscillator frequency	1	200	kHz
$f_{sw}$	Switching frequency	100	10000	Hz
$f_{sw}$	Switching frequency	1.5	20.0	kHz
$T_A$	Operating free-air temperature	-65	150	°C
		$\theta_{JA}$	$\theta_{JC}$	°C/W



Figure C.3: TL494, PWM Control Circuit - Page3

**TL494**  
**PULSE-WIDTH-MODULATION CONTROL CIRCUITS**

www.ti.com | SNVA555 | REVISED 2009-01-20

electrical characteristics over recommended operating free-air temperature range,  $V_{CC} = 15\text{ V}$ ,  $f = 10\text{ kHz}$  (unless otherwise noted)

**reference section**

PARAMETER	TEST CONDITIONS†	TL494C, TL494I			UNIT
		MIN	TYP†	MAX	
Output voltage (BMT)	$V_{CC} = 15\text{ V}$	1.5	1.5	1.5	V
Output frequency	100 kHz, $V_{CC} = 15\text{ V}$		10	10	kHz
TL494 frequency	100 kHz, $V_{CC} = 15\text{ V}$		10	10	kHz
TL494 duty cycle (variable error amplifier)	$V_{CC} = 15\text{ V}$ , $V_{EE} = 0\text{ V}$		50	50	%
TL494 duty cycle (variable error amplifier)	$V_{CC} = 15\text{ V}$		50	50	%

† For conditions not specified by the manufacturer, the manufacturer assumes that the number of test devices is large enough so that the sample mean and standard deviation are close to the true mean and standard deviation of the actual production process. The number of test devices is not specified, but the inherent variability of the manufacturing process is considered. The number of test devices is not specified, but the inherent variability of the manufacturing process is considered.

**oscillator section,  $C_T = 0.01\ \mu\text{F}$ ,  $R_T = 12\ \text{k}\Omega$  (see Figure 1)**

PARAMETER	TEST CONDITIONS†	TL494, TL494I			UNIT
		MIN	TYP†	MAX	
Frequency			10		kHz
Standard deviation of frequency <sup>‡</sup>	All values at $V_{CC} = 15\text{ V}$ and $T_A$ unspecified		1%		(100 Hz)
Frequency drift with temperature <sup>§</sup>	$V_{CC} = 15\text{ V}$ , $T_A = 40^\circ\text{C}$ to $125^\circ\text{C}$		1		ppm/°C
Frequency drift with propagation <sup>¶</sup>	$V_{CC} = 15\text{ V}$ , $T_A = 25^\circ\text{C}$		1%		ppm/ppm

† For conditions not specified by the manufacturer, the manufacturer assumes that the number of test devices is large enough so that the sample mean and standard deviation are close to the true mean and standard deviation of the actual production process. The number of test devices is not specified, but the inherent variability of the manufacturing process is considered.

‡ Standard deviation is a measure of the statistical distribution of the measured values derived from the formula:

$$\sigma = \sqrt{\frac{\sum_{i=1}^N (x_i - \bar{x})^2}{N - 1}}$$

¶ Propagation is the effect of timing repeatability and propagation delay on the measured frequency.

**error-amplifier section (see Figure 2)**

PARAMETER	TEST CONDITIONS	TL494, TL494I			UNIT
		MIN	TYP†	MAX	
Input offset voltage	$V_{CC} = 15\text{ V}$ , $V_{EE} = 0\text{ V}$		0	15	mV
Input offset current	$V_{CC} = 15\text{ V}$ , $V_{EE} = 0\text{ V}$		0	100	nA
Input bias current	$V_{CC} = 15\text{ V}$ , $V_{EE} = 0\text{ V}$		0	10	nA
Common-mode input voltage range	$V_{CC} = 15\text{ V}$ , $V_{EE} = 0\text{ V}$	0.5	10	14.5	V
Common-mode input voltage range	$V_{CC} = 15\text{ V}$ , $V_{EE} = 0\text{ V}$ , $V_{CM} = 0\text{ V}$ to $10\text{ V}$	0	10	14.5	V
Common-mode input voltage range	$V_{CC} = 15\text{ V}$ , $V_{EE} = 0\text{ V}$ , $V_{CM} = 0\text{ V}$ to $10\text{ V}$ , $R_T = 12\ \text{k}\Omega$	0	10	14.5	V
Common-mode rejection ratio	$V_{CC} = 15\text{ V}$ , $V_{EE} = 0\text{ V}$ , $V_{CM} = 0\text{ V}$ to $10\text{ V}$	60	80	80	dB
Output load current (FEEDBACK)	$V_{CC} = 15\text{ V}$ , $V_{EE} = 0\text{ V}$ , $V_{OUT} = 10\text{ V}$	0	10	10	mA
Output short-circuit current (FEEDBACK)	$V_{CC} = 15\text{ V}$ , $V_{EE} = 0\text{ V}$ , $V_{OUT} = 0\text{ V}$	0	10	10	mA

† All values are typical, except for common-mode input range, which is guaranteed at  $T_A = 25^\circ\text{C}$ .



Figure C.4: TL494, PWM Control Circuit - Page 4

TL494  
PULSE-WIDTH-MODULATION CONTROL CIRCUITS

electrical characteristics over recommended operating free-air temperature range,  $V_{CC} = 15\text{ V}$ ,  $f = 10\text{ kHz}$  (unless otherwise noted)

output section

PARAMETER	TEST CONDITIONS	MIN	TYPT	MAX	UNIT
Output current (continuous)	See Figure 1	0	1.0	1.5	A
Output current (pulse)	See Figure 1	0	1.0	1.5	A
Output voltage regulation (V <sub>OUT</sub> )	Load regulation: $R_{L} = 10\ \Omega$ to $100\ \Omega$ Line regulation: $V_{IN} = 12\text{ V}$ to $15\text{ V}$	0	0.1	0.2	%
Output voltage (no load)	See Figure 1	0	1.0	1.5	V

\* All typical values except for temperature coefficient are at  $T_A = 25^\circ\text{C}$ .

dead-time control section (see Figure 1)

PARAMETER	TEST CONDITIONS	MIN	TYPT	MAX	UNIT
Minimum dead-time (DEAD-TIME <sub>MIN</sub> )	See Figure 1	0	0.5	1.0	$\mu\text{s}$
Maximum dead-time (DEAD-TIME <sub>MAX</sub> )	See Figure 1	0	1.0	1.5	$\mu\text{s}$
Minimum dead-time (DEAD-TIME <sub>MIN</sub> )	Temperature	0	0.5	1.0	$\mu\text{s}$
	Manufacturing	0	0.5	1.0	$\mu\text{s}$

\* All typical values except for manufacturing coefficient are at  $T_A = 25^\circ\text{C}$ .

PWM comparator section (see Figure 1)

PARAMETER	TEST CONDITIONS	MIN	TYPT	MAX	UNIT
Input threshold voltage (REF <sub>THRESH</sub> )	See Figure 1	0	1.0	1.5	V
Input hysteresis voltage (REF <sub>HYST</sub> )	See Figure 1	0	0.1	0.2	V

\* All typical values except for temperature coefficient are at  $T_A = 25^\circ\text{C}$ .

total device

PARAMETER	TEST CONDITIONS	MIN	TYPT	MAX	UNIT
Efficiency (continuous)	$R_T = V_{OUT} / I_{OUT}$ (All other inputs with outputs open)	$V_{OUT} = 12\text{ V}$	0	80	%
		$V_{OUT} = 0\text{ V}$	0	70	%
Warranty period (years)	At 25°C, 100% (1000 h)	See Figure 1	0	10	years

\* All typical values except for temperature coefficient are at  $T_A = 25^\circ\text{C}$ .

switching characteristics,  $T_A = 25^\circ\text{C}$

PARAMETER	TEST CONDITIONS	MIN	TYPT	MAX	UNIT
Rise time	Common-emitter configuration (see Figure 1)	0	0.5	1.0	$\mu\text{s}$
Fall time		0	0.5	1.0	$\mu\text{s}$
Rise time	Emitter-coupled configuration (see Figure 1)	0	0.5	1.0	$\mu\text{s}$
Fall time		0	0.5	1.0	$\mu\text{s}$

\* All typical values except for temperature coefficient are at  $T_A = 25^\circ\text{C}$ .



Figure C.5: TL494, PWM Control Circuit - Page5



TL494  
PULSE-WIDTH-MODULATION CONTROL CIRCUITS

www.ti.com/lit/ug/tl494-ug

PARAMETER MEASUREMENT INFORMATION

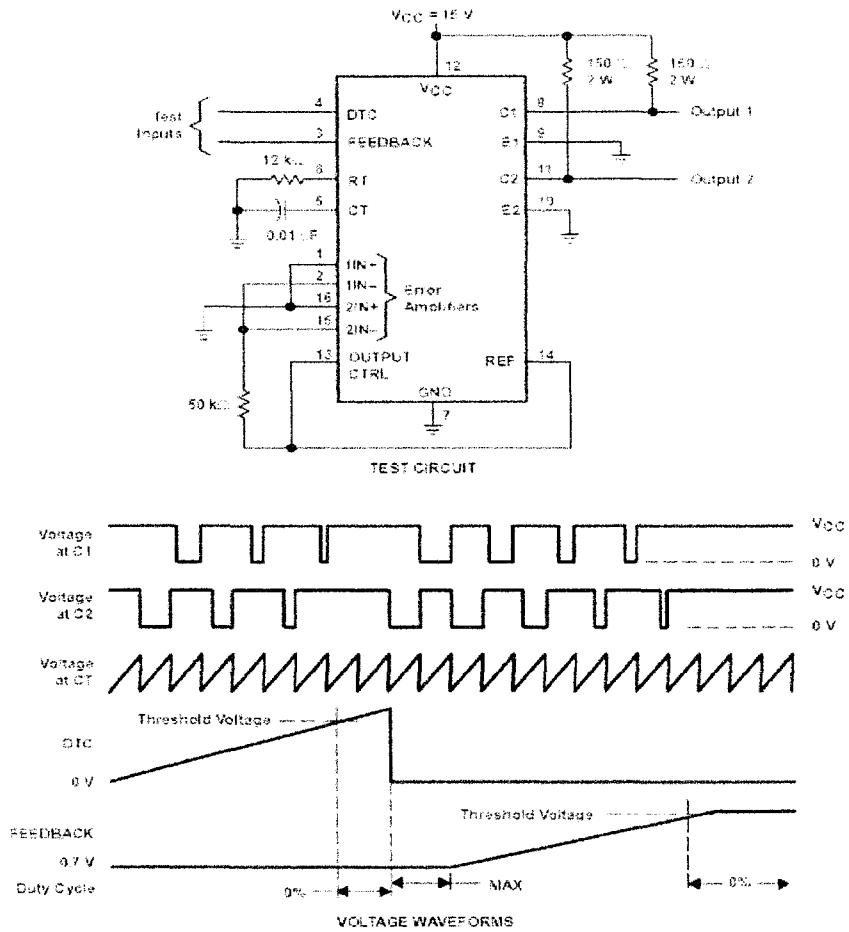


Figure 1. Operational Test Circuit and Waveforms



Figure C.6: TL494, PWM Control Circuit - Page6

PARAMETER MEASUREMENT INFORMATION

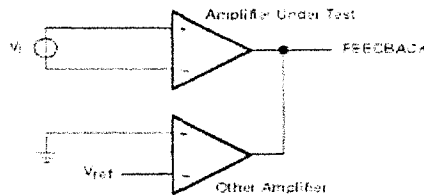
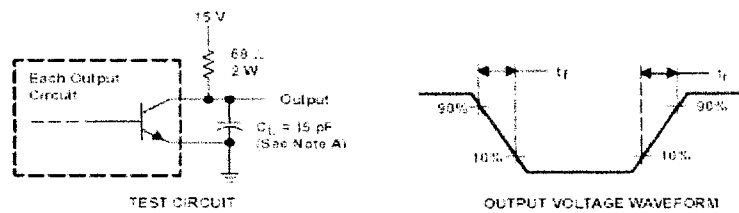
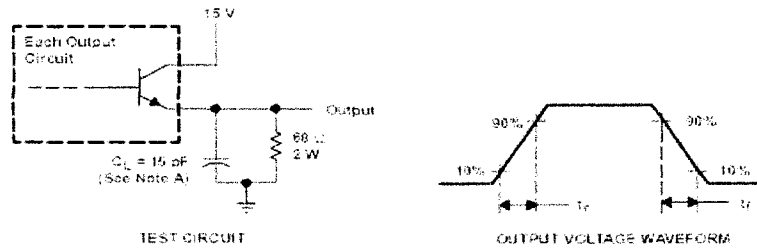


Figure 2 Amplifier Characteristics



NOTE 1: \$C\_L\$ includes probe and any cable inductance.

Figure 3. Common Emitter Configuration



NOTE 1: \$C\_L\$ includes probe and any cable inductance.

Figure 4. Emitter Follower Configuration



Figure C.7: TL494, PWM Control Circuit - Page7

TL494  
PULSE-WIDTH-MODULATION CONTROL CIRCUITS

TYPICAL CHARACTERISTICS

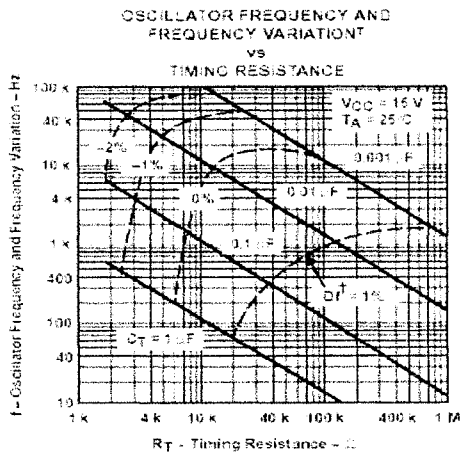


Figure 5

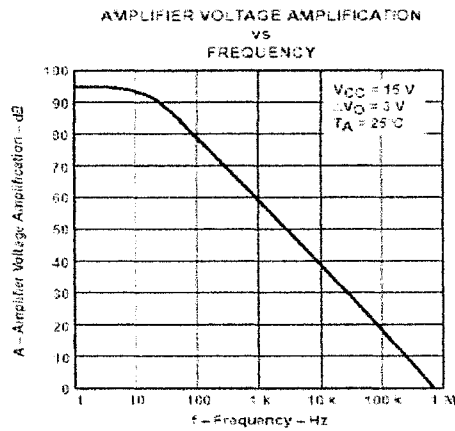


Figure 6



Figure C.8: TL494, PWM Control Circuit - Page8

# Appendix D

## Cut Sheets - Servo Systems Encoder

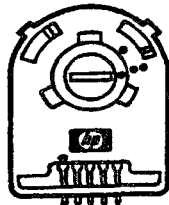


A Full Service Motion Control Distributor and Systems Integrator.  
Motion Control • Robotics • Avionic • Marine • Components and Systems

Hewlet Packard model  
Incremental Encoder Specifications

Supply Voltage, Vcc.....-.05 to 7V  
Output Voltage, Vo.....-.05 to Vcc  
Output Current per Channel.....-1.0 ma to 5 ma

PIN OUT	
[1]	GND
[2]	
[3]	Channel A
[4]	+ Vcc
[5]	Channel B



• Pin One

115 Main Road • P.O. Box 97 • Montville, NJ 07045-0097 • (973) 335-1007 Toll Free: (800) 922-1103 Fax: (973) 335-1661  
www.servosystems.com • e-mail: info@servosystems.com

Figure D.1: Servo Systems Encoder

# Appendix E

## Cut Sheets - DC Motor

**9XXX MOTOR SIZE DATA (25° C)**

PARAMETER	SYMBOL	UNITS	9X12	9X32	9X13	9X33	9X14	9X34
1 Motor Constant	K <sub>M</sub>	oz-in <sup>2</sup> /W	1.16	1.62	1.94	2.66	2.05	3.01
2 Peak Torque (Stall)	T <sub>P</sub>	oz-in	8.35	13.8	15.8	31.8	23.9	41.3
3 No Load Speed	S <sub>0</sub>	rpm	8251	7015	5592	5993	7666	6151
4 Motor Friction Torque	T <sub>F</sub>	oz-in	0.40	0.50	0.50	0.60	0.50	0.60
5 Viscous Damping Factor	D	oz-in/krpm	0.0086	0.0272	0.0113	0.0335	0.0125	0.0367
6 Damping Constant	K <sub>D</sub>	oz-in <sup>2</sup> /krpm	1.00	1.94	2.78	5.23	3.11	5.68
7 Electrical Time Constant	T <sub>E</sub>	ms	0.53	0.63	0.74	0.84	0.80	0.85
8 Mechanical Time Constant	T <sub>M</sub>	ms	22.8	14.4	14.7	9.29	18.1	9.25
9 Thermal Time Constant	T <sub>TH</sub>	min	7.21	7.21	11.1	11.1	12.0	12.0
10 Thermal Impedance	R <sub>TH</sub>	deg C/W	22.7	22.7	19.1	19.1	17.1	17.1
11 Maximum Winding Temperature	Θ <sub>MX</sub>	deg C max	155	155	155	155	155	155
12 Motor inertia	J <sub>M</sub>	oz-in-s <sup>2</sup>	2.2x10 <sup>-4</sup>	2.7x10 <sup>-4</sup>	3.9x10 <sup>-4</sup>	4.5x10 <sup>-4</sup>	5.4x10 <sup>-4</sup>	5.9x10 <sup>-4</sup>
13 Motor Weight	W <sub>M</sub>	oz	8.96	6.98	8.98	8.90	10.1	10.1
14 Motor Length, 94XX, 92XX	L <sub>1</sub>	in max	1.828	1.828	2.203	2.203	2.403	2.403
15 Motor Length, 95XX	L <sub>1</sub>	in max	1.779	1.779	2.154	2.154	2.354	2.354

**9XX2 MOTOR WINDING DATA (25° C)**

PARAMETER	SYMBOL	UNITS	9X12				9X32			
			WDG #1	WDG #3	WDG #4	WDG #1	WDG #2	WDG #3	WDG #4	
16 Voltage	E	V	6.00	12.0	19.1	24.0	12.0	19.1	24.0	30.3
17 Torque Constant	K <sub>T</sub>	oz-in/A	0.93	1.86	2.95	3.72	2.20	3.50	4.40	5.53
18 Back EMF Constant	K <sub>E</sub>	V/krpm	0.89	1.38	2.18	2.75	1.63	2.59	3.25	4.09
19 Terminal Resistance	R <sub>T</sub>	ohms	0.75	2.63	6.46	10.2	1.93	4.70	7.38	11.6
20 Inductance	L	mH	0.34	1.35	3.40	5.42	1.16	2.94	4.84	7.34
21 No Load Current	I <sub>0</sub>	A	0.51	0.26	0.16	0.13	0.32	0.20	0.18	0.13
22 Peak Current (Stall)	I <sub>P</sub>	A	8.03	4.56	2.96	2.35	6.22	4.06	3.25	2.60

**9XX3 MOTOR WINDING DATA (25° C)**

PARAMETER	SYMBOL	UNITS	9X13				9X33			
			WDG #1	WDG #2	WDG #3	WDG #4	WDG #1	WDG #2	WDG #3	WDG #4
23 Voltage	E	V	6.00	12.0	19.1	24.0	12.0	19.1	24.0	30.3
24 Torque Constant	K <sub>T</sub>	oz-in/A	1.42	2.80	4.47	5.60	2.67	4.20	5.25	6.68
25 Back EMF Constant	K <sub>E</sub>	V/krpm	1.05	2.07	3.31	4.14	1.98	3.10	3.90	4.94
26 Terminal Resistance	R <sub>T</sub>	ohms	0.64	2.17	5.32	8.33	1.08	2.53	3.94	6.21
27 Inductance	L	mH	0.40	1.54	3.99	6.17	0.84	2.08	3.29	5.27
28 No Load Current	I <sub>0</sub>	A	0.40	0.20	0.13	0.10	0.30	0.19	0.15	0.12
29 Peak Current (Stall)	I <sub>P</sub>	A	9.36	5.54	3.59	2.88	11.1	7.65	6.09	4.88

**9XX4 MOTOR WINDING DATA (25° C)**

PARAMETER	SYMBOL	UNITS	9X14				9X34			
			WDG #1	WDG #2	WDG #3	WDG #4	WDG #1	WDG #2	WDG #3	WDG #4
30 Voltage	E	V	12.0	19.1	24.0	30.3	12.0	19.1	24.0	30.3
31 Torque Constant	K <sub>T</sub>	oz-in/A	2.06	3.27	4.13	5.22	2.58	4.07	5.17	6.50
32 Back EMF Constant	K <sub>E</sub>	V/krpm	1.53	2.42	3.05	3.86	1.91	3.01	3.82	4.81
33 Terminal Resistance	R <sub>T</sub>	ohms	1.10	2.59	4.06	6.40	0.83	1.89	2.96	4.62
34 Inductance	L	mH	0.81	2.04	3.25	5.19	0.63	1.56	2.51	3.97
35 No Load Current	I <sub>0</sub>	A	0.28	0.18	0.14	0.11	0.33	0.21	0.15	0.13
36 Peak Current (Stall)	I <sub>P</sub>	A	10.9	7.36	5.91	4.73	14.5	10.1	8.11	6.55

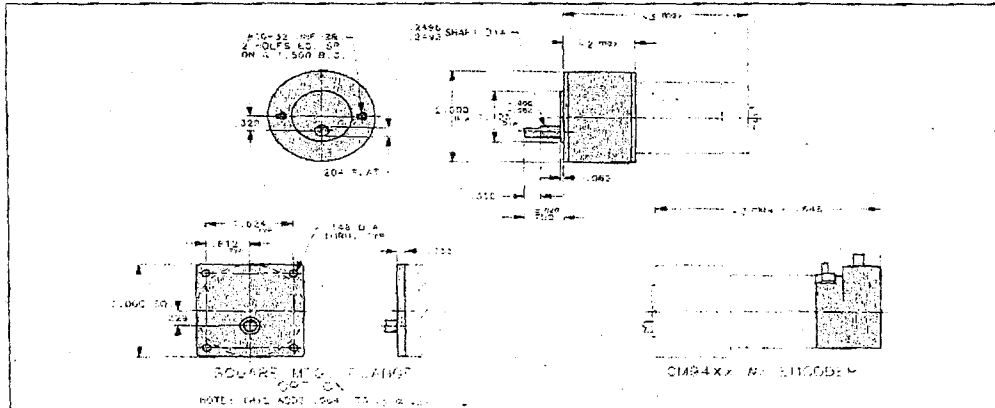
Figure E.1: DC Motor - Page1

**GM9XXX SPUR GEARMOTOR DATA (25° C)**

PARAMETER	SYM	UNITS	GEAR RATIOS															
			5.8974	11.500	19.858	38.333	65.527	127.78	218.42	425.93	728.08	1419.8	2426.9	4732.5				
37 Load, Standard Gearing	T <sub>L</sub>	oz-in max	175	175	175	175	175	175	175	175	175	175	175	175	175	175	175	
38 Load, High Torque Option	T <sub>L</sub>	oz-in max	—	—	300	300	300	300	300	300	300	300	300	300	300	300	300	
39 Load, Wide Face Option	T <sub>L</sub>	oz-in max	—	—	500	500	500	500	500	500	500	500	500	500	500	500	500	
40 N.L. Speed, GM9X12	S <sub>g</sub>	rpm	1399	717	420	215	128	64.6	37.8	19.4	11.3	5.81	3.40	1.74	—	—	—	
41 N.L. Speed, GM9X12	S <sub>g</sub>	rpm	1189	610	357	183	107	54.9	32.1	16.5	9.63	4.94	2.89	1.48	—	—	—	
42 N.L. Speed, GM9X13	S <sub>g</sub>	rpm	948	486	284	146	85.3	43.8	25.6	13.1	7.88	3.94	2.30	1.18	—	—	—	
43 N.L. Speed, GM9X33	S <sub>g</sub>	rpm	1016	521	305	156	91.5	46.9	27.4	14.1	8.23	4.22	2.47	1.27	—	—	—	
44 N.L. Speed, GM9X14	S <sub>g</sub>	rpm	1300	667	390	200	117	60.0	35.1	18.0	10.5	5.40	3.16	1.62	—	—	—	
45 N.L. Speed, GM9X34	S <sub>g</sub>	rpm	1043	535	313	160	93.9	48.1	28.2	14.4	8.45	4.33	2.53	1.30	—	—	—	
46 Gearbox Shaft Rotation	—	—	—	—	cw	ccw	ccw	ccw	ccw	ccw	ccw	ccw	ccw	ccw	ccw	ccw	ccw	ccw
47 Gearbox Efficiency	—	%	81	81	73	73	66	66	59	59	53	53	48	48	—	—	—	
48 Gearbox Weight, Std./H.T.	WG	oz	5.90	5.90	8.26	8.26	6.62	6.62	6.98	6.98	7.34	7.34	8.18	8.18	6.16	6.16	6.16	
49 Gearbox Weight, Wide Face	WG	oz	—	—	6.52	6.52	6.88	6.88	7.24	7.24	8.08	8.08	—	—	—	—	—	
50 Gearbox Length, Std./H.T.	L <sub>2</sub>	in max	1.373	1.373	1.373	1.373	1.373	1.373	1.373	1.373	1.373	1.373	1.528	1.528	1.528	1.528	1.528	
51 Gearbox Length, Wide Face	L <sub>2</sub>	in max	—	—	1.373	1.373	1.373	1.373	1.373	1.373	1.373	1.373	1.528	1.528	—	—	—	
52 Length, GM94X2, Std./H.T.	L <sub>3</sub>	in max	3.101	3.101	3.101	3.101	3.101	3.101	3.101	3.101	3.101	3.101	3.256	3.256	3.256	3.256	3.256	
53 Length, GM94X2, Wide Face	L <sub>3</sub>	in max	—	—	3.101	3.101	3.101	3.101	3.101	3.101	3.101	3.101	3.256	3.256	—	—	—	
54 Length, GM94X3, Std./H.T.	L <sub>3</sub>	in max	3.476	3.476	3.476	3.476	3.476	3.476	3.476	3.476	3.476	3.476	3.476	3.631	3.631	3.631	3.631	
55 Length, GM94X3, Wide Face	L <sub>3</sub>	in max	—	—	3.476	3.476	3.476	3.476	3.476	3.476	3.476	3.476	3.631	3.631	—	—	—	
56 Length, GM94X4, Std./H.T.	L <sub>3</sub>	in max	3.676	3.676	3.676	3.676	3.676	3.676	3.676	3.676	3.676	3.676	3.676	3.831	3.831	3.831	3.831	
57 Length, GM94X4, Wide Face	L <sub>3</sub>	in max	—	—	3.676	3.676	3.676	3.676	3.676	3.676	3.676	3.676	3.831	3.831	—	—	—	
58 Length, GM95X2, Std./H.T.	L <sub>3</sub>	in max	3.052	3.052	3.052	3.052	3.052	3.052	3.052	3.052	3.052	3.052	3.052	3.207	3.207	3.207	3.207	
59 Length, GM95X2, Wide Face	L <sub>3</sub>	in max	—	—	3.052	3.052	3.052	3.052	3.052	3.052	3.052	3.052	3.207	3.207	—	—	—	
60 Length, GM95X3, Std./H.T.	L <sub>3</sub>	in max	3.427	3.427	3.427	3.427	3.427	3.427	3.427	3.427	3.427	3.427	3.427	3.582	3.582	3.582	3.582	
61 Length, GM95X3, Wide Face	L <sub>3</sub>	in max	—	—	3.427	3.427	3.427	3.427	3.427	3.427	3.427	3.427	3.582	3.582	—	—	—	
62 Length, GM95X4, Std./H.T.	L <sub>3</sub>	in max	3.627	3.627	3.627	3.627	3.627	3.627	3.627	3.627	3.627	3.627	3.627	3.782	3.782	3.782	3.782	
63 Length, GM95X4, Wide Face	L <sub>3</sub>	in max	—	—	3.627	3.627	3.627	3.627	3.627	3.627	3.627	3.627	3.782	3.782	—	—	—	

† Represents gearbox capability only. Continuous load torque capability will vary with gear ratio, motor selection, and operating conditions. See pages 3 and 4, section IV, in "Servo Motor Application" Notes.  
 ‡ Shaft rotation is designated while looking at output shaft of gearbox with positive voltage (+) on number 1 terminal. Gearmotor is polarity reversible.

**GM9XXX SPUR GEARMOTOR DIMENSIONS**



**HEDS 90X0 OPTICAL ENCODER DATA (25° C)**

PARAMETER	SYMBOL	UNITS	Min.	Typ.	Max.
64 Encoder Resolution, HEDS 91X0	N	CPR	96	500	512
65 Encoder Inertia, HEDS 91X0	J <sub>E</sub>	oz-in-s <sup>2</sup>	—	8.0 x 10 <sup>-4</sup>	—
66 Encoder Weight, HEDS 91X0	W <sub>E</sub>	oz	—	1.58	—
67 Encoder Length, HEDS 91X0	L <sub>E</sub>	in max	—	—	0.595

Figure E.2: DC Motor - Page2